Journal of Medicinal Chemistry

pubs.acs.org/jmc Article

Gut-Restricted Selective Cyclooxygenase-2 (COX-2) Inhibitors for Chemoprevention of Colorectal Cancer

Zhuming Zhang,* Avijit Ghosh, Peter J. Connolly, Peter King, Thomas Wilde, Jianyao Wang, Yawei Dong, Xueliang Li, Daohong Liao, Hao Chen, Gaochao Tian, Javier Suarez, William G. Bonnette, Vineet Pande, Karen A. Diloreto, Yifan Shi, Shefali Patel, Beth Pietrak, Lawrence Szewczuk, Carlo Sensenhauser, Shannon Dallas, James P. Edwards, Kurtis E. Bachman, and David C. Evans*

Cite This: *J. Med. Chem.* 2021, 64, 11570−11596 Read Online

ACCESS | Metrics & More | Article Recommendations | Supporting Information

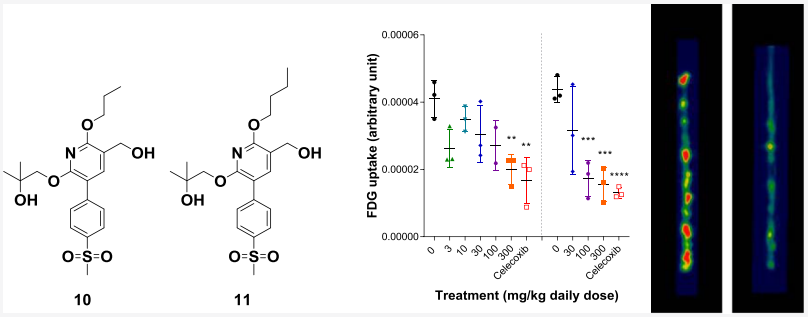

ABSTRACT: Selective cyclooxygenase (COX)-2 inhibitors have been extensively studied for colorectal cancer (CRC) chemoprevention. Celecoxib has been reported to reduce the incidence of colorectal adenomas and CRC but is also associated with an increased risk of cardiovascular events. Here, we report a series of gut-restricted, selective COX-2 inhibitors characterized by high colonic exposure and minimized systemic exposure. By establishing acute ex vivo ^{18}F-FDG uptake attenuation as an efficacy proxy, we identified a subset of analogues that demonstrated statistically significant in vivo dose-dependent inhibition of adenoma progression and survival extension in an APC$^{min/+}$ mouse model. However, in vitro−in vivo correlation analysis showed their chemoprotective effects were driven by residual systemic COX-2 inhibition, rationalizing their less than expected efficacies and highlighting the challenges associated with COX-2-mediated CRC disease chemoprevention.

INTRODUCTION

Colorectal cancer (CRC) is the third leading cause of cancer-related death in both men and women in the United States and also one of the most preventable malignancies.[1,2] It is well accepted that most CRCs occur via a metachronous adenoma−carcinoma sequence characterized by well-staged genetic alterations and oncogenic transformation over many years.[2−4] A long-term use of a single or combination of chemoprotective agents has been shown to impede, arrest, or even reverse the development of adenomas in the colon, and interfere with their progression from premalignant adenomas to carcinomas.[5−7] In this regard, nonsteroidal anti-inflammatory drugs (NSAIDs), particularly selective cyclooxygenase COX-2 inhibitors, have been one of the most studied class of drugs in CRC chemoprevention.[8−10] Recently, extensive epidemiological and randomized clinical studies have unequivocally established the chemopreventive effects of NSAIDs.[11−16] Celecoxib (**1**, Figure 1), a modestly selective COX-2 inhibitor, was approved by the FDA for adenoma prevention in patients with familial adenomatous polyposis (FAP), an inherited genetic predisposition to CRC.[14−16]

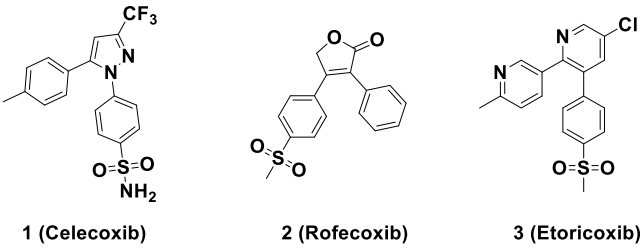

Figure 1. Chemical structures of celecoxib (**1**) and etoricoxib (**3**).

NSAIDs act by inhibiting the synthesis of prostanoids, a family of biologically active mediators generated by the activity

Received: May 17, 2021
Published: July 19, 2021

https://doi.org/10.1021/acs.jmedchem.1c00890
J. Med. Chem. 2021, 64, 11570−11596

Table 1. Inhibitory Potency in Human COX-2/COX-1 Enzymes, and COX-2/COX-1-Driven PGE_2 Synthesis in HEK293 Cells of 1, 3−12

Cpd	hCOX-2 IC_{50} (μM)[a]	hCOX-1 IC_{50} (μM)[a]	PGE_2 COX-2 IC_{50} (μM)[b]	PGE_2 COX-1 IC_{50} (μM)[b]
1	0.028 ± 0.027	9.2 ± 0.81	0.057 ± 0.021	0.41 ± 0.20
3	0.43 ± 0.03	>50	0.56 ± 0.19	>50
4	0.39 ± 0.04	>50	1.50 ± 0.23	>50
5	6.36[c]	>50	1.89 ± 0.49	>50
6	3.24[c]	>50	0.95 ± 0.16	>50
7	>50	>50	>50	>50
8	17.1 ± 1.8	>50	>50	>50
9	4.10 ± 0.14	>50	>50	>50
10	0.84 ± 0.06	>50	0.60 ± 0.43	>50
11	0.226 ± 0.042	>50	0.047 ± 0.036	14.1 ± 4.2
12	18.2[c]	>50	2.95[c]	>50

[a]Peroxidase fluorescent kinetic activities were measured (IC_{50} ± S.D.) using 10-acetyl-3,7-dihydroxyphenoxazine (ADHP) as an electron donor after preincubation with inhibitors for 60 min. [b]Production of PGE_2 was measured over time (IC_{50} ± S.D.) by tandem MS/MS analysis after pretreatment with inhibitors for 60 min in 10% FBS. [c]Tested only once. The number of replicates for other tested compounds was at least twice.

of COXs.[17,18] On the basis of pharmacodynamic (PD) features at therapeutic doses, NSAIDs are classified as either nonselective COX-1/COX-2 inhibitors or selective COX-2 inhibitors. The precise molecular mechanism of colorectal tumorigenesis inhibition by NSAIDs has not been fully delineated, and likely involves a combination of COX-dependent and COX-independent pathways.[19−21] A prolonged use of nonselective NSAIDs is associated with side effects such as gastrointestinal bleeding and ulceration that is partially attributed to COX-1 inhibition in the cases of SC-560 and indomethacin.[22−24]

COX-2 and COX-1 are two isoenzymes that catalyze the initial step of the conversion of arachidonic acid to bioactive prostaglandins (PGs).[18,25,26] Constitutive COX-1 is ubiquitously expressed in almost all tissues for housekeeping PG synthesis, whereas inducible COX-2 is upregulated via stimulation of inflammatory cytokines or growth factors.[18,27] Increased expression of COX-2 occurs during all stages of the multistep progression of CRC,[28−30] and overexpression of COX-2 correlates with the colon tumor size, invasiveness, and increased PG levels.[31] It is now understood that proinflammatory and immune-suppressive PGE_2 plays a central role in colorectal tumor growth by promoting proliferation, survival, motility, angiogenesis, and DNA methylation and potentiating Wnt signaling.[32−36] In preclinical studies, inhibition of COX-2 reduced the size and number of polyps in multiple adenoma and inflammation mouse models.[37−40] In a randomized clinical study conducted in FAP patients, a significant dose-dependent reduction in polyp burden was observed in patients who received celecoxib (**1**).[15] Rofecoxib (**2**, Figure 1) was also found to significantly reduce the risk of recurrent adenomas in another clinical trial focusing on maintaining a polyp-free colon in FAP patients.[13] In the Prevention of Sporadic Adenomatous Polyps (PreSAP) clinical trial, the use of celecoxib was correlated with a reduced relative risk (RR of 0.64) for adenomas detected during a 3 year period.[14] However, these studies also showed that cardiovascular (CV) adverse events increased with the administration of selective COX-2 inhibitors.[16,41,42] The elevated CV hazard was associated with COX-2 dependent pathways, putatively attributed to blocked prostacyclin (PGI_2) production.[42] This serious CV risk has rendered celecoxib (**1**) and rofecoxib (**2**) unsuitable for a long-term use in a wider population of patients.[12−16,41,42]

To minimize the risk of CV adverse effects, but maintain the beneficial property of attenuating colon polyp progression, colon-specific prodrugs of celecoxib have been investigated.[43,44] Other approaches to overcome systemic adverse events, including the use of formulations to deliver active drugs to different regions of the gastrointestinal tract, have also been reported.[45,46] Instead, we pursued an alternative strategy to modulate the physicochemical properties of potent and selective COX-2 inhibitor candidate drugs in order to restrict them to the intestinal tract. In so doing, local on-target concentrations in the gastrointestinal tract are maximized while systemic exposure is minimized.[47] Our objective, therefore, was to identify a colon-targeted, orally administered, COX-2-selective inhibitor that would suppress local PGE_2 production in the target tissue (lamina propria), reduce adenoma progression for CRC chemoprevention, and be devoid of systemically mediated CV adverse effects.

We chose etoricoxib (**3**, Figure 1) as the starting point based on two key factors.[48,49] First, we recently described the use of reoptimized MS-based COX enzymatic assays to investigate previously unpublished time-dependent inhibition kinetics of COX-2 inhibitors from several chemical series.[50] Our studies confirmed high specificity of COX-2 inhibition associated with etoricoxib (**3**) and close analogues (**4−12**) sharing a common pyridyl core ring (Table 1). In contrast, celecoxib (**1**) displayed only moderate selectivity for COX-2 over COX-1 inhibition (Tables 1 and 5). Moreover, celecoxib (**1**) exhibited high overall thermodynamic potency indicated by the intrinsic inhibition constant (*Ki**), but also associated with a short dissociation half-life ($t_{1/2(dissociation)}$). By contrast, etoricoxib (**3**) and its analogues **10** and **11** (Figure 3), while less potent than **1**, showed a longer kinetic residence time ($t_{1/2(dissociation)}$) for target occupancy.[51] We envisaged that long residence time kinetics would be important for robust target engagement in local colon tissues by minimizing systemic drug recirculation resulting from gut-restricted distribution.

Second, compared to celecoxib (**1**, clog *P* 4.57), etoricoxib (**3**, clog *P* 2.35) was a more hydrophilic starting point for our exploration. Previously, the physicochemical property-based approach proved to be quite effective in identifying gut-restricted JAK inhibitors with low intrinsic permeability, which translated into high colonic retention and low systemic exposure after oral dosing.[47] Our initial plan was centered on lowering clog *P* to reduce permeability while balancing potency of COX-2 inhibition, a similar strategy utilized for enteric JAK inhibitors.[47,52] However, an inverse correlation of potency and

https://doi.org/10.1021/acs.jmedchem.1c00890
J. Med. Chem. 2021, 64, 11570−11596

clog *P* counteracted our efforts for further lowering the permeability of these inhibitors. The high clearance of these analogues was recognized as a key attribute to minimize systemic exposure for the small fraction of drug that was absorbed. Herein, we describe our coordinated multidimensional optimization efforts for a series of potent, selective COX-2 inhibitors highlighting their gut-restricted pharmacological characterization in vitro and in vivo.

RESULTS AND DISCUSSION

Analysis of cocrystal structures of celecoxib (**1**), close analogues, and rofecoxib (**2**) bound to COX-2 enzymes (PDB IDs: 3LN1; 5KIR) indicated the phenylsulfonamide or methylsulfonylphenyl groups were optimal and critical in occupying the COX-2-binding pocket surrounded by key residues, especially Arg499 and Val509.[53−55] As etoricoxib (**3**) was also shown to share a similar binding orientation to COX-2 (Section S11, Figure S5), these structures served as the basis for our exploration (Figure 2). We recently reoptimized COX enzymatic assays to evaluate COX-2 inhibitors.[50] Because COX enzymes are intracellular targets localized in subcellular compartments such as endoplasmic reticulum (ER) and the nuclear envelope, we also established MS-based orthogonal assays to confirm cellular penetration and uptake as well as COX-1/COX-2 selectivity of these inhibitors by measuring production of PGE_2 from arachidonic acid in stably transfected human embryonic kidney (HEK) 293 TRex cells overexpressing COX-1 or COX-2 controlled by an inducible tetracycline promoter.[56]

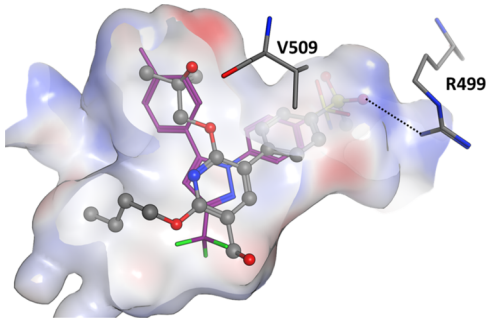

Figure 2. Docking model of compound **11** (balls and sticks) in complex with COX-2 (side chains as sticks and binding pocket depicted as an electrostatic surface map—blue: positive and red: negative potential). Celecoxib (**1**, PDB ID: 3LN1) is superimposed as purple sticks for reference.

The 5-CF_3 analogue **4** (clog *P* 2.06; hCOX-2 IC_{50} 0.39 μM), with a less planar, gem-dimethyl-substituted glycol replacing its peripheral pyridinyl ring, was identified to have lower clog *P* but still retain similar enzymatic potency and selectivity to etoricoxib (**3**, clog *P* 2.35; hCOX-2 IC_{50} 0.43 μM) (Figure 3, Table 1). The 5-CF_3 moiety of **4** was anticipated to occupy a similar region in the COX-2 active site to 3-CF_3 of celecoxib (**1**). The nonfluorinated analogues **5** (5-Me; clog *P* 1.60; hCOX-2 IC_{50} 6.36 μM) and **6** (5-Et; clog *P* 2.13; hCOX-2 IC_{50} 3.24 μM) lost enzymatic potency but still maintained cellular COX-2 potency in the low micromolar range (IC_{50} 1−2 μM). However, by reducing clog *P* below 1, analogue **7** (5-CH_2OH; clog *P* 0.51; hCOX-2 IC_{50} > 50 μM) became inactive in both enzymatic and cellular assays (PGE_2 COX-2 > 50 μM). Introducing an additional 6-methoxy (R^1 = Me) or 6-isopropoxy (R^1 = *i*-Pr) in **7** led to an improvement in enzymatic activity in **8** (clog *P* 0.89; hCOX-2 IC_{50} 17.1 μM) and **9** (clog *P* 1.73; hCOX-2 IC_{50} 4.10 μM) but did not confer cellular activity (PGE_2 COX-2 IC_{50} > 50 μM). Fortunately, continued SAR development with 6-propoxy (R^1 = *n*-Pr) and 6-butoxy (R^1 = *n*-Bu) improved both enzymatic and cellular potencies as shown in analogues **10** (clog *P* 1.95; hCOX-2 IC_{50} 0.84 μM; PGE_2 COX-2 IC_{50} 0.6 μM) and **11** (clog *P* 2.48; hCOX-2 IC_{50} 0.226 μM; PGE_2 COX-2 IC_{50} 0.047 μM). In particular, **11** displayed comparable potency to etoricoxib (**3**, PGE_2 COX-2 IC_{50} 0.56 μM) and celecoxib (**1**, PGE_2 COX-2 IC_{50} 0.057 μM). Like etoricoxib (**3**, PGE_2 COX-1 IC_{50}/COX-2 IC_{50} ratio >80), compounds **10** (PGE_2 COX-1 IC_{50} > 50 μM) and **11** (PGE_2 COX-1 IC_{50} = 14.1 μM) remained more selective than celecoxib (**1**, PGE_2 COX-1 IC_{50}/COX-2 IC_{50} ratio ∼ 7). However, by lowering clog *P* below 1, compound **12** (R^1 = $(CH_2)_2OMe$; clog *P* 0.78) lost significant potency (hCOX-2

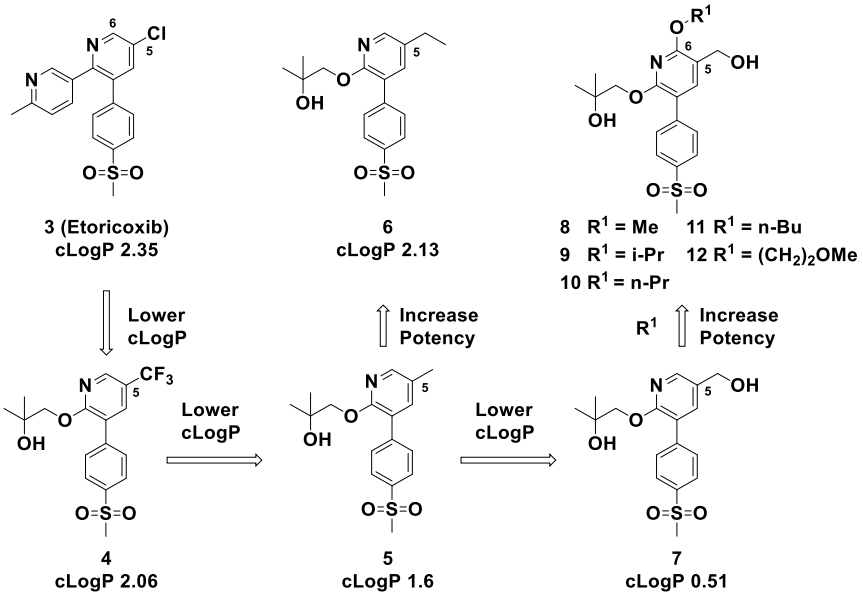

Figure 3. Evolution of etoricoxib (**3**) and analogues **4**−**12** for local enteric delivery.

https://doi.org/10.1021/acs.jmedchem.1c00890
J. Med. Chem. 2021, 64, 11570−11596

IC_{50} 18.2 μM; PGE_2 COX-2 IC_{50} 2.95 μM) compared to corresponding compound **11** (R^1 = *n*-Bu; clog *P* 2.48).

Compounds **1**, **3**, **4**, **6**, **10**, and **11** were screened in cassette PO dosing PK studies for their systemic (plasma) and colonic exposures at 2 and 4 h time points following oral dosing of 10 mg/kg in C57BL mice (T_{max} ranging from 0.25 to 3 h). In vivo clearance (CL), volume of distribution (V_{dss}), and half-life ($T_{1/2}$) of these compounds were also determined in cassette IV dosing PK studies in mice to correlate with in vitro human or mouse liver microsomal and hepatocyte stability (Table 2).

Table 2. Human/Mouse Liver Microsomal, Hepatic Clearance, and Mean Cassette Dosing PK Parameters of Compounds 1, 3, 4, 6, 10, and 11 in C57BL Mice by PO (10 mg/kg) and IV Dosing (2 mg/kg)

Compound	1	3	4	6	10	11
HLM $T_{1/2}$ (min)[a]	67.2	>184	>184	68.7	>184	27.8
MLM $T_{1/2}$ (min)[a]	59.3	53.8	>184	13.2	19.6	2.7
human Hep $T_{1/2}$ (min)[b]	57.4	>371	>371	84.2	3.1	2.4
mouse Hep $T_{1/2}$ (min)[b]	33.1	29.2	>371	3.2	3.0	1.9
CL (mL/min/kg)[c]	10.5	41.3	0.54	65.6	92.7	101.2
V_{dss} (L/kg)[c]	0.94	1.27	1.55	1.35	3.05	4.92
$T_{1/2}$ (h)[c]	1.27	0.78	38.5	0.32	NA[f]	0.23
colon (ng/g), 4 h[d]	9460	55.7	8400	51.6	5336	4352
plasma (ng/mL), 4 h[d]	2553	36.4	9803	21.8	5.7	3.0
ratio colon/plasma, 4 h[e]	3.8	1.5	0.9	2.5	1276	1616

[a]For HLM/MLM $T_{1/2}$: high stability > 184 min; 33 min < medium stability <184 min; and low stability < 33 min. [b]For hepatocytes $T_{1/2}$: high stability > 371 min; 60 min < medium stability < 371 min; and low stability < 60 min. [c]IV cassette dosing of **2**–**4** compounds in each group, solution in 70% PEG/H_2O. [d]Oral cassette dosing, solution in 70% PEG/H_2O, values shown are the average concentration for individual animals at time point of 4 h. [e]The ratios were calculated as averages of ratios from individual animals. [f]$T_{1/2}$ was not obtained due to *R*-squared (R_{sq}) < 0.75.

Compound **4** was highly stable in human and mouse liver microsomes and hepatocytes in vitro, which was consistent with its low clearance (CL 0.54 mL/min/kg) and long half-life ($T_{1/2}$ 38.5 h) in a cassette 2 mg/kg IV PK study. Compound **4** also had good exposure and equal distribution in colon (8400 ng/g) and plasma (9803 ng/mL) at 4 h (T_{max} 3 h) following a cassette 10 mg/kg oral dosing in vivo. Celecoxib (**1**) showed modest metabolic stability in vitro but moderate clearance (CL 10.5 mL/min/kg) and half-life ($T_{1/2}$ 1.27 h) in mice in vivo, which was consistent with a high exposure in colon (9460 ng/g) and a relatively lower exposure in plasma (2553 ng/mL). Etoricoxib (**3**) was metabolically stable in human liver microsomes and hepatocytes but unstable in mouse and showed higher clearance (CL 41.3 mL/min/kg) and a short half-life ($T_{1/2}$ 0.78 h), leading to a low exposure in colon (55.7 ng/g) and plasma (36.4 ng/mL) in mice. Similarly, compound **6** was metabolically unstable in mouse in vitro and unsurprisingly showed a low exposure in colon (51.6 ng/g) and plasma (21.8 ng/mL) consistent with its higher clearance (CL 65.6 mL/min/kg) and a shorter half-life ($T_{1/2}$ 0.32 h) in vivo. There were no signs of gut restriction for compounds **1**, **3**, **4**, and **6** despite a wide range of physicochemical and ADME properties such as clog *P*, metabolic stability, and clearance. Their volume of distribution (V_{dss}) was in a narrow range of 1–2 L/kg. Unexpectedly, compounds **10** and **11** displayed high colonic exposures (>4300 ng/g) and a low systemic exposure (<6 ng/mL) with a distribution ratio of C/P > 1200 at 4 h (T_{max} ~ 0.25 h) following cassette 10 mg/kg oral dosing. Both compounds exhibited high clearance (>90 mL/min/kg) with a volume of distribution (V_{dss}) above others (>2 L/kg) after 2 mg/kg IV cassette dosing (Table 2). The gut-restricted characteristics of compounds **10** and **11** were confirmed by single-dose time-course PK studies following colon exposures as well as systemic plasma concentration in expanded time points after an oral dosing (10 mg/kg) in C57BL Mice (Table 5, also Section S4, Figures S1 and S2).

The PK results suggested that unique metabolism of compounds **10** and **11** played a critical role in the observed high colon/plasma (C/P) ratio distinct from that of compound **6**. To study its metabolic fate, compound **11** was incubated with human and mouse hepatocytes, and metabolites were identified by liquid chromatography interfaced with tandem mass spectrometric (LC–MS/MS) analysis and their relative percentages were quantitatively assessed based on peak areas in the mass spectral response (Table 3). Compound **11** was found to undergo extensive metabolism with a turnover of ~100 and 79.6% in human and mouse hepatocytes, respectively. Glucuronidation was the major metabolic pathway in both species with a single O-glucuronide M6 identified as the major metabolite in human (92.5%) and mouse (24.7%). The hydroxyl group in 5-CH_2OH was the putative site for the formation of O-glucuronide M6. However, efforts to confirm the structure of M6 were unsuccessful due to the inability to isolate the putative M6 or synthesize an authentic sample for authentication. A subsequent in vitro UDP-glucuronosyltransferase (UGT) phenotyping screening identified UGT1A9 as the primary isoform responsible for driving clearance via glucuronidation (Section S6). Consistent with these findings, the single-dose oral and IV PK studies confirmed a minimal systemic plasma exposure and low oral bioavailability in mouse (4.25%), rat (1.5%), and monkey (4.87%) (Section S5, Table S4). Dog was the exception, showing high oral bioavailability (74%, Table S4), possibly resulting from different UGT1A9 expression levels or substrate affinity, as reported with other human UGT1A9 substrates (Section S7).[57]

The in vitro metabolism study also identified oxidative hydroxylation of the 6-butoxy chain as the other major metabolic clearance pathway in mouse. However, this path was less significant in human hepatocytes indicated by the formation of a variable amount of hydroxylated metabolites M4 and M5 (Table 3). Minor metabolites such as o-dealkylated M2 (loss of *n*-butyl) and carboxylic acid M7 from oxidation of 5-CH_2OH were also observed in human and/or mouse hepatocytes. These putative metabolites M2, M4, M5, and M7 were synthesized and found to be inactive in the COX-2 enzymatic (COX-2 IC_{50} > 50 μM) assay and would not contribute to in vivo pharmacology (Section S3, Table S2). The metabolite study confirmed that compound **10** was metabolized similar to compound **11** with glucuronidation representing the dominant metabolic pathway in both human and mouse species in vitro. Hydroxylation of the 6-propoxy moiety and oxidation of 5-CH_2OH to the carboxylic acid were major pathways in mouse but less significant in human hepatocytes (Section S2). Like compound **11**, single-dose oral and IV PK studies of compound **10** also generally demonstrated gut-restricted characteristics across species with low oral bioavailability in mouse (4.25%), rat

https://doi.org/10.1021/acs.jmedchem.1c00890
J. Med. Chem. 2021, 64, 11570–11596

Table 3. In Vitro Metabolite Profiling and Identification from Incubations of Compound 11 with Human and Mouse Hepatocytes[a]

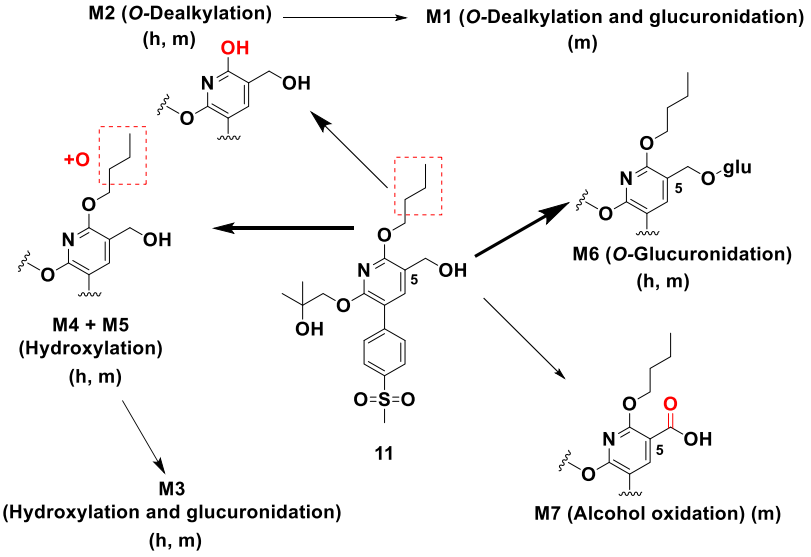

	% peak area		
metabolite	human	mouse	biotransformation
M1	0.1	0.51	O-dealkylation and glucuronidation
M2	3.08	7.97	O-dealkylation
M3	1.15	1.56	hydroxylation and glucuronidation
M4	2.63	**38.44**	hydroxylation
M5	0.53	2.23	hydroxylation
M6	**92.51**	**24.76**	O-glucuronidation
M7		4.14	alcohol oxidation
compound **11**		**20.40**	

[a]Final compound **11** concentration of 10 μM and a cell concentration of 1×10^6 cells/mL (1000 μL final incubation volume). Cells were incubated for 0 and 2 h. The percent compositions of parent drug and its metabolites were based on peak areas from 5 ppm accurate mass measurements and with assumptions of equal positive ESIs.

Table 4. Inhibitory Potency in COX-2/COX-1-Driven PGE_2 Synthesis in HEK293 Cells, and Mean Cassette Dosing PK Parameters of Compounds 13-20 in C57BL Mice by IV Dosing (2 mg/kg) and PO (10 mg/kg)

cpd	PGE_2, COX-2, IC_{50} (μM)[b]	PGE_2, COX-1, IC_{50} (μM)[b]	CL (mL/min/kg)[c]	colon (ng/g), 4 h[d]	plasma (ng/mL), 4 h[d]	ratio of colon/plasma[e]
11	0.047 ± 0.036	14.1 ± 4.2	101.2	4352	3.0	1616
13	2.34[f]	7.69[f]	48.2	2810	22.8	134.3
14	1.21 ± 0.30	>50	58.8	85.8	35.8	2.5
15	0.54 ± 0.46	>50	55.4	478.2	28.7	16.5
16	0.049	0.511	32.2	1942	75.9	24.9
17	0.036 ± 0.009	2.46 ± 0.99	101.5	1872	6.7	402.3
18	1.32 ± 0.33	>50	68.6	11920	7.7	1596
19	0.21[f]	>50[f]	89.3	1854	2	1040
20	0.037 ± 0.027	7.23 ± 2.31	100.4	5394	9.9	545.2

[a]Peroxidase fluorescent kinetic activities were measured (IC_{50} ± S.D.) using ADHP as an electron donor after preincubation with inhibitors for 60 min. [b]The production of PGE_2 and PGD_2 was measured over time (IC_{50} ± S.D.) by tandem MS/MS analysis after pretreatment with inhibitors for 60 min in 10% FBS. [c]IV cassette dosing, solution in 70% PEG/H_2O. [d]Oral cassette dosing, solution in 70% PEG/H_2O, values shown are the average concentration for individual animals at a time point of 4 h. [e]The ratios were calculated as averages of ratios from individual animals. [f]Tested only once. The number of replicates for other tested compounds was at least twice.

(2.3%), and monkey (20.0%); dog was an exception (79.5%) (Section S4, Table S3).

To better understand the critical role of the primary hydroxyl group (5-CH_2OH) in compound **10** or **11** leading to high in vivo clearance and high colon/plasma (C/P) ratios, compounds **13**−**20** were prepared for characterization (Figure 4, Table 4). Introducing a methyl group (R^2 = −CH_2(OH)Me) led to compound **13** with lower clearance (CL 48.2 mL/min/kg) and a reduced colon/plasma ratio (C/P: 134.3). Adding two geminal methyl groups (R^2 = −CH(OH)Me_2) resulted in compound **14** with a diminished colon concentration (85.8 ng/g) and a colon/plasma ratio (C/P: 2.5). Extending compound **11** (R^2 = −CH_2OH) with a hydroxyethyl group provided compound **15** (R^2 = −$CH_2O(CH_2)_2OH$) with an attenuated colon/plasma ratio (C/P: 16.5), presumably attributed to the alteration of metabolism for hepatic clearance or less dependence on the

https://doi.org/10.1021/acs.jmedchem.1c00890
J. Med. Chem. 2021, 64, 11570−11596

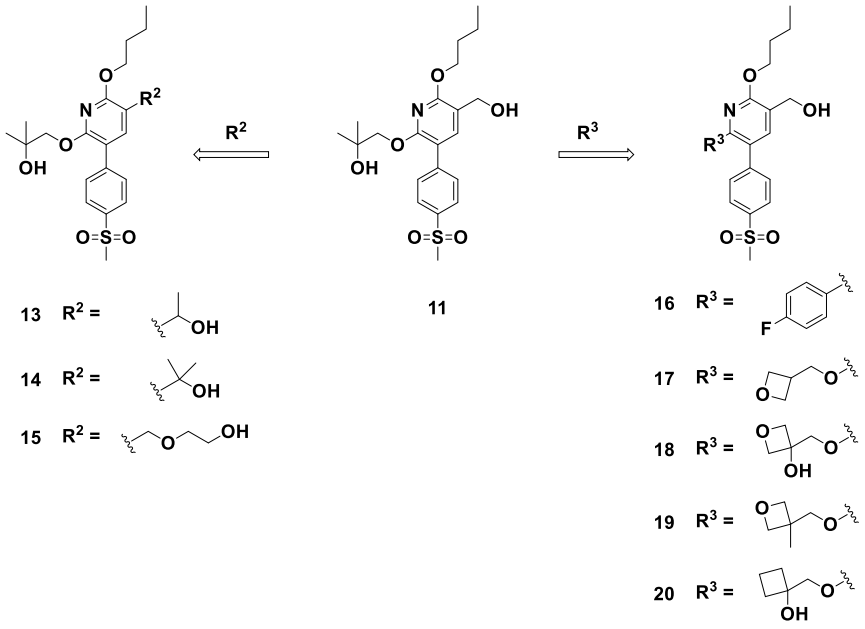

Figure 4. Analogues **13**−**20** with modifications at R^2 or R^3 on the pyridine ring sites of compound **11**.

glucuronidation pathway. These results provided direct evidence in support of the primary benzylic hydroxyl moiety (R^2 = −CH_2OH) as the major metabolic site for glucuronidation driving clearance and resultant high colon/plasma exposure ratios.

Turning our attention to the aliphatic gem-dimethyl-substituted glycol in compound **11**, we found that replacing this group with an aromatic 4-fluorophenyl led to a lower clearance (CL 32.2 mL/min/kg) and a lower colon/plasma exposure ratio (C/P: 24.9) as shown in compound **16** (Table 4). Also, compound **16** showed narrow selectivity in the cellular COX-1/COX-2 assays (PGE2 COX-1 IC_{50}/COX-2 IC_{50} ratio ∼ 10, Table 4), highlighting that aromatic substitution at R^3 was unfavorable. Compounds **17**, **18**, and **19**, sharing a terminal oxetanyl group with or without an attached tertiary hydroxyl moiety, all maintained high colon/plasma ratios (C/P: >400). This finding indicated the tertiary hydroxyl group might be additive but not essential for driving the clearance and high colon/plasma ratio. It should be pointed out that modification of gem-dimethyl groups to an oxetane ring altered COX-2 potency or selectivity and colonic exposure. For example, compared to compound **11** (PGE2 COX-1 IC_{50}/COX-2 IC_{50} ratio ∼ 300; colon concentration 6506 ng/g at 2 h) (Tables 1 and 2), analogue **17** was potent in COX-2 inhibition but 4-fold less selective (PGE2 COX-2 IC_{50} 0.047 μM; PGE2 COX-1 IC_{50}/COX-2 IC_{50} ratio ∼ 70). Compound **18** was relatively less potent in cellular COX-2 activity (PGE2 COX-2 IC_{50} 1.32 μM). The colonic exposure of compound **19** was noticeably lower (1854 ng/g). By contrast, cyclizing the terminal gem-dimethyl to a cyclobutyl group led to compound **20** with overall in vitro and in vivo properties comparable with compound **11** (Tables 4 and 5).

To support the selection of compounds for in vivo PD studies, additional analogues were synthesized. Modifications to the 6-butoxy (R^4) site on compounds **10** and **11** were made by varying alkoxy length and hydrophobicity, resulting in identification of the fluorinated analogues **21** (clog *P* 2.30) and **22** (clog *P* 2.03) for further studies (Figure 7). By correlating COX-2 cellular and enzymatic potency with physicochemical or ADME properties in this subset of COX-2 inhibitors (Figure 5), we observed a direct relationship between clog *P* (log *D*) and COX-2 activities. Compounds with low clog *P* (<1) were unlikely to have acceptable cellular COX-2 potency (PGE2 COX-2 pIC_{50} > 6 or IC_{50} < 1 μM). This observation was not totally unexpected given the intracellular localization of the COX-2 enzyme and the subcellular microenvironment of the COX-2-binding site, which is surrounded by hydrophobic residues. Low clog *P* (<1) would not only attenuate permeability for cellular uptake but also affect lipophilicity required for biochemical affinity. The correlation was in line with the weaker potency associated with compounds **8** (clog *P* 0.89; Figure 3, Table 1), **12** (clog *P* 0.78; Figure 3, Table 1), and putative (inactive) metabolites M2, M4, and M5 (clog *P* < 1; Table 3, also Table S2).

Conversely, an empirically inverse correlation seemed to exist between a lower clog *P* (<2) and a higher colon/portal vein (PV) plasma ratio (>150) at 4 h following oral dosing (10 mg/kg) cassette PK in C57BL mice, presumably resulting from limited absorption through reduced permeability (Figure 6). Careful analysis of single-dose PK studies of compounds **10** (PV plasma 98.6 ng/mL; systemic plasma 25 ng/mL), **20** (PV plasma 82.4 ng/mL; systemic plasma 3 ng/mL), **21** (PV plasma 178.4 ng/mL; systemic plasma 3.4 ng/mL), and **22** (PV plasma 230.3 ng/mL; systemic plasma 3.8 ng/mL) revealed the PV plasma concentrations were consistently higher than systemic plasma exposures, indicating that some drug was being absorbed across the gut epithelium but subsequently cleared first pass to result in apparent gut restriction (Table 5). To minimize this effect, we incorporated bioisosteric replacements in the phenyl region (R^5) aimed at attenuating clog *P* (log *D*) and permeability (Figure 7). A pyridinyl sulfonamide analogue **23** (clog *P* 1.94; PGE_2 COX-2 0.23 μM) was identified having acceptable, though decreased, cellular potency. Compound **23** showed the lowest MDCK based passive permeability ($P_{app\ A>B}$ 8.15 cm/s $\times 10^{-6}$) and the narrowest gap between PV and systemic plasma exposures (7.1 ng/mL vs 5.5 ng/mL); its similar colon/PV plasma and colon/plasma ratios (2179 vs 1692) were indicative of limited absorption via restricted permeability (Table 5).

https://doi.org/10.1021/acs.jmedchem.1c00890
J. Med. Chem. 2021, 64, 11570−11596

Table 5. Summary of Inhibitory Potency in Human COX-2/COX-1 Enzymes, Calculated Intrinsic Inhibition Constant (*Ki), Dissociation Half-Life ($t_{1/2(\text{dissociation})}$), COX-2-Driven PGE_2 Synthesis in HEK293 Cells, Human Whole Blood COX-2/COX-1 Assays, ADME, and Mean Cassette or Single-Dosing PK Exposure Parameters in C57BL Mice by PO (10 mg/kg), ^{18}F-FDG Uptake, Polyp Area Tumor Growth Inhibition, and Survival Extension in $Apc^{Min/+}$ Mice of Compounds 1, 3, 10, 11, and 20−23**

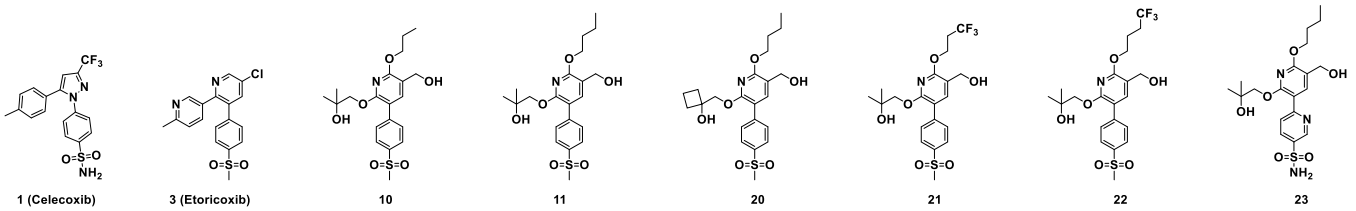

1 (Celecoxib) 3 (Etoricoxib) 10 11 20 21 22 23

compound	**1** (celecoxib)	**3** (etoricoxib)	**10**	**11**	**20**	**21**	**22**	**23**
hCOX-2 IC_{50} (μM)[b]	0.028 ± 0.027	0.43 ± 0.03	0.84 ± 0.06	0.226 ± 0.042	0.12 ± 0.05	0.50 ± 0.07	0.36 ± 0.10	0.45 ± 0.09
hCOX-2 *Ki** (nM)	0.47 ± 0.08	69 ± 4	114 ± 9	12 ± 1	3.0 ± 0.2	32 ± 3	12 ± 2	19 ± 1
hCOX-2 $t_{1/2(\text{dissociation})}$ (h)	0.71 ± 0.03	6.1 ± 0.3	8.9 ± 0.7	18 ± 1	39 ± 2	22 ± 2	27 ± 3	23 ± 1
hCOX-1 IC_{50} (μM)[b]	9.2 ± 0.81	>50	>50	>50	>50	>50	>50	>50
PGE_2 COX-2 IC_{50} (μM)[d]	0.057 ± 0.021	0.56 ± 0.19	0.60 ± 0.43	0.047 ± 0.036	0.037 ± 0.027	0.13 ± 0.03	0.078 ± 0.049	0.23 ± 0.11
PGE_2 COX-1 IC_{50} (μM)[d]	0.41 ± 0.20	>50	>50	14.1 ± 4.2	7.23 ± 2.31	>50	21.8 ± 16.4	>50
HWB COX-2 IC_{50} (μM)[e]	0.44 ± 0.37	0.611 ± 0.055	2.341 ± 0.002	0.346[j]	0.146[j]	0.877 ± 0.378	0.345 ± 0.126	7.232[j]
HWB COX-1 IC_{50} (μM)[e]	14.8 ± 10.7	93.8 ± 54.0	193 ± 43	>180[j]	>60[j]	181 ± 20	>180	>60[j]
human PPB (fu %)	0.3	11.4	1.6	0.9	0.5	1.0	1.1	0.2
human colon (fu %)	0.31	NA	6.6	2.5	5.5	22.4	20.4	7.5
clog *P* (log *D*)	4.57 (3.55)	2.35	1.95 (2.68)	2.48 (3.15)	2.67 (3.41)	2.30 (2.53)	2.03 (2.97)	1.94 (2.56)
Papp $_{A>B}$ (+inh.) (cm/s $\times 10^{-6}$)[f]	22.4	35.9	++	19.88	16.19	21.5	20.19	8.15
solubility FaSSIF (μM)[g]	133.5	357.8	25	66.5	56.1	44.4	110.6	63.1
colon (ng/g), 4 h[h]	9460 ± 2423	55.7 ± 3.9	2910 ± 1324*	802.6 ± 679.4*	5290 ± 2745*	15520 ± 2417	15980 ± 2739	12040 ± 3242*
plasma (ng/mL), 4 h[h]	2553 ± 422	36.4 ± 2.5	25 ± 31*	16.2 ± 15.1*	3 ± 1*	3.4 ± 1.7	3.8 ± 1.2	5.5 ± 0.9*
PV plasma (ng/mL), 4 h[h]	2150 ± 544	48.6 ± 8.9	98.6 ± 45.1*	24.8 ± 5.1*	82.4 ± 52.6*	178.7 ± 90.2	230.3 ± 112.3	7.1 ± 0.5*
ratio colon/plasma, 4 h[i]	3.8 ± 1.2	1.5 ± 0.2	492 ± 612*	91.5 ± 79.3*	1718 ± 392*	5264 ± 2245	4473 ± 1204	2179 ± 245*
ratio colon/PV plasma, 4 h[i]	4.6 ± 1.6	1.2 ± 0.3	38 ± 29*	29.7 ± 19.5*	69.9 ± 21.4*	101 ± 44	77 ± 25	1692 ± 336*
ex vivo ^{18}F-FDG uptake (%)[k]	31.4 ($P < 0.001$)	43.5 ($P < 0.01$)	35.6 ($P < 0.01$)	48.9 ($P < 0.01$)	61.2 ($P < 0.001$)	48.6 ($P < 0.05$)	NA[m]	54.8 ($P < 0.001$)
ex vivo ^{18}F-FDG IC50 (μM) (95% CI, μM)[l]	NA	NA	4.4 (2.4−47)	13 (7.5−53)	5.5 (2.7−98)	4.2 (1.6−376)	NA[m]	14 (7.5−42)
in vivo polyp area TGI %[n]	65.9	NT	41.9	35.1	NT	48.7	39.8	25.0
in vivo survival (days)[o]	>82	>82	>82[p]	NT	NT	74	62.5	NT

[a]Single-dose PK at 2 h following oral dosing of 10 mg/kg by solution formulation in 70% PEG/H_2O. [b]Peroxidase fluorescent kinetic activities were measured (IC_{50} ± S.D.) using ADHP as an electron donor after preincubation with inhibitors for 60 min. [c]Calculated intrinsic inhibition constant. [d]Production of PGE_2 was measured over time (IC_{50} ± S.D.) by tandem MS/MS analysis after pretreatment with inhibitors for 60 min in 10% FBS. [e]HWB = human whole blood. [f]Passive permeability (cm/s $\times 10^{-6}$) was measured from the apical (A) to the basolateral side (B) of MDCK-MDR1 cells in the presence of a P-gp inhibitor with mass balance >60%. [g]Equilibrium solubility assay, simulated intestinal fluid under fasted physiological conditions (FaSSIF pH 6.5). [h]Oral cassette dosing of 10 mg/mg, solution in 70% PEG/H_2O, the average concentration of individual animals at a time point of 4 h, PV = portal vein. [i]Ratios were calculated as averages of ratios from individual animals. [j]Tested only in one donor ($N = 1$). [k]Ileum ex vivo percentage change was the mean difference between a dose of 0 *vs* 300 mg/kg oral daily dosing either incorporated into a chow diet or suspension by gavage for 2 weeks in curative setting (mice starting age of 16 week old). [l]FDG uptake was plotted against the total compound concentration in ileum at >12 h. IC_{50} was fitted for each compound in GraphPad Prism using the parameters assuming: (1) vehicle FDG uptake = no inhibition; (2) celecoxib FDG uptake = complete inhibition; (3) Hill coefficient = 1; (4) weighting = $1/y^2$; and (5) 95% confidence interval (CI). [m]Not conclusive due to animal death. [n]Tumor growth inhibition (TGI) values from total ileum polyp area (sum of all polyp areas with diameter > 1 mm) following a daily oral dosing of 300 mg/kg as a suspension for 10−12 weeks, %TGI = $1 - (T_t/C_t)$, T_t = median tumor volume of treated at time *t*, and C_t = median tumor volume of control at time *t*. [o]Kaplan−Meier survival days were recorded until 50% mortality reached in each group in curative setting (mice starting at age of 16 weeks, Section S8) with a daily oral dosing of 100 mg/kg as a suspension unless specified otherwise. Study was terminated at day 82. [p]Oral daily dosing of 30 mg/kg as a suspension.

https://doi.org/10.1021/acs.jmedchem.1c00890
J. Med. Chem. 2021, 64, 11570−11596

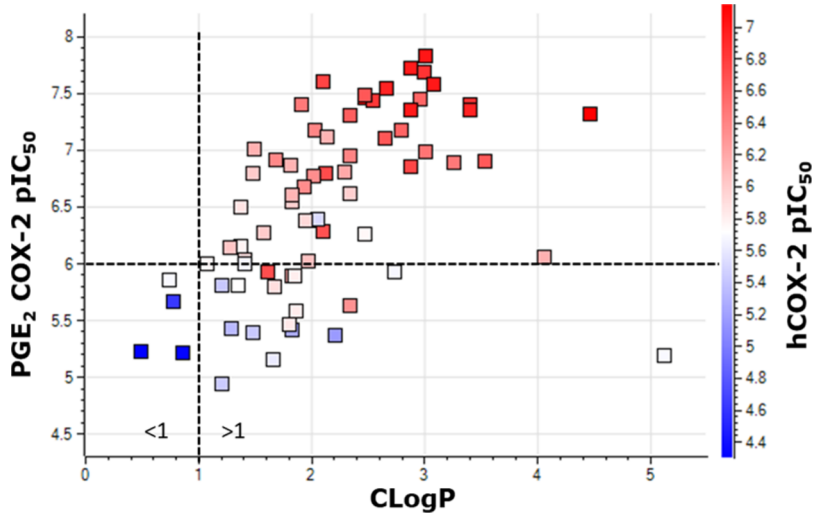

Figure 5. Correlation between cellular PGE_2 COX-2 potency (pIC_{50}) and clog *P* with human COX-2 enzymatic potency (pIC_{50}, color coding) [$pIC_{50} = -\log_{10}(IC_{50}\ \mu M)$].

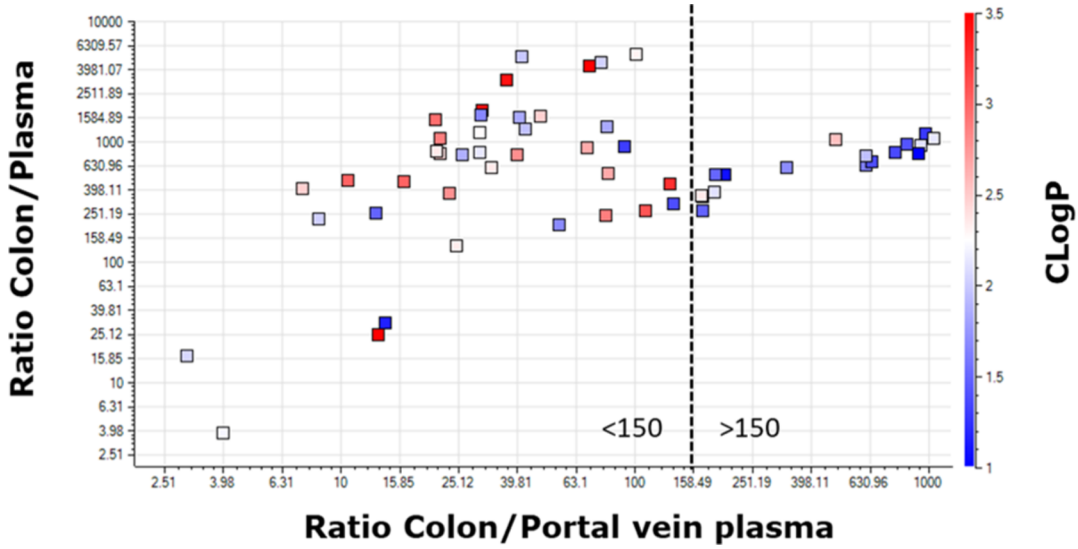

Figure 6. Comparison of the mouse exposure colon/plasma ratio to the colon/PV plasma ratio (both measured at 4 h) in cassette PK following an oral dosing of 10 mg/kg in C57BL mice. All points were color coded in relation to clog *P*. Logarithmic scale was used on all axes.

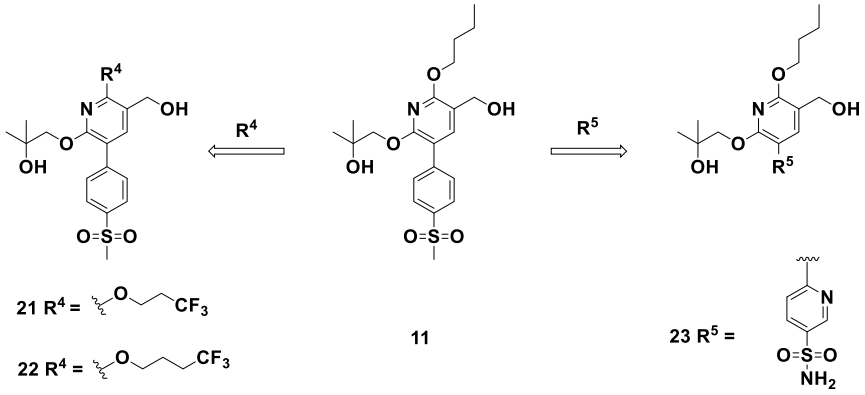

Figure 7. Analogues **21**−**23** as selected representatives with modifications at various sites of compounds **11** (or **10**).

To confirm COX-1/COX-2 selectivity in a more physiologically relevant system, compounds **10**, **11**, and **20**−**23** were evaluated in human whole blood (HWB) for COX-2 inhibition by measuring PGE_2 production stimulated by LPS, and COX-1 inhibition by measuring TXB_2 synthesis stimulated by a calcium ionophore.[58,59] All analogues displayed concentration-dependent inhibition of PGE_2 and achieved ∼100% inhibition at the highest tested concentration, with COX-2 IC_{50} values ranging

https://doi.org/10.1021/acs.jmedchem.1c00890
J. Med. Chem. 2021, 64, 11570−11596

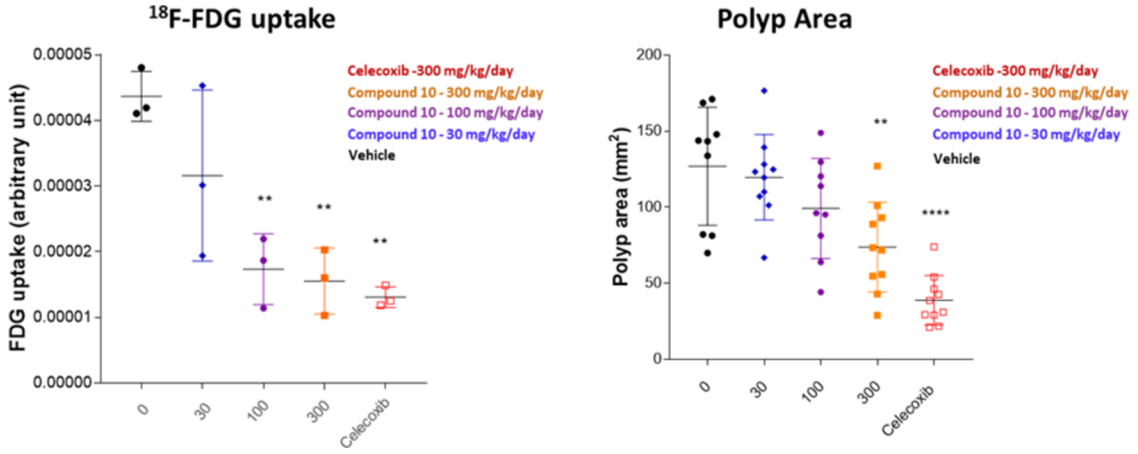

Figure 8. Side-by-side comparison of the [^{18}F]-FDG PET signal (expressed as average injected dose per gram (% ID/g, 20% threshold) in 2-week curative setting) and polyp area attenuation in APC$^{Min/+}$ mice in prophylactic setting (12 weeks) for compound **10**. Vehicle and celecoxib groups (300 mg/kg/daily in chow diet) served as negative and positive controls, respectively. Analyses were performed in R, version 3.3.2. ANOVA, adjusted for multiple comparisons in a linear regression model. *P < 0.05; **P < 0.01; ***P < 0.001; and ****P < 0.0001.

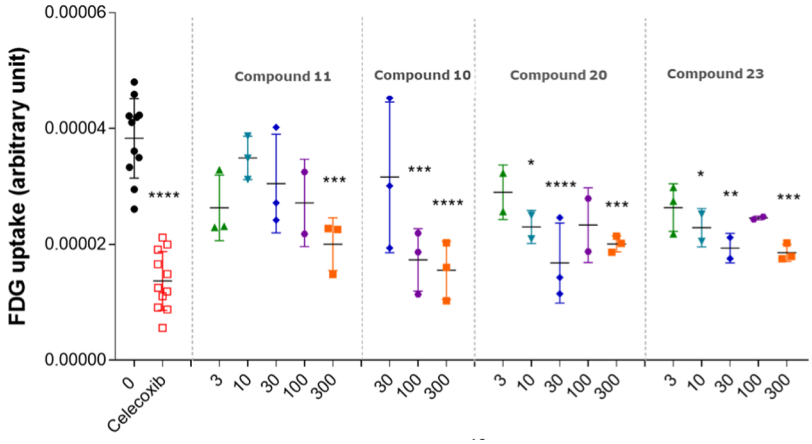

Figure 9. Compounds **11**, **20**, and **23** for [^{18}F]-FDG PET in curative setting (dosing in chow diet, mice received daily doses of 3, 10, 30, 100, and 300 mg/kg for 2 weeks from the age of >16 weeks) compared to compound **10**. ^{18}F-FDG PET signal expressed as average injected dose per gram (% ID/g, 20% threshold). The percentage injected dose per gram (% ID/g) was calculated as follows: % ID/g = ROI activity divided by injected dose multiplied by 100%. Vehicle and celecoxib (300 mg/kg/daily) served as negative and positive controls, respectively. Analyses were performed in R, version 3.3.2. ANOVA, adjusted for multiple comparisons in a linear regression model. *P < 0.05; **P < 0.01; ***P < 0.001; and ****P < 0.0001.

from 0.15 to 7.5 μM (Table 5). By contrast, none of these compounds significantly inhibited COX-1 (IC_{50} > 60 μM), consistent with their COX-1/COX-2 selectivities in stably transfected HEK293 cells. Except for compounds **10** (HWB COX-2 IC_{50} 2.3 μM) and **23** (HWB COX-2 IC_{50} 7.2 μM), compounds **11** and **20**−**22** showed similar potencies to celecoxib (**1**, HWB COX-2 IC_{50} 0.44 μM) and etoricoxib (**3**, HWB COX-2 IC_{50} 0.611 μM). Compounds **11** and **20**−**22** showed higher selectivity (HWB COX-1 IC_{50}/COX-2 IC_{50} > 200) than etoricoxib (**3**, HWB COX-1 IC_{50}/COX-2 IC_{50} ∼ 150). The selectivity of compound **10** (HWB COX-1 IC_{50}/COX-2 IC_{50} ∼ 80) was still higher than that of celecoxib (**1**, HWB COX-1 IC_{50}/COX-2 IC_{50} ∼ 37). The potency of compound **23** (HWB COX-2 IC_{50} 7.2 μM) was weaker than anticipated, presumably attributable in part to high human plasma/serum protein binding as evidenced by very low unbound fractions (human PPB fu % = 0.2%) compared to others in this group (human PPB fu % in a range of 0.5−1.6%). Interestingly, the unbound fraction of compound **23** was significantly higher in colon tissue (human colon fu % = 7.5%). In contrast to compounds **10** and **11** (human colon fu % = 6.6, 2.5% respectively), fluorinated analogues **21** and **22** displayed much higher unbound fractions (human colon fu % = 22.4, 20.4% respectively) though their human plasma protein-binding values (human PPB fu %: 0.9−1.6%) were similar. All analogues showed a narrow range of solubility (FaSSIF, 25−110 μM). It was notable that compound **20** was the most potent COX-2 inhibitor (hCOX-2 IC_{50} 0.12 μM; PGE_2 COX-2 IC_{50} 0.037 μM; and HWB COX-2 IC_{50} 0.146 μM) with low nanomolar COX-2 enzyme kinetic potency (Ki* 2.9 nM) and a long residence time ($T_{1/2(dissociation)}$ 39 h) for target occupancy.[50]

To evaluate the in vivo chemoprotective effects of these gut-restricted COX-2 inhibitors, we first measured attenuation of ex vivo local ileum acute glucose (as ^{18}F-FDG) uptake from short-term treatment (2 weeks) as an indirect PD surrogate and predictor of long-term efficacy (12 weeks) in a multiple intestinal neoplasia (MIN) mouse model by utilizing molecular tomographic imaging.[60] This Apc mutant (Apc$^{Min/+}$) mouse model, widely used in colorectal carcinogenesis and chemoprevention research, simulates human adenoma progression, in which loss of function (LOF) of tumor suppressor adenomatous polyposis coli (APC) gene by deletion/mutation leads to the

https://doi.org/10.1021/acs.jmedchem.1c00890
J. Med. Chem. 2021, 64, 11570−11596

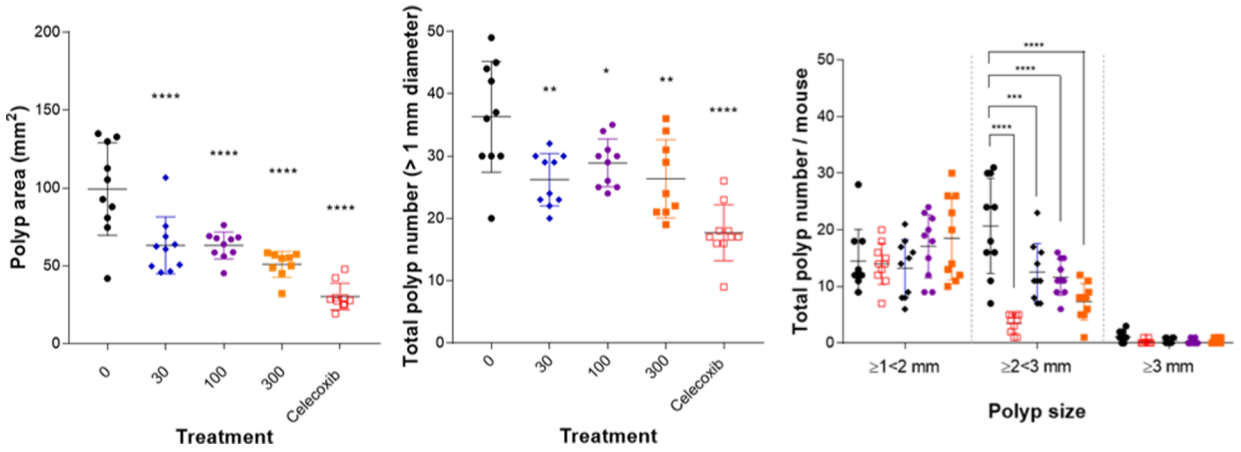

Figure 10. Oral in vivo efficacy of compound **21** in prophylactic setting (dosing as a suspension by gavage, mice received doses of 30, 100, and 300 mg/kg for 10 weeks from the age of 5−6 weeks). Celecoxib (300 mg/kg/daily in a suspension by gavage) served as a positive control. Polyp area/number in treatment: One-way ANOVA with Dunnett's multiple comparison test; polyp number vs polyp size: Two-way ANOVA with Dunnett's multiple comparison test. GraphPad Prism 7.0.

Table 6. Comparison of In Vitro and In Vivo IC_{50} Values (nM, Unbound)

	in vivo potency[a]		in vitro potency[b]	
compound	systemic (IC_{50} nM)	gut (IC_{50} nM)	HWB COX-2 (fu % × IC_{50} nM)	HWB COX-1 (fu % × IC_{50} nM)
1 (celecoxib)[c]	3.2	3.2	1.32	44.4
10	35	2384	37.5	3088
21	1.3	741.8	8.77	1810
22	1.9	160	3.8	>1980

[a]Calculated based on in vivo polyp area TGI (%, 300 mg/kg oral daily dosing) and relevant plasma and ileum exposures 4 h after the last dose in a 12 week prophylactic setting in $APC^{min/+}$ mice. [b]Calculation (IC_{50} × fu %) based on measured in vitro human whole blood COX-2/COX-1 potency (IC_{50}) and human plasma protein-binding free faction (fu %) (Table 5). [c]Based on 9 week PK exposure in prophylactic setting (300 mg/kg oral daily dosing), assuming equal exposure in plasma and ileum, fit using Mathematica 11.

initiation of adenomatous polyp formation and growth, recapitulating clinically relevant CRC tumorigenesis observed in FAP patients.[61−63] Celecoxib (1) has been shown to be effective in suppressing adenoma formation and growth in this $Apc^{Min/+}$ mouse model over a study period of 1−2 months.[64] To shorten the turnaround time, we hypothesized that ^{18}F-FDG uptake attenuation could represent a sensitive biomarker for predicting efficacy as it is a common assumption that metabolic changes precede morphologic responses in the polyp size and/or number.[65] By using compound **10**, we first established that there was a direct correlation between ^{18}F-FDG signals from the abdominal region in vivo and ileum ex vivo in APC mice (data not shown). We then confirmed a positive correlation between short-term dose-dependent reduction in ex vivo ileum ^{18}F-FDG PET signal from treatment with compound **10** in curative setting (dosing in chow diet, mice received doses of 30, 100, and 300 mg/kg for 2 weeks starting from the age of 16 weeks with established adenomas) and long-term does-dependent polyp area inhibition in $Apc^{Min/+}$ mice in a prophylactic setting (dosing of compounds in chow diet, mice received doses of 30, 100, or 300 mg/kg for 12 weeks from the age of 5−6 weeks) using celecoxib (**1**, chow diet, 300 mg/kg daily) and vehicle as positive and negative controls (Figure 8). The correlation established acute ^{18}F-FDG PET signal attenuation as a prognostic biomarker to predict efficacy and quickly eliminate ineffective compounds that failed to reduce glucose uptake within 2 weeks.

Compound **10** showed short-term, dose-dependent reduction of ^{18}F-FDG uptake (35.6%, $P < 0.01$; IC_{50}, 4.4 μM) at 300 mg/kg oral daily dosing in a curative setting (2 week), which translated into a statistically significant polyp area tumor growth inhibition (TGI 41.9%) for total ileum polyp area (sum all of all polyp areas with diameter > 1 mm) in a prophylactic setting (300 mg/kg daily, 12 weeks) over celecoxib (^{18}F-FDG, 31.4% $P < 0.001$; TGI 65.9%) (Table 5). Etoricoxib (**3**, ^{18}F-FDG, 43.5%, $P < 0.01$), compounds **11** (^{18}F-FDG, 48.9%, $P < 0.01$; IC_{50}, 13 μM), **20** (^{18}F-FDG, 61.2%, $P < 0.001$; IC_{50}, 5.5 μM), and **23** (^{18}F-FDG, 54.8%, $P < 0.01$; IC_{50}, 14 μM) all showed short-term dose-dependent ^{18}F-FDG uptake decreases (Table 5), but the magnitude and ranges of the decrease for compounds **11**, **20**, and **23** were smaller compared to compound **10** (Figure 9). Compound **23** showed much weaker polyp area tumor growth inhibition (TGI 25.0%, $p > 0.05$) in a long-term prophylactic setting (300 mg/kg daily, 12 weeks). Surprisingly, compound **11** was also weaker with respect to polyp area tumor growth inhibition (TGI 35.1%) despite a significant reduction of ^{18}F-FDG uptake (48.9%, $P < 0.01$; IC_{50}, 13 μM). Based on the results, compound **20** was not considered for long-term studies. Compounds **21** (TGI 48.7%, Figure 10) and **22** (TGI 39.8%) showed comparable and statistically significant tumor growth inhibition in a prophylactic setting (300 mg/kg daily as a suspension by gavage, 10 weeks). It should be pointed out that compounds **10**, **21**, and **22** showed a statistically significant reduction of the polyp area and polyp number at all doses (30, 100, and 300 mg/kg) driven primarily by reduction in polyps of size ranging from >2 to <3 mm, as exemplified by compound **21** in Figure 10. Compounds **10** (>82 days, 80% survival, 30 mg/kg), **21** (74 days, 50% survival, 100 mg/kg), and **22** (62.5 days, 50% survival, 100 mg/kg) all extended survival of $Apc^{min/+}$ mice

https://doi.org/10.1021/acs.jmedchem.1c00890
J. Med. Chem. 2021, 64, 11570−11596

Scheme 1. Syntheses of Compounds 5, 6, and 7[a]

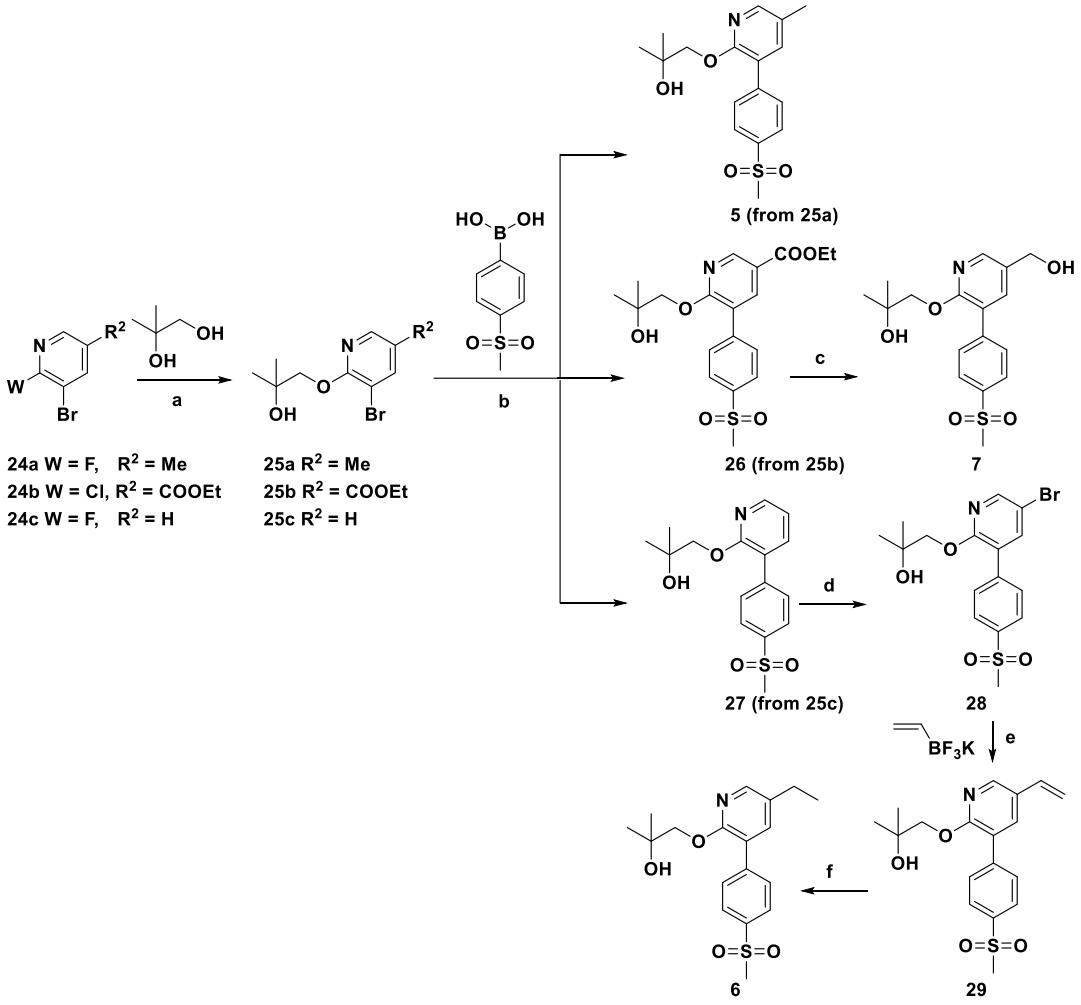

[a]Reagents and Conditions: (a) *tert*-BuOK, DMF, rt; (b) $Pd(dppf)Cl_2$ (cat) or $Pd(dppf)Cl_2$·DCM (cat), Na_2CO_3, 1,4-dioxane/H_2O, 80 °C; (c) Red-Al, THF, rt; (d) NBS, DMF, 70 °C; (e) $Pd(dppf)Cl_2$ (cat), Na_2CO_3, 1,4-dioxane/H_2O, 80 °C; and (f) Pd−C (10%), H_2, EtOH, rt.

(dosing by gavage P.O., daily starting at age of 4−6 weeks) compared to positive controls celecoxib (**1**) (>82 days, 100% survival, 100 mg/kg) and etoricoxib (**3**) (>82 days, 80% survival, 100 mg/kg) and negative control (vehicle treatment, 20 days, 50% survival) (Table 5, also Section S8). Nevertheless, compounds **10**, **21**, or **22** failed to demonstrate superior in vivo chemopreventive effects over celecoxib at the highest doses tested.

To test the hypothesis that GI tissue exposure and COX-2 inhibition drive efficacy rather than systemic exposure/inhibition, separate IC_{50}s for celecoxib (**1**) and compounds **10**, **21**, and **22** were derived using the in vivo tumor (polyp) area and either systemic or ileum concentrations. These values are shown for four compounds in Table 6 (plots shown in Section S9), along with in vitro IC_{50} values for HWB COX-1 and COX-2 inhibition, adjusted for unbound drug concentrations. Comparison of in vitro with in vivo potencies provides insights into factors driving efficacy. For example, by looking at the clinical comparator celecoxib, the systemic and gut in vivo IC_{50}s are similar to the adjusted in vitro COX-2 IC_{50}, consistent with the hypothesis that systemic or gut inhibition of COX-2 drives efficacy. The observation that celecoxib's in vivo IC_{50} is 14-fold lower than its adjusted in vitro COX-1 IC_{50} suggests a minimal contribution of COX-1 inhibition driving in vivo efficacy.

In contrast, in vivo gut IC_{50} values for the gut-restricted compounds **10**, **21**, and **22** are 40- to 85-fold higher than the adjusted in vitro COX-2 potency (IC_{50}). This extreme "right-shift" of in vivo IC_{50} and lack of in vitro−in vivo correlation (IVIVC) suggest that gut COX-2 inhibition is not driving efficacy. Assuming gut COX-2 inhibition is not driving efficacy, three other possibilities should be considered: (1) systemic COX-2 inhibition, (2) systemic COX-1 inhibition, and (3) gut COX-1 inhibition. Our results suggest systemic COX-2 is the most likely driver of efficacy both because of good IVIVC (in vitro and adjusted in vivo potency (IC_{50}s) are within 1.0- to 6.7-fold of each other) for the gut-restricted compounds and because celecoxib, with its high systemic exposure, is effective at reducing the polyp area. Systemic COX-1 inhibition can be ruled out due to the large disconnect between in vitro and adjusted in vivo potency (88- to 1,400-fold difference in IC_{50}s for gut-restricted compounds). Interestingly, gut COX-1 inhibition has reasonable IVIVC (1.3- to 12.4-fold difference between in vitro and adjusted in vivo potency IC_{50}s for gut-restricted compounds), and therefore cannot be ruled out as a driver of efficacy. However, because celecoxib works systemically with minimal COX-1 inhibition, systemic COX-2 inhibition is the more likely driver of tumor growth inhibition in this mouse model.[66,67]

https://doi.org/10.1021/acs.jmedchem.1c00890
J. Med. Chem. 2021, 64, 11570−11596

Scheme 2. Syntheses of Compounds 8 and 12[a]

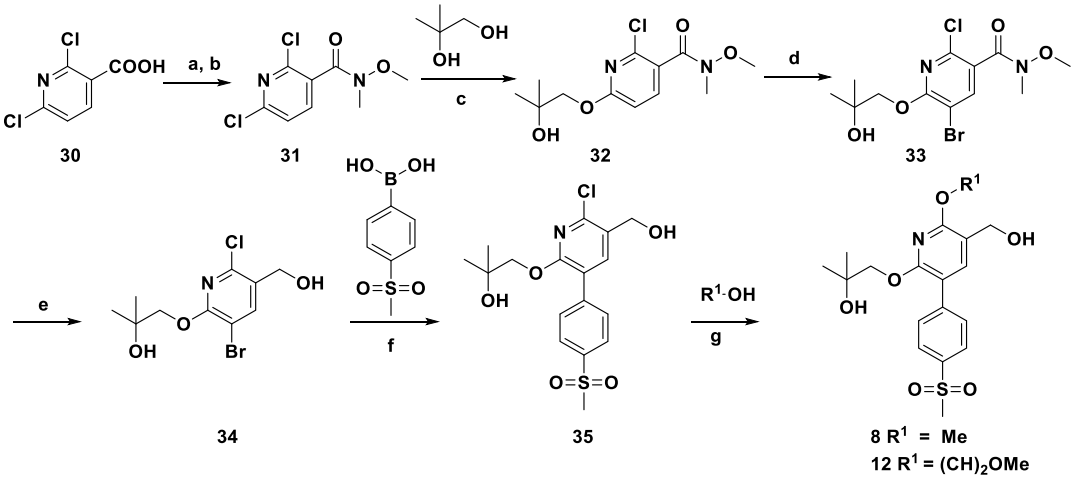

[a]Reagents and Conditions: (a) $SOCl_2$, DMF, $CHCl_3$, 80 °C; (b) CH_3NHOCH_3·HCl, TEA, DCM, rt; (c) *tert*-BuOK, DMF, 60 °C; (d) Br_2, NaOAc, AcOH, 80 °C; (e) $NaBH_4$, MeOH, rt; (f) Pd(dppf)Cl_2 (cat), Na_2CO_3, 1,4-dioxane/H_2O, 60 °C; and (g) NaH, DMF, rt.

Scheme 3. Synthetic Route for Preparation of Compounds 9, 10, 11, 21, and 22[a]

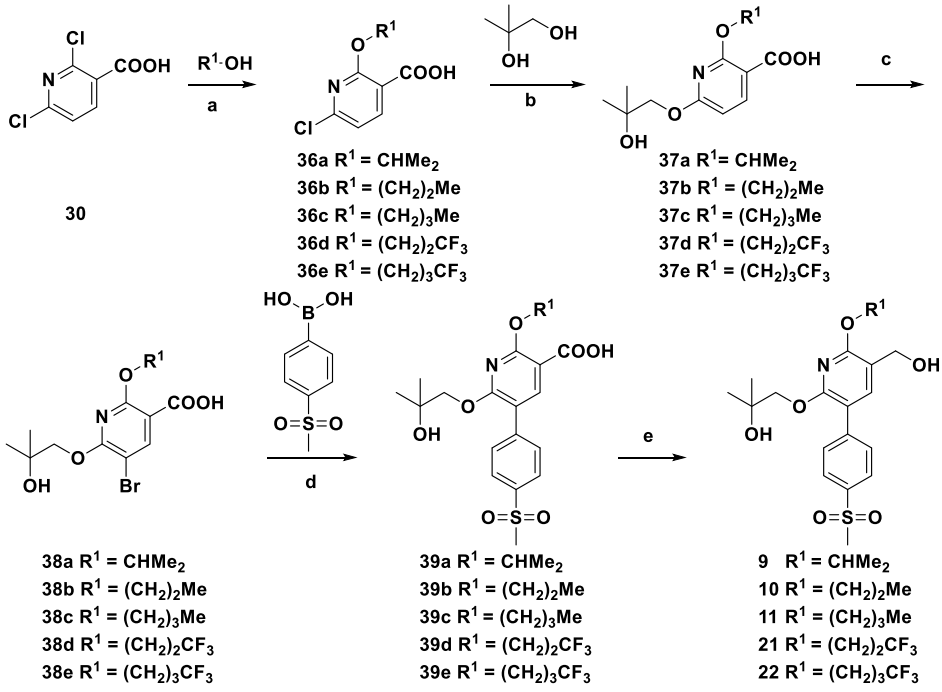

[a]Reagents and Conditions: (a) NaH, DMF or THF; (b) Xphos Pd G3 (cat), Cs_2CO_3, toluene, 90 °C; (c) NBS, MeCN, rt; (d) Pd(PPh_3)$_4$ (cat), Na_2CO_3, 1,4-dioxane/H_2O, 80 °C; and (e) BH_3·THF, THF.

Chemistry. Preparation of compound **4** has been reported.[68] The synthesis of compounds **5**−**7** is outlined in Scheme 1 and described in detail in Section S1. Commercially available **24a**−**c** were reacted with 2-methylpropane-1,2-diol in the presence of potassium *tert*-butoxide in DMF to afford the corresponding ethers **25a**−**c**, which were coupled with commercially available 4-(methanesulfonyl)phenylboronic acid under palladium-mediated Suzuki reaction conditions to give compound **5** and intermediates **26** (R^2 = COOEt) and **27** (R^2 = H). Intermediate **26** was reduced with sodium bis(2-methoxyethoxy)aluminum hydride (Red-Al) in THF to provide compound **7**. Selective bromination of **27** with *N*-bromosuccinimide (NBS) in DMF led to bromide **28**. Subsequent Suzuki−Miyaura coupling of potassium trifluoro(vinyl)borate with **28** installed a vinyl group in **29**, which was reduced by palladium catalyst-mediated hydrogenation to generate compound **6**.

Several flexible synthetic routes were used to access compounds **8**−**23**. The initial route outlined in Scheme 2 was developed for preparation of compounds **8** and **12**. Commercially available 2,6-dichloronicotinic acid **30** was converted into Weinreb amide **31** by reacting with thionyl chloride followed by coupling with dimethylhydroxylamine hydrochloride under basic conditions. Treatment of **31** with 2-methylpropane-1,2-diol in the presence of potassium *tert*-butoxide generated **32** as the major product. Selective bromination of **32** with bromine in acetic acid provided bromide **33**. The reduction of Weinreb

https://doi.org/10.1021/acs.jmedchem.1c00890
J. Med. Chem. 2021, 64, 11570−11596

Scheme 4. Syntheses of Compounds 13, 14, and 15[a]

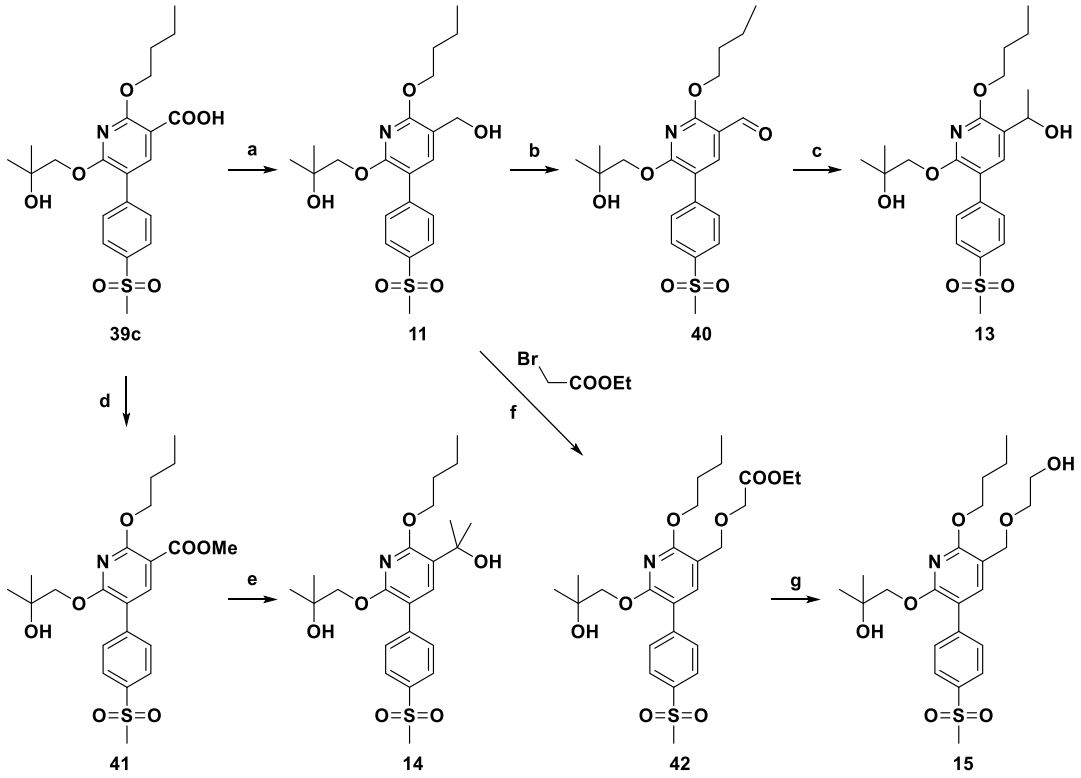

[a]Reagents and Conditions: (a) BH_3·THF, THF; (b) Dess–Martin periodinane, DCM, rt; (c) MeMgCl, THF, rt; (d) $TMSCHN_2$, MeOH, toluene, rt; (e) MeMgCl, THF, rt; (f) NaH, THF, rt; and (g) $LiAlH_4$, THF, 0 °C.

Scheme 5. Synthesis of Compound 16[a]

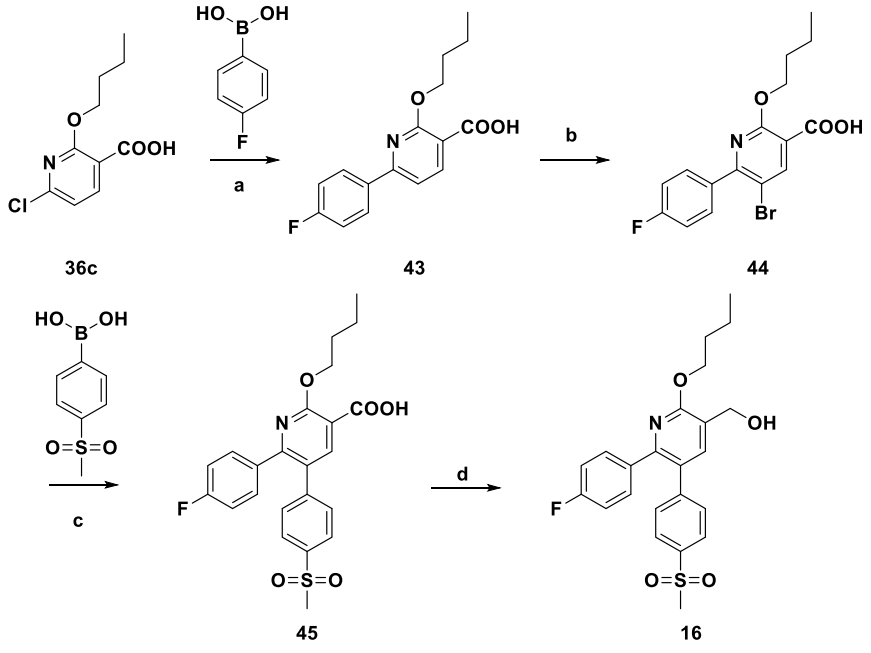

[a]Reagents and Conditions: (a) $Pd(PPh_3)_4$ (cat), K_2CO_3, 1,4-dioxane/H_2O, 80 °C; (b) NBS, TFA, MeCN, rt; (c) $Pd(PPh_3)_4$ (cat), K_2CO_3, 1,4-dioxane/H_2O, 80 °C; and (d) BH_3·THF, THF.

amide **33** was achieved by using sodium borohydride to provide **34**. The coupling reaction of **34** with 4-(methanesulfonyl)-phenylboronic acid under palladium-mediated Suzuki reaction conditions gave compound **35**. Finally, treatment of **35** with methanol or 2-methoxyethanol in the presence of sodium hydride-furnished compounds **8** or **12**, respectively.

Analogues **9**, **10**, **11**, **21**, and **22** were synthesized by the route outlined in Scheme 3. In this route, ortho-regioselective alkoxylation of 2,6-dichloronicotinic acid **30** was achieved

https://doi.org/10.1021/acs.jmedchem.1c00890
J. Med. Chem. 2021, 64, 11570–11596

Scheme 6. Synthetic Route for Preparation of Compounds 17, 18, 19, and 20[a]

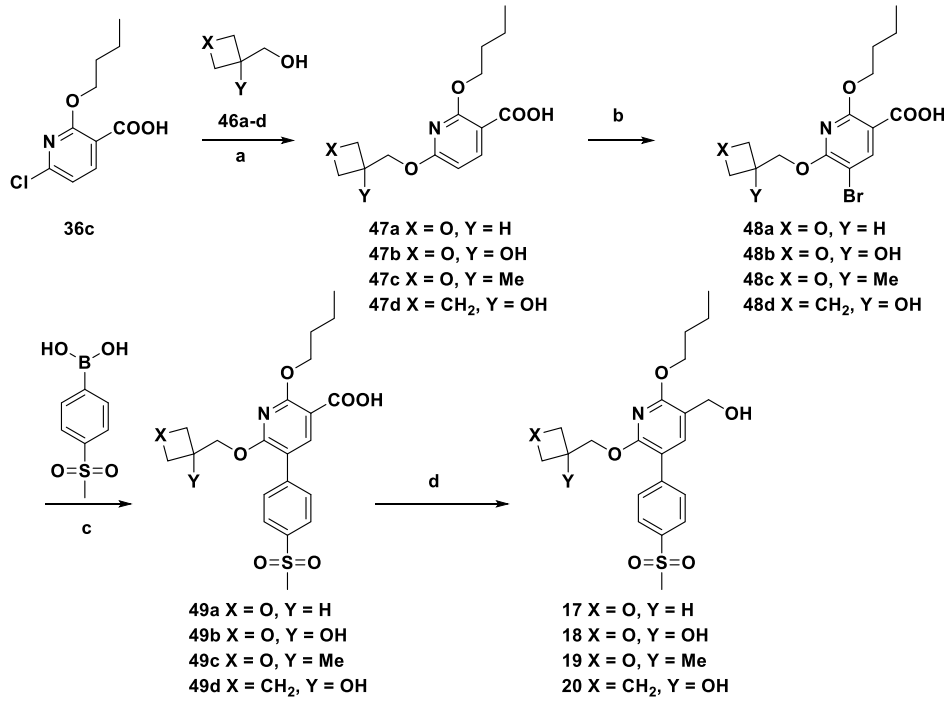

[a]Reagents and Conditions: (a) Xphos Pd G3 (cat), Cs_2CO_3, toluene, 90 °C; (b) NBS, AcOH, MeCN, rt; (c) $Pd(PPh_3)_4$ (cat), K_2CO_3, 1,4-dioxane/H_2O, 80 °C; and (d) (i) TEA, ClC(═O)O−iBu, THF; then $NaBH_4$; or (ii) BH_3·THF, THF.

Scheme 7. Synthesis of Compound 23[a]

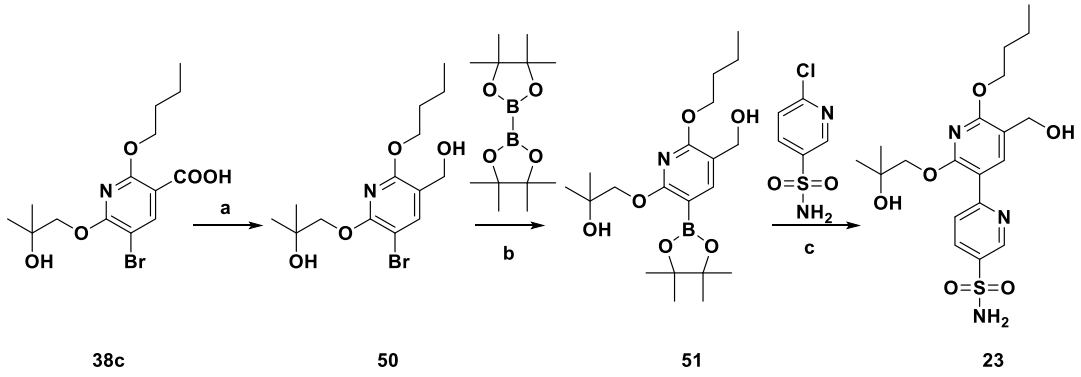

[a]Reagents and conditions: (a) BH_3·THF, THF; (b) $Pd(dppf)Cl_2$ (cat), KOAc, 1,4-dioxane, 100 °C; and (c) $Pd(dppf)Cl_2$ (cat), Na_2CO_3, 1,4-dioxane/H_2O, 65 °C.

using various alcohols (R^1-OH) in the presence of sodium hydride under controlled conditions to afford intermediates **36a−e**.[69] Treatment of **36a−e** with 2-methylpropane-1,2-diol under palladium catalyzed reaction conditions to provide corresponding 2,6-di-alkoxylated acids **37a−e**. Our efforts to produce **37a−e** directly from **30** by combining steps a and b without purification of **36a−e** were unsuccessful due to difficult separation at the end. Selective bromination of **37a−e** with NBS in acetonitrile led to bromides **38a−e** in good yields, followed by coupling with 4-(methanesulfonyl)phenylboronic acid under Suzuki reaction conditions to give **39a−e** as the major products. The carboxylic acids **39a−e** were reduced by the borane−tetrahydrofuran complex to afford corresponding analogues **9**, **10**, **11**, **21**, and **22**.

Compounds **13**, **14**, and **15** were prepared according to Scheme 4. Oxidation of compound **11** using Dess−Martin periodinane gave aldehyde **40** in >90% yield. Subsequent nucleophilic addition of methylmagnesium chloride led to the formation of analogue **13**. Similarly, gem-dimethyl analogue **14** was obtained through nucleophilic addition of methylmagnesium chloride to methyl ester **41**, which was prepared by esterification of acid **39c** with $TMSCHN_2$, described previously in Scheme 2. Selective alkylation of compound **11** was accomplished using ethyl bromoacetate and sodium hydride to afford ester **42**, which was readily reduced to alcohol **15** using lithium aluminum hydride under controlled anhydrous conditions.

Scheme 5 shows the preparation of compound **16**. Intermediate carboxylic acid **36c**, described previously in Scheme 2, was coupled with 4-fluorophenylboronic acid under palladium-mediated Suzuki conditions to generate intermediate **43** in modest yield (40%). Subsequent transformations

https://doi.org/10.1021/acs.jmedchem.1c00890
J. Med. Chem. 2021, 64, 11570−11596

(selective bromination, palladium-mediated Suzuki coupling, and reduction of the acid moiety) led to the formation of analogue **16**.

In a similar manner to the synthetic route as described in Scheme 3, compounds **17** and **18** were prepared as illustrated in Scheme 6. The previously described ortho-alkylated intermediate **36c** was coupled with commercially available oxetanyl or cyclobutyl reagents **46a−d** (X = O or CH_2; Y = H, Me, or OH) to provide corresponding dialkoxylated **47a−d** under palladium-mediated reaction conditions. Treatment of **47a−d** with NBS generated bromides **48a−d**. Subsequent Suzuki coupling of 4-(methanesulfonyl)phenylboronic acid with **48a−d** installed a 4-(methanesulfonyl)phenyl group in **49a−d**. The carboxylic acids **49a−c** were reduced by first reacting with isobutyl chloroformate in the presence of triethylamine to generate mixed anhydrides in situ, followed by treatment with sodium borohydride, to give analogues **17**, **18**, and **19**. Alternatively, a reduction of acid **49d** with borane tetrahydrofuran complex directly afforded analogue **20**.

Scheme 7 was used to prepare compound **23**. The previously described acid **38c** was first reduced to alcohol **50**, and then converted into boronic pinacol ester **51** by reacting with bis(pinacolato)diboron (Pin_2B_2)-mediated by $Pd(dppf)_2Cl_2$ and potassium acetate under anhydrous and heated conditions. Suzuki coupling of **51** with commercially available 2-chloro-5-(methylsulfonyl)pyridine under palladium-mediated reaction conditions furnished analogue **23**.

CONCLUSIONS

In summary, we described a series of gut-restricted, selective COX-2 inhibitors with a central pyridine core as a common structural feature. These compounds were characterized by high colonic exposure and minimized systemic exposure mediated by attenuated permeability and clearance through a glucuronidation pathway via UGT1A9. By establishing short-term ex vivo ^{18}F-FDG uptake attenuation in an acute setting as an indirect, surrogate readout to predict efficacy, we evaluated a subset of analogues in long-term in vivo chemopreventive studies in $APC^{min/+}$ mouse models. Compounds **10**, **21**, and **22** showed dose-dependent suppression of adenoma formation and growth as well as extension of survival. Unexpectedly, in vitro potent analogues such as compounds **11** and **23** showed much weaker in vivo efficacy in terms of the polyp area and multiplicity inhibition. An IVIVC demonstrated that in vivo efficacy was not driven by local gut COX-2 inhibition. Rather, efficacy was consistent with residual systemic COX-2-driven inhibition, which may explain why none of these locally targeted inhibitors demonstrated superior in vivo effects for inhibiting adenoma progression relative to celecoxib in $APC^{min/+}$ mice. Our results could not rule out that gut COX-1- or COX-independent mechanisms alternatively play a significant role in driving adenoma growth inhibition, which warrants further investigation.

EXPERIMENTAL SECTION

Chemistry. All commercial reagents and anhydrous solvents were purchased and used without further purification, unless otherwise specified. Mass spectra (MS) were obtained on a SHIMADZU LCMS-2020 MSD or an Agilent 1200\G6110A MSD instrument using electrospray ionization (ESI) in positive mode unless otherwise indicated. Calculated (calcd) mass corresponds to the exact mass. Nuclear magnetic resonance (NMR) spectra were obtained on a Bruker model AVIII 300 MHz or 400 MHz spectrometer. Definitions for multiplicity are as follows: s = singlet, d = doublet, t = triplet, q = quartet, dd = doublet of doublets, ddd = doublet of doublet of doublets, td = triplet of doublets, dq = doublet of quartet, dt = doublet of triplets, spt = septet, quin = quintet, m = multiplet, and br = broad. ^{1}H NMR chemical shifts are expressed in parts per million (δ) downfield from tetramethylsilane as a standard. Normal-phase silica gel chromatography (FCC) was performed on silica gel (SiO_2) using prepacked cartridges. All compounds sent for biological tests were confirmed with purity >95% in quantitative HPLC analysis [method: Gilson GX-281-RP-HPLC with Phenomenex Gemini C18 (10 μm, 150 × 25 mm), or Waters XBridge C18 column (5 μm, 150 × 30 mm), the mobile phase of 5−99% MeCN in water (10 mM NH_4HCO_3) over 10 min, and then held at 100% MeCN for 2 min, at a flow rate of 25 mL/min] or elemental analysis in addition to LCMS and ^{1}H NMR. Celecoxib (**1**), etoricoxib (**3**), and compound **4** were purchased from Combi-Blocks, Inc (San Diego), Carbosynth Ltd (UK), and Aurora Fine Chemicals LLC (San Diego), respectively.

Preparation of 2,6-Dichloro-*N*-methoxy-*N*-methylnicotinamide (31). To a mixture of 2,6-dichloronicotinic acid (30 g, 156 mmol) and DMF (1 mL) in $CHCl_3$ (300 mL) under nitrogen at 0 °C was added $SOCl_2$ (55.8 g, 469 mmol). The reaction mixture was then heated and stirred at 60 °C for 1 h. The mixture was cooled to room temperature and concentrated to give crude 2,6-dichloronicotinoyl chloride as a gum (35 g), which was used directly in the next step.

To the solution of crude 2,6-dichloronicotinoyl chloride (35 g) in DCM (300 mL) at 0 °C were added triethylamine (50.9 g, 499 mmol) and *N*,*O*-dimethylhydroxylamine hydrochloride (19.5 g, 200 mmol). The reaction mixture was stirred at room temperature for 2 h. The reaction was quenched by the addition of water (300 mL). The mixture was extracted with DCM (2 × 100 mL). The combined organic extract was washed with brine (300 mL), dried over anhydrous Na_2SO_4, filtered, and concentrated. The crude product (44 g) was recrystallized in ethyl acetate and petroleum ether (1:5) to give the title compound as a white solid (35 g, 95% yield). LCMS (ESI): mass calcd for $C_8H_8Cl_2N_2O_2$, 234.0; *m*/*z* found, 235.0 $[M + H]^+$.

Preparation of 2-Chloro-6-(2-hydroxy-2-methylpropoxy)-*N*-methoxy-*N*-methylnicotinamide (32). To a solution of 2-methylpropane-1,2-diol (12.7 g, 140 mmol) in anhydrous DMF (200 mL) at 0 °C was added potassium *tert*-butoxide (17.2 g, 153 mmol) under nitrogen. The mixture was stirred for 0.5 h, and then 2,6-dichloro-*N*-methoxy-*N*-methylnicotinamide (30 g, 128 mmol) was added. The reaction mixture was heated and stirred at 60 °C overnight. The mixture was cooled to room temperature, quenched with water (200 mL), and then extracted with ethyl acetate (2 × 200 mL). The combined organic extract was washed with brine (200 mL), dried over anhydrous Na_2SO_4, filtered, and concentrated. The residue was purified by flash chromatography (50% ethyl acetate in petroleum ether as the eluent) to give the title compound as a white solid (24.5 g, 67% yield). LCMS (ESI): mass calcd for $C_{12}H_{16}BrClN_2O_4$, 288.1; *m*/*z* found, 289.1 $[M + H]^+$.

Preparation of 5-Bromo-2-chloro-6-(2-hydroxy-2-methylpropoxy)-*N*-methoxy-*N*-methylnicotinamide (33). To a solution of 2-chloro-6-(2-hydroxy-2-methylpropoxy)-*N*-methoxy-*N*-methylnicotinamide (12 g, 41.6 mmol) in glacial acetic acid (120 mL) was added sodium acetate (6.98 g, 83.1 mmol), followed by the dropwise addition of bromine (6.66 mL, 129 mmol). The reaction mixture was heated and stirred at 80 °C overnight. The mixture was cooled to room temperature, quenched with water (400 mL), and then extracted with ethyl acetate (2 × 400 mL). The combined organic extract was washed with brine (2 × 400 mL), dried over anhydrous Na_2SO_4, and concentrated. The residue was purified by flash chromatography (50% ethyl acetate in petroleum ether as the eluent) to give the title compound as a white solid (7.5 g, 49% yield). LCMS (ESI): mass calcd for $C_{12}H_{17}ClN_2O_4$, 366.0; *m*/*z* found, 367.0 $[M + H]^+$.

Preparation of 1-((3-Bromo-6-chloro-5-(hydroxymethyl)-pyridin-2-yl)oxy)-2-methylpropan-2-ol (34). To a solution of 5-bromo-2-chloro-6-(2-hydroxy-2-methylpropoxy)-*N*-methoxy-*N*-methylnicotinamide (27 g, 70.7 mmol) in MeOH (200 mL) at 0 °C was added $NaBH_4$ (16.1 g, 424 mmol). The resulting reaction mixture was stirred at room temperature for 2 h. The mixture was concentrated

https://doi.org/10.1021/acs.jmedchem.1c00890
J. Med. Chem. 2021, 64, 11570−11596

under reduced pressure, and water was added. The resulting mixture was extracted with ethyl acetate (2 × 200 mL). The combined organic extract was washed with brine (100 mL), dried over anhydrous Na_2SO_4, and concentrated to give the crude product as a gum (22 g, 100% yield), which was used directly into the next step. LCMS (ESI): mass calcd for $C_{10}H_{13}BrClNO_3$, 309.0; m/z found, 310.0 $[M + H]^+$.

Preparation of 1-((6-Chloro-5-(hydroxymethyl)-3-(4-(methylsulfonyl)phenyl)pyridin-2-yl)oxy)-2-methylpropan-2-ol (35). To a mixture of crude 1-(3-bromo-6-chloro-5-(hydroxymethyl)pyridin-2-yloxy)-2-methylpropan-2-ol (**34**, 5 g, 16.1 mmol), 4-(methylsulfonyl)phenylboronic acid (3.86 g, 19.3 mmol), and aqueous Na_2CO_3 (2.0 M, 16.1 mL, 32 mmol) in 1,4-dioxane (40 mL) was added $Pd(dppf)Cl_2$ (1.18 g, 1.61 mmol) under nitrogen. The reaction mixture was heated with stirring at 60 °C for 3 h. The mixture was cooled to room temperature, quenched with water (40 mL), and extracted with ethyl acetate (2 × 80 mL). The combined organic extract was washed with brine (40 mL), dried over anhydrous Na_2SO_4, and concentrated. The residue was purified by flash chromatography (50% ethyl acetate in petroleum ether as the eluent) to give the title compound as a yellow solid (5 g, 80% yield). LCMS (ESI): mass calcd for $C_{17}H_{20}ClNO_5S$, 385.1; m/z found, 386.2 $[M + H]^+$; ^1H NMR (300 MHz, DMSO-d_6): δ 8.01 (d, J = 8.7 Hz, 2H), 7.98 (s, 1H), 7.92 (d, J = 8.7 Hz, 2H), 4.54 (s, 2H), 4.10 (s, 2H), 3.84 (br s, 2H), 3.25 (s, 3H), 1.15 (s, 6H) ppm.

Preparation of 1-((5-(Hydroxymethyl)-6-methoxy-3-(4-(methylsulfonyl)phenyl)pyridin-2-yl)oxy)-2-methylpropan-2-ol (8). To a solution of anhydrous methanol (1.25 g, 38.9 mmol) in DMF (30 mL) at 0 °C was added NaH (60%, 1.56 g, 38.9 mmol). The mixture was stirred for 0.5 h, and then 1-((6-chloro-5-(hydroxymethyl)-3-(4-(methylsulfonyl)phenyl)pyridin-2-yl)oxy)-2-methylpropan-2-ol (1.5 g, 3.89 mmol) was added. The reaction mixture was stirred at room temperature overnight. The mixture was quenched with water (40 mL), and then extracted with ethyl acetate (2 × 50 mL). The combined organic extract was washed with brine (2 × 60 mL), dried over anhydrous Na_2SO_4, filtered, and concentrated. The residue was purified by flash chromatography (60% ethyl acetate in petroleum ether as the eluent), and the crude product was further purified by prep-HPLC (10−90% MeCN in water) to give the title compound as a white solid (280 mg, 19% yield). LCMS (ESI): mass calcd. for $C_{18}H_{23}NO_6S$, 381.1; m/z found, 382.2 $[M + H]^+$; ^1H NMR (300 MHz, DMSO-d_6): δ 7.95 (d, J = 8.7 Hz, 2H), 7.89 (d, J = 8.7 Hz, 2H), 7.83 (s, 1H), 5.09 (t, J = 5.7 Hz, 1H), 4.63 (s, 1H), 4.45 (d, J = 5.7 Hz, 2H), 4.16 (s, 2H), 3.94 (s, 3H), 3.25 (s, 3H), 1.17 (s, 6H) ppm.

Preparation of 1-((5-(Hydroxymethyl)-6-(2-methoxyethoxy)-3-(4-(methylsulfonyl)phenyl)pyridin-2-yl)oxy)-2-methylpropan-2-ol (12). To a solution of anhydrous 2-methoxyethanol (2.96 g, 38.9 mmol) in DMF (30 mL) at 0 °C was added NaH (60%, 1.56 g, 38.9 mmol). The mixture was stirred for 0.5 h, and then 1-((6-chloro-5-(hydroxymethyl)-3-(4-(methylsulfonyl)phenyl)pyridin-2-yl)oxy)-2-methylpropan-2-ol (**35**, 1.5 g, 3.89 mmol) was added. The reaction mixture was stirred at room temperature overnight. The mixture was quenched with water (40 mL), and then extracted with ethyl acetate (2 × 50 mL). The combined organic extract was washed with brine (2 × 60 mL), dried over anhydrous Na_2SO_4, filtered, and concentrated. The residue was purified by flash chromatography (60% ethyl acetate in petroleum ether as the eluent), and the crude product was further purified by prep-HPLC (10−90% MeCN in water) to give the title compound as a white solid (100 mg, 19% yield). LCMS (ESI): mass calcd for $C_{20}H_{27}NO_7S$, 425.2; m/z found, 426.1 $[M + H]^+$; ^1H NMR (300 MHz, DMSO-d_6): δ 7.95 (d, J = 8.4 Hz, 2H), 7.89 (d, J = 8.4 Hz, 2H), 7.84 (s, 1H), 5.11 (t, J = 5.7 Hz, 1H), 4.64 (s, 1H), 4.44−4.49 (m, 4H), 4.13 (s, 2H), 3.69−3.72 (m, 2H), 3.33 (s, 3H), 3.26 (s, 3H, s), 1.16 (s, 6H) ppm.

Preparation of 6-Chloro-2-isopropoxynicotinic Acid (36a). To a solution of 2-propanol (2.35 g, 39.1 mmol) in anhydrous THF (150 mL) was added NaH (60%, 2.29 g, 57.3 mmol). The mixture was stirred at 50 °C for 0.5 h, and then 2,6-dichloropyridine-3-carboxylic acid (5 g, 26.0 mmol) was added. The reaction mixture was heated and stirred at 70 °C for 3 h. The mixture was cooled to room temperature, quenched with water (2 L), and concentrated to a small volume. The mixture was acidified to "pH" 1 using aqueous HCl (1 M) and extracted with ethyl acetate (3 × 100 mL). The organic layers were combined, dried over anhydrous Na_2SO_4, and concentrated to give the title compound as a yellow solid (5 g, 89% yield). LCMS (ESI): mass calcd for $C_9H_{10}ClNO_3$, 215.0; m/z found, 216.1 $[M + H]^+$.

Preparation of 6-chloro-2-propoxynicotinic acid (36b). To a solution of 1-propanol (46.4 g, 772 mmol) in anhydrous DMF (2.6 L) at 0 °C was added NaH (60%, 56.6 g, 1415 mmol). The mixture was stirred at 0 °C for 1 h, and then 2,6-dichloropyridine-3-carboxylic acid (130 g, 643 mmol) was added in several portions. The reaction mixture was stirred at room temperature for 30 h. The mixture was quenched with iced water (7.8 L). The mixture was acidified to "pH" 1 using aqueous HCl (1 M). The organic layers were combined, dried over anhydrous Na_2SO_4, The precipitate was collected and dried to give the title compound as a white solid (91 g, 66% yield). LCMS (ESI): mass calcd. for $C_9H_{10}ClNO_3$, 215.0; m/z found, 216.1 $[M+H]^+$.

Preparation of 2-Butoxy-6-chloronicotinic Acid (36c). To a solution of 1-butanol (63.7 g, 859 mmol) in anhydrous DMF (200 mL) at 0 °C was added NaH (60%, 65.6 g, 1.64 mol). The mixture was stirred at 0 °C for 1 h, and then 2,6-dichloropyridine-3-carboxylic acid (10 g, 52 mmol) was added in several batches. The reaction mixture was stirred at room temperature overnight. The mixture was quenched with ice water (2 L). The mixture was acidified to "pH" 5 using aqueous HCl (1 M) and extracted with ethyl acetate (3 × 2 L). The organic layers were combined, dried over anhydrous Na_2SO_4, and concentrated to give the title compound as a white solid (165 g, 89% yield). LCMS (ESI): mass calcd for $C_{10}H_{12}ClNO_3$, 229.1; m/z found, 228.0 $[M-H]^+$.

Preparation of 6-Chloro-2-(3,3,3-trifluoropropoxy)nicotinic Acid (36d). To a solution of 3,3,3-trifluoropropan-1-ol (267 g, 2.34 mol) in anhydrous THF (9 L) was added NaH (60%, 137.5 g, 3.44 mol). The mixture was stirred at room temperature for 1 h, and then 2,6-dichloropyridine-3-carboxylic acid (300 g, 1.56 mmol) was added. The reaction mixture was stirred at room temperature for 48 h. The mixture was quenched with water (5 L), acidified to "pH" 1 using aqueous HCl (1 M), and then extracted with ethyl acetate (3 × 3.5 L). The organic layers were combined, dried over anhydrous Na_2SO_4, and concentrated. The residue was purified by Flash-Prep-HPLC (Column, C-18, mobile phase, water (a)/MeCN (b), b %: 30%−55%, 30 min; detector, UV 210 nm) to give the title compound as a white solid (170 g, 40% yield). LCMS (ESI): mass calcd for $C_9H_7ClF_3NO_3$, 269.0; m/z found, 270.0 $[M + H]^+$.

Preparation of 6-Chloro-2-(4,4,4-trifluorobutoxy)nicotinic Acid (36e). To a solution of 4,4,4-trifluorobutan-1-ol (150 g, 1.17 mol) in anhydrous THF (4.5 L) was added NaH (60%, 68.7 g, 1.72 mol). The mixture was stirred at 50 °C for 0.5 h, and then 2,6-dichloropyridine-3-carboxylic acid (150 g, 0.781 mol) was added. The reaction mixture was heated and stirred at 70 °C for 3 h. The mixture was cooled to room temperature, quenched with water (2 L), acidified to "pH" 1 with aqueous HCl (1 M), and then extracted with ethyl acetate (3 × 2 L). The organic layers were combined, dried over anhydrous Na_2SO_4, and concentrated to give the title compound as a white solid (156 g, 70% yield). LCMS (ESI): mass calcd for $C_{10}H_9ClF_3NO_3$, 283.0; m/z found, 284.1 $[M + H]^+$.

Preparation of 6-(2-Hydroxy-2-methylpropoxy)-2-isopropoxynicotinic Acid (37a). To a mixture of 6-chloro-2-(propan-2-yloxy)pyridine-3-carboxylic acid (**36a**, 5 g, 23.2 mmol), Cs_2CO_3 (18.9 g, 57.8 mmol), and 2-methylpropane-1,2-diol (4.18 g, 46.4 mmol) in toluene (150 mL) under nitrogen was added XPhos Pd G3 (196 mg, 0.23 mmol). The reaction mixture was heated and stirred at 90 °C overnight. The mixture was cooled to room temperature and then quenched with water (200 mL). The organic layer was separated, and the "pH" of the aqueous layer was adjusted to 1 with aqueous HCl (1 M). The aqueous solution was extracted with ethyl acetate (3 × 150 mL). The organic layers were combined, dried over anhydrous Na_2SO_4, and concentrated to give the title compound as a white solid (5.5 g, 88% yield). LCMS (ESI): mass calcd for $C_{13}H_{19}NO_5$, 269.1; m/z found, 270.1 $[M + H]^+$.

Preparation of 6-(2-Hydroxy-2-methylpropoxy)-2-propoxynicotinic Acid (37b). To a mixture of 6-chloro-2-propoxynicotinic acid (**36b**, 91 g, 422 mmol), Cs_2CO_3 (344 g, 1055 mmol), and 2-

https://doi.org/10.1021/acs.jmedchem.1c00890
J. Med. Chem. 2021, 64, 11570−11596

methylpropane-1,2-diol (57.0 g, 633 mmol) in toluene (270 mL) under nitrogen was added XPhos Pd G3 (7.1 g, 8.74 mmol). The reaction mixture was heated and stirred at 90 °C overnight. The mixture was cooled to room temperature and then quenched with water. The organic layer was separated, and the "pH" of the aqueous layer was adjusted to 1 with aqueous HCl (1 M). The aqueous solution was extracted with ethyl acetate. The organic layers were combined, dried over anhydrous Na_2SO_4, and concentrated to give the title compound as a brown oil (100 g, 88% yield). LCMS (ESI): mass calcd for $C_{13}H_{19}NO_5$, 269.1; *m/z* found, 270.2 $[M + H]^+$.

Preparation of 2-Butoxy-6-(2-hydroxy-2-methylpropoxy)-nicotinic Acid (37c). To a mixture of 2-butoxy-6-chloronicotinic acid (**36c**, 5 g, 21.4 mmol), Cs_2CO_3 (27.9 g, 85.4 mmol), and 2-methylpropane-1,2-diol (4.8 g, 53.4 mmol) in toluene (150 mL) under nitrogen were added dicyclohexyl(2′,6′-dimethoxybiphenyl-2-yl)-phosphine (876 mg, 2.1 mmol) and $Pd(OAc)_2$ (1.03 g, 4.3 mmol). The reaction mixture was heated and stirred at 90 °C overnight. The mixture was cooled to room temperature and then quenched with water (500 mL). The mixture was filtered through a short celite pad, and the filtrate was extracted with ethyl acetate (200 mL). The "pH" of the aqueous layer was adjusted to 1 using aqueous HCl (1 M), and then extracted with ethyl acetate (2 × 200 mL). The organic layers were combined, dried over anhydrous Na_2SO_4, and concentrated to give the title compound as a light yellow oil (5 g, 60% yield). LCMS (ESI): mass calcd for $C_{14}H_{21}NO_5$, 283.1; *m/z* found, 282.2 $[M - H]^+$.

Preparation of 6-(2-Hydroxy-2-methylpropoxy)-2-(3,3,3-trifluoropropoxy)nicotinic Acid (37d). To a mixture of 6-chloro-2-(3,3,3-trifluoropropoxy)nicotinic acid (**36d**, 130 g, 482 mmol), Cs_2CO_3 (393 g, 1210 mmol), and 2-methylpropane-1,2-diol (86.9 g, 964 mmol) in toluene (3.9 L) under nitrogen was added XPhos Pd G3 (4.08 g, 4.82 mmol). The reaction mixture was heated and stirred at 90 °C overnight. The mixture was cooled to room temperature and then quenched with water (3 L). The mixture was extracted with ethyl ether (1 L). The organic layer was separated, and the "pH" of the aqueous layer was adjusted to 1 with aqueous HCl (1 M). The aqueous solution was extracted with ethyl acetate (2 × 2 L). The organic layers were combined, washed with brine (2 L), dried over anhydrous Na_2SO_4, and concentrated to give the title compound as a brown oil (130 g, 83% yield). LCMS (ESI): mass calcd for $C_{13}H_{16}F_3NO_5$, 323.1; *m/z* found, 324.1 $[M + H]^+$.

Preparation of 6-(2-Hydroxy-2-methylpropoxy)-2-(4,4,4-trifluorobutoxy)nicotinic Acid (37e). To a mixture of 6-chloro-2-(4,4,4-trifluorobutoxy)nicotinic acid (**36e**, 156 g, 550 mmol), Cs_2CO_3 (448 g, 1375 mmol), and 2-methylpropane-1,2-diol (99 g, 1100 mmol) in toluene (4.68 L) under nitrogen was added XPhos Pd G3 (4.6 g, 5.5 mmol). The reaction mixture was heated and stirred at 90 °C overnight. The mixture was cooled to room temperature and then quenched with water (3 L). The organic layer was separated, and the "pH" of the aqueous layer was adjusted to 1 with aqueous HCl (1 M). The aqueous solution was extracted with ethyl acetate (3 × 1 L). The organic layers were combined, dried over anhydrous Na_2SO_4, and concentrated to give the title compound as a yellow solid (130 g, 83% yield). LCMS (ESI): mass calcd for $C_{14}H_{18}F_3NO_5$, 337.1; *m/z* found, 338.2 $[M + H]^+$.

Preparation of 5-Bromo-6-(2-hydroxy-2-methylpropoxy)-2-isopropoxynicotinic Acid (38a). To a solution of 6-(2-hydroxy-2-methylpropoxy)-2-isopropoxynicotinic acid (**37a**, 5.5 g, 20.4 mmol) and acetic acid (6.13 g, 102 mmol) in acetonitrile (55 mL) was added NBS (4.36 g, 74.1 mmol). The reaction mixture was stirred at room temperature for 2 h, quenched by the addition of water (50 mL), and then extracted with ethyl acetate (3 × 100 mL). The organic layers were combined, dried over Na_2SO_4, and concentrated. The residue was recrystallized in acetonitrile to give the title compound as a white solid (3.3 g, 46% yield). LCMS (ESI): mass calcd for $C_{13}H_{18}BrNO_5$, 347.0; *m/z* found, 348.1 $[M + H]^+$.

Preparation of 5-Bromo-6-(2-hydroxy-2-methylpropoxy)-2-propoxynicotinic Acid (38b). To a solution of 5-bromo-6-(2-hydroxy-2-methylpropoxy)-2-propoxynicotinic acid (**37b**, 109 g, 340 mmol) in acetonitrile (2.7 L) was added NBS (72.9 g, 410 mmol). The reaction mixture was stirred at room temperature for 3 h. The mixture was concentrated and the residue was purified by flash chromatography (5% MeOH in DCM) to give the title compound as a white solid (119 g, 92% yield). LCMS (ESI): mass calcd for $C_{13}H_{18}BrNO_5$, 347.0; *m/z* found, 348.1 $[M + H]^+$.

Preparation of 5-Bromo-2-butoxy-6-(2-hydroxy-2-methylpropoxy)nicotinic Acid (38c). To a solution of 2-butoxy-6-(2-hydroxy-2-methylpropoxy)nicotinic acid (**37c**, 5.1 g, 14.1 mmol) in acetonitrile (130 mL) was added NBS (2.8 g, 15.5 mmol). The reaction mixture was stirred at room temperature for 2 h. Water was added (500 mL). The precipitate was collected by filtration and dried in vacuo to give the title compound as a white solid (4.5 g, 72% yield). LCMS (ESI): mass calcd for $C_{14}H_{20}BrNO_5$, 361.1; *m/z* found, 362.2 $[M + H]^+$.

Preparation of 5-Bromo-6-(2-hydroxy-2-methylpropoxy)-2-(3,3,3-trifluoropropoxy)nicotinic Acid (38d). To a solution of 6-(2-hydroxy-2-methylpropoxy)-2-(3,3,3-trifluoropropoxy)nicotinic acid (**37d**, 130 g, 402 mmol) and acetic acid (120.7 g, 2.01 mol) in acetonitrile (1.3 L) was added NBS (78.7 g, 442 mmol). The reaction mixture was stirred at room temperature for 2 h. The precipitate was collected by filtration, washed with cold acetonitrile (200 mL) and water (1 L), and then dried in vacuo to give the title compound as a white solid (116 g, 72% yield). LCMS (ESI): mass calcd for $C_{13}H_{15}BrF_3NO_5$, 401.0; *m/z* found, 402.0 $[M + H]^+$.

Preparation of 5-Bromo-6-(2-hydroxy-2-methylpropoxy)-2-(4,4,4-trifluorobutoxy)nicotinic Acid (38e). To a solution of 6-(2-hydroxy-2-methylpropoxy)-2-(4,4,4-trifluoro-butoxy)nicotinic acid (**37e**, 180 g, 533 mmol) and acetic acid (160 g, 2.67 mol) in acetonitrile (1.8 L) was added NBS (114 g, 640 mmol). The reaction mixture was stirred at room temperature for 2 h, and then quenched with water (1.5 L). The mixture was concentrated to half of its volume under reduced pressure. The precipitate was collected by filtration and recrystallized in acetonitrile to give the title compound as a yellow solid (140 g, 63% yield). LCMS (ESI): mass calcd for $C_{14}H_{17}BrF_3NO_5$, 415.0; *m/z* found, 416.1 $[M + H]^+$.

Preparation of 6-(2-Hydroxy-2-methylpropoxy)-2-isopropoxy-5-(4-(methylsulfonyl)phenyl)nicotinic Acid (39a). To a mixture of 5-bromo-6-(2-hydroxy-2-methylpropoxy)-2-isopropoxynicotinic acid (**38a**, 1 g, 2.87 mmol), 4-(methylsulfonyl)phenylboronic acid (689 mg, 3.44 mmol), and aqueous Na_2CO_3 (2.0 M, 5.7 mL, 11.4 mmol) in 1,4-dioxane (8 mL) was added $Pd(dppf)Cl_2$ (210 mg, 0.29 mmol) under nitrogen. The reaction mixture was heated with stirring at 80 °C for 3 h. The mixture was cooled to room temperature and quenched with water (20 mL). The mixture was acidified to "pH" 1 with aqueous HCl solution (1 M) and then extracted with ethyl acetate (2 × 50 mL). The combined organic extract was washed with brine (40 mL), dried over anhydrous Na_2SO_4, and concentrated. The residue was purified by reverse-phase Combi-Flash chromatography (column, C18; eluent, 25−55% MeCN in water; time, 30 min) to give the title compound as a yellow solid (0.8 g, 66% yield). LCMS (ESI): mass calcd for $C_{20}H_{25}NO_7S$, 423.1; *m/z* found, 424.2 $[M + H]^+$.

Preparation of 6-(2-Hydroxy-2-methylpropoxy)-5-(4-(methylsulfonyl)phenyl)-2-propoxynicotinic Acid (39b). To a mixture of 5-bromo-2-butoxy-6-((1-hydroxycyclobutyl)methoxy)-nicotinic acid (**38b**, 115 g, 342 mmol), 4-(methylsulfonyl)-phenylboronic acid (82 g, 410 mmol), and aqueous Na_2CO_3 (2.0 M, 513 mL, 1.03 mol) in 1,4-dioxane (1.2 L) was added $Pd(dppf)Cl_2$ (25 g, 34.2 mmol) under nitrogen. The reaction mixture was heated with stirring at 100 °C for 2 h. The mixture was cooled to room temperature and quenched with water. The mixture was acidified to "pH" 1 with aqueous HCl solution (1 M) and then extracted with a mixture of ethyl acetate and THF (1:1). The combined organic extract was washed with brine, dried over anhydrous Na_2SO_4, and concentrated. The residue was purified by flash chromatography (4% MeOH in DCM as the eluent) to give the title compound as a light yellow solid (70 g, 48% yield). LCMS (ESI): mass calcd for $C_{20}H_{25}NO_7S$, 423.1; *m/z* found, 424.2 $[M + H]^+$; ^1H NMR (300 MHz, $CDCl_3$): δ 8.48 (s, 1H), 8.02 (d, J = 8.4 Hz, 2H), 7.78 (d, J = 8.4 Hz, 2H), 4.61 (d, J = 6.6 Hz, 2H), 4.30 (s, 2H), 3.13 (s, 3H), 1.91−2.01 (m, 2H), 1.33 (s, 6H), 1.13 (t, J = 7.5 Hz, 6H) ppm.

https://doi.org/10.1021/acs.jmedchem.1c00890
J. Med. Chem. 2021, 64, 11570−11596

Preparation of 2-Butoxy-6-(2-hydroxy-2-methylpropoxy)-5-(4-(methylsulfonyl)phenyl)nicotinic Acid (39c). To a mixture of 5-bromo-2-butoxy-6-(2-hydroxy-2-methylpropoxy)nicotinic acid (**38c**, 2 g, 4.5 mmol), 4-(methylsulfonyl)phenylboronic acid (1.2 g, 5.9 mmol), and K_2CO_3 (2.8 g, 20.4 mmol) in 1,4-dioxane (40 mL) and water (4 mL) was added $Pd(Ph_3P)_4$ (524 mg, 0.45 mmol) under nitrogen. The reaction mixture was heated with stirring at 80 °C overnight. The mixture was cooled to room temperature and quenched with water. The mixture was acidified to "pH" 1 using aqueous HCl solution (1 M) and then extracted with ethyl acetate (3 × 90 mL). The combined organic extract was washed with brine, dried over anhydrous Na_2SO_4, and concentrated. The residue was purified by flash chromatography (3−10% MeOH in DCM as the eluent) to give the title compound as a white solid (1.2 g, 52% yield). LCMS (ESI): mass calcd for $C_{21}H_{27}NO_7S$, 437.2; *m/z* found, 438.1 $[M + H]^+$; ^1H NMR (300 MHz, $CDCl_3$): δ 8.48 (s, 1H), 8.02 (d, *J* = 8.4 Hz, 2H), 7.78 (d, *J* = 8.4 Hz, 2H), 4.65 (d, *J* = 6.6 Hz, 2H), 4.30 (s, 2H), 3.13 (s, 3H), 1.88−2.02 (m, 2H), 1.49−1.60 (m, 2H), 1.33 (s, 6H), 1.05 (t, *J* = 7.5 Hz, 6H) ppm.

Preparation of 6-(2-Hydroxy-2-methylpropoxy)-5-(4-(methylsulfonyl)phenyl)-2-(3,3,3-trifluoropropoxy)nicotinic Acid (39d). To a mixture of 5-bromo-6-(2-hydroxy-2-methylpropoxy)-2-(3,3,3-trifluoropropoxy) nicotinic acid (**38d**, 116 g, 288 mmol), 4-(methylsulfonyl)phenylboronic acid (86.5 g, 433 mmol), and Na_2CO_3 (91.7 g, 865 mmol) in 1,4-dioxane (928 mL) and water (232 mL) was added $Pd(dppf)Cl_2$ (21.1 g, 28.8 mmol) under nitrogen. The reaction mixture was heated with stirring at 100 °C for 5 h. The mixture was cooled to room temperature and quenched with water. The mixture was acidified to "pH" 1 using aqueous HCl solution (1 M) and then extracted with ethyl acetate (2 × 1 L). The combined organic extract was washed with brine, dried over anhydrous Na_2SO_4, and concentrated. The residue was purified by reverse-phase prep-HPLC (column, C18; eluent, 25−55% MeCN in water; time, 30 min; detector, UV 210 nm) to give the title compound as a white solid (100 g, 73% yield). LCMS (ESI): mass calcd for $C_{20}H_{22}F_3NO_7S$, 477.1; *m/z* found, 478.2 $[M + H]^+$.

Preparation of 6-(2-Hydroxy-2-methylpropoxy)-5-(4-(methylsulfonyl)phenyl)-2-(4,4,4-trifluorobutoxy)nicotinic Acid (39e). To a mixture of 5-bromo-6-(2-hydroxy-2-methylpropoxy)-2-(4,4,4-trifluorobutoxy)nicotinic acid (**38e**, 140 g, 336 mmol), 4-(methylsulfonyl)phenylboronic acid (80.7 g, 404 mmol), and aqueous Na_2CO_3 (2 M, 504 mL, 1.0 mol) in 1,4-dioxane (1.4 L) was added $Pd(dppf)Cl_2$ (24.6 g, 33.6 mmol) under nitrogen. The reaction mixture was heated with stirring at 100 °C for 1 h. The mixture was cooled to room temperature and quenched with water. The mixture was acidified to "pH" 1 using aqueous HCl solution (1 M) and then extracted with ethyl acetate (3 × 1 L). The combined organic extract was washed with brine, dried over anhydrous Na_2SO_4, and concentrated. The residue was purified by reverse-phase Combi-Flash (column, C18; eluent, 25−55% MeCN in water) to give the title compound as a white solid (90 g, 54% yield). LCMS (ESI): mass calcd for $C_{21}H_{24}F_3NO_7S$, 491.1; *m/z* found, 492.2 $[M + H]^+$.

Preparation of 1-((5-(Hydroxymethyl)-6-isopropoxy-3-(4-(methylsulfonyl)phenyl)pyridin-2-yl)oxy)-2-methylpropan-2-ol (9). To a solution of 6-(2-hydroxy-2-methylpropoxy)-2-isopropoxy-5-(4-(methylsulfonyl)phenyl)nicotinic acid (**39a**, 0.8 g, 1.89 mmol) in anhydrous THF (24 mL) at 0 °C was added a THF solution (1 M) of BH_3·THF (5.7 mL, 5.7 mmol). The reaction mixture was stirred at room temperature for 1 h. The mixture was quenched with MeOH (5 mL) and brine (10 mL), and the organic layer was separated. The aqueous layer was extracted with ethyl acetate (3 × 30 mL). The combined organic extract was washed with brine (2 × 30 mL), dried over anhydrous Na_2SO_4, filtered, and concentrated. The residue was purified by reverse-phase Combi-Flash (column, C18; eluent, 25−60% MeCN in water) to give the title compound as a white solid (435 mg, 56% yield). LCMS (ESI): mass calcd for $C_{20}H_{27}NO_6S$, 409.2; *m/z* found, 410.1 $[M + H]^+$; ^1H NMR (300 MHz, DMSO-d_6): δ 7.95 (d, *J* = 8.7 Hz, 2H), 7.88 (d, *J* = 8.7 Hz, 2H), 7.82 (s, 1H), 5.27 (sept, *J* = 6.3 Hz, 1H), 5.05 (t, *J* = 5.7 Hz, 1H), 4.63 (s, 1H), 4.42 (d, *J* = 5.7 Hz, 2H), 4.11 (s, 2H), 3.25 (s, 3H), 1.34 (d, *J* = 6.3 Hz, 6H), 1.17 (s, 6H) ppm.

Preparation of 1-((5-(Hydroxymethyl)-3-(4-(methylsulfonyl)phenyl)-6-propoxypyridin-2-yl)oxy)-2-methylpropan-2-ol (10). To a solution of 6-(2-hydroxy-2-methylpropoxy)-5-(4-(methylsulfonyl)phenyl)-2-propoxynicotinic acid (**39b**, 72.8 g, 163 mmol) in anhydrous THF (1.4 L) at 0 °C was added a THF solution (1 M) of BH_3·THF (653 mL, 653 mmol). The reaction mixture was stirred at room temperature for 3 h. MeOH (1 L) and SiliaMrtS DMT (7 g) were added. The mixture was stirred at room temperature for 12 h, filtered, and concentrated. The residue was purified by reverse-phase Combi-Flash (column, C18; eluent, 25−55% MeCN in water; time, 40 min), followed by recrystallization in acetonitrile to give the title compound as a white solid (45.1 g, 67% yield). LCMS (ESI): mass calcd for $C_{20}H_{27}NO_6S$, 409.2; *m/z* found, 410.2 $[M + H]^+$; ^1H NMR (400 MHz, DMSO-d_6): δ 7.95 (d, *J* = 8.8 Hz, 2H), 7.88 (d, *J* = 8.8 Hz, 2H), 7.83 (s, 1H), 5.07 (t, *J* = 5.6 Hz, 1H), 4.62 (s, 1H), 4.46 (d, *J* = 5.6 Hz, 2H), 4.31 (t, *J* = 6.6 Hz, 2H), 4.13 (s, 2H), 3.25 (s, 3H), 1.79−1.74 (m, 2H), 1.17 (s, 6H), 0.99 (t, *J* = 7.6 Hz, 3H) ppm; Anal. Calcd for $C_{20}H_{27}NO_6S$: C, 58.66; H, 6.65; N, 3.42. Found: C, 58.63; H, 6.68; N, 3.37; Pd level < 1 ppm.

Preparation of 1-((5-(Hydroxymethyl)-3-(4-(methylsulfonyl)phenyl)-6-propoxypyridin-2-yl)oxy)-2-methylpropan-2-ol (11). To a solution of 2-butoxy-6-(2-hydroxy-2-methylpropoxy)-5-(4-(methylsulfonyl)phenyl)nicotinic acid (**39c**, 1.2 g, 2.74 mmol) in anhydrous THF (24 mL) at 0 °C was added a THF solution (1 M) of BH_3·THF (7.05 mL, 7.05 mmol). The reaction mixture was stirred at room temperature for 2 h. The mixture was quenched with MeOH (10 mL) and water (60 mL), and the organic layer was separated. The aqueous layer was extracted with ethyl acetate (3 × 30 mL). The combined organic extract was washed with saturated aqueous $NaHCO_3$ (30 mL), brine (30 mL), dried over anhydrous Na_2SO_4, filtered, and concentrated. The residue was recrystallized in acetonitrile to give the title compound as a white solid (860 mg, 74% yield). LCMS (ESI): mass calcd for $C_{21}H_{29}NO_6S$, 423.2; *m/z* found, 424.2 $[M + H]^+$; ^1H NMR (300 MHz, DMSO-d_6): δ 7.95 (d, *J* = 8.7 Hz, 2H), 7.88 (d, *J* = 8.7 Hz, 2H), 7.82 (s, 1H), 5.08 (t, *J* = 5.7 Hz, 1H), 4.63 (s, 1H), 4.45 (d, *J* = 5.4 Hz, 2H), 4.36 (t, *J* = 6.6 Hz, 2H), 4.13 (s, 2H), 3.25 (s, 3H), 1.68−1.78 (m, 2H), 1.40−1.50 (m, 2H), 1.16 (s, 6H), 0.99 (t, *J* = 7.5 Hz, 3H) ppm; Anal. Calcd for $C_{21}H_{29}NO_6S$: C, 59.56; H, 6.90; N, 3.31. Found: C, 59.54; H, 7.04; N, 3.32; Pd level 1 ppm.

Preparation of 1-((5-(Hydroxymethyl)-3-(4-(methylsulfonyl)phenyl)-6-(3,3,3-trifluoropropoxy)pyridin-2-yl)oxy)-2-methylpropan-2-ol (21). To a solution of 6-(2-hydroxy-2-methylpropoxy)-5-(4-(methylsulfonyl)phenyl)-2-(3,3,3-trifluoropropoxy)nicotinic acid (**39d**, 100 g, 209 mmol) in anhydrous THF (3 L) at 0 °C was added a THF solution (1 M) of BH_3·THF (628 mL, 628 mmol). The reaction mixture was stirred at room temperature for 3 h. The mixture was quenched with MeOH (100 mL) and concentrated. The residue was triturated in acetonitrile (500 mL) and water (1 L). The precipitate was collected by filtration, washed with water, and then recrystallized in acetonitrile (200 mL) to give the title compound as a white solid (71.3 g, 73% yield). LCMS (ESI): mass calcd for $C_{20}H_{24}F_3NO_6S$, 463.1; *m/z* found, 464.4 $[M + H]^+$; ^1H NMR (400 MHz, DMSO-d_6): δ 7.96 (d, *J* = 8.4 Hz, 2H), 7.89 (d, *J* = 8.4 Hz, 2H), 7.86 (s, 1H), 5.10 (br s, 1H), 4.61 (s, 1H), 4.60 (t, *J* = 6.0 Hz, 2H), 4.45 (s, 2H), 4.14 (s, 2H), 3.25 (s, 3H), 2.78−2.90 (m, 2H), 1.17 (s, 6H) ppm; ^{19}F NMR (376 MHz, DMSO-d_6): δ −63.05 ppm; Anal. Calcd for $C_{20}H_{24}F_3NO_6S$: C, 51.83; H, 5.22; N, 3.02. Found: C, 51.82; H, 5.24; N, 2.96; Pd level < 5.4 ppm.

Preparation of 1-((5-(Hydroxymethyl)-3-(4-(methylsulfonyl)phenyl)-6-(4,4,4-trifluorobutoxy)pyridin-2-yl)oxy)-2-methylpropan-2-ol (22). To a solution of 6-(2-hydroxy-2-methylpropoxy)-5-(4-(methylsulfonyl)phenyl)-2-(4,4,4-trifluorobutoxy)nicotinic acid (**39e**, 90 g, 183 mmol) in anhydrous THF (2.5 L) at 0 °C was added a THF solution (1 M) of BH_3·THF (550 mL, 550 mmol). The reaction mixture was stirred at room temperature for 3 h. The mixture was slowly quenched with MeOH (500 mL) dropwise and concentrated. The residue was diluted with water (3 L). The precipitate was collected by filtration, washed with water, and then recrystallized in acetonitrile (150 mL) and ethanol (150 mL) to give the title compound as a white solid (62.1 g, 70% yield). LCMS (ESI): mass calcd for $C_{21}H_{26}F_3NO_6S$, 477.1; *m/z* found, 478.1

https://doi.org/10.1021/acs.jmedchem.1c00890
J. Med. Chem. 2021, 64, 11570−11596

$[M + H]^+$; ^{1}H NMR (400 MHz, DMSO-d_6): δ 7.95 (d, J = 8.4 Hz, 2H), 7.89 (d, J = 8.4 Hz, 2H), 7.84 (s, 1H), 5.06 (t, J = 5.6 Hz, 1H), 4.60 (s, 1H), 4.46 (d, J = 5.6 Hz, 2H), 4.31 (t, J = 6.4 Hz, 2H), 4.13 (s, 2H), 3.25 (s, 3H), 2.41−2.46 (m, 2H), 1.95−2.02 (m, 2H), 1.16 (s, 6H) ppm; ^{19}F NMR (376 MHz, DMSO-d_6): δ −64.70 ppm; Anal. Calcd for $C_{21}H_{26}F_3NO_6S$: C, 52.82; H, 5.49; N, 2.93. Found: C, 52.76; H, 5.50; N, 2.89; Pd level < 4.1 ppm.

Preparation of 2-Butoxy-6-(2-hydroxy-2-methylpropoxy)-5-(4-(methylsulfonyl)phenyl)nicotinaldehyde (40). To a solution of 1-[[6-butoxy-5-(hydroxymethyl)-3-(4-methanesulfonylphenyl)-pyridin-2-yl]oxy]-2-methylpropan-2-ol (**11**, 860 mg, 2.03 mmol) in dichloromethane (20 mL) at 0 °C was added Dess−Martin periodinane (2.34 g, 5.52 mmol) in several batches. The resulting reaction mixture was stirred at room temperature overnight. The reaction was then quenched by aqueous $KHCO_3$ solution (60 mL). The resulting solution was extracted with ethyl acetate (3 × 30 mL). The combined organic extract was washed with brine (30 mL), dried over anhydrous Na_2SO_4, filtered, and concentrated. The residue was purified by chromatography (33% ethyl acetate in petroleum ether as the eluent) to give the title compound as a white solid (810 mg, 95% yield). LCMS (ESI): mass calcd for $C_{21}H_{27}NO_6S$, 421.2; m/z found, 422.3 $[M + H]^+$.

Preparation of 1-((6-Butoxy-5-(1-hydroxyethyl)-3-(4-(methylsulfonyl)phenyl)pyridin-2-yl)oxy)-2-methylpropan-2-ol (13). To a solution of 2-butoxy-6-(2-hydroxy-2-methylpropoxy)-5-(4-(methylsulfonyl)phenyl)nicotinaldehyde (**40**, 810 mg, 1.83 mmol) in anhydrous THF (20 mL) at 0 °C was added a THF solution (3 M) of methylmagnesium chloride (1.8 mL, 5.4 mmol). The reaction mixture was stirred at 0 °C for 2 h. The reaction was then quenched by aqueous saturated NH_4Cl solution (40 mL). The resulting solution was extracted with ethyl acetate (3 × 20 mL). The combined organic extract was washed with brine (40 mL), dried over anhydrous Na_2SO_4, filtered, and concentrated. The residue was purified by reverse-phase prep-HPLC [Column, XBridge Prep C18 OBD 19 × 150 mm 5 μm C-0013; mobile phase, phase A: water(0.1% NH_4HCO_3+0.1%$NH_3.H_2O$), phase B: MeCN from 43 to 54; detector, 254 nm] to give the title compound as a white solid (423 mg, 53% yield). LCMS (ESI): mass calcd for $C_{22}H_{31}NO_6S$, 437.2; m/z found, 438.1 $[M + H]^+$; ^{1}H NMR (300 MHz, DMSO-d_6): δ 7.96 (d, J = 8.4 Hz, 2H), 7.87 (d, J = 8.4 Hz, 2H), 7.86 (s, 1H), 5.12 (d, J = 4.2 Hz, 1H), 4.84−4.90 (m, 1H), 4.62 (s, 1H), 4.36 (dq, J = 4.2, 6.6 Hz, 2H), 4.13 (s, 2H), 3.25 (s, 3H), 1.70−1.79 (m, 2H), 1.39−1.46 (m, 2H), 1.32 (d, J = 6.3 Hz, 3H), 1.17 (s, 6H), 0.93 (t, J = 6.6 Hz, 3H) ppm.

Preparation of Methyl 2-Butoxy-6-(2-hydroxy-2-methylpropoxy)-5-(4-(methylsulfonyl)phenyl)nicotinate (41). To a stirring solution of 2-butoxy-6-(2-hydroxy-2-methylpropoxy)-5-(4-(methylsulfonyl)phenyl)nicotinic acid (**39c**, 1.2 g, 2.4 mmol) in MeOH (12 mL) and toluene (12 mL) at 0 °C was added a hexane solution (1 M) of (trimethylsilyl)diazomethane (3.5 mL, 3.5 mmol) dropwise. The resulting reaction mixture was stirred at 0 °C for 0.5 h. The reaction was then quenched by water (60 mL). The resulting solution was extracted with ethyl acetate (3 × 30 mL). The combined organic extract was washed with brine (30 mL), dried over anhydrous Na_2SO_4, and concentrated. The residue was purified by flash chromatography (25% ethyl acetate in petroleum ether as the eluent) to give the title compound as a white solid (1.1 g, 71%). LCMS (ESI): mass calcd for $C_{22}H_{29}NO_7S$, 451.2; m/z found, 452.3 $[M + H]^+$.

Preparation of 1-((6-Butoxy-5-(2-hydroxypropan-2-yl)-3-(4-(methylsulfonyl)phenyl)pyridin-2-yl)oxy)-2-methylpropan-2-ol (14). To a solution of methyl 2-butoxy-6-(2-hydroxy-2-methylpropoxy)-5-(4-(methylsulfonyl)phenyl)nicotinate (**41**, 1.3 g, 2.88 mmol) in anhydrous THF (20 mL) at 0 °C was added a THF solution (3 M) of methylmagnesium chloride (10 mL, 30 mmol). The reaction mixture was stirred at room temperature overnight. The reaction was then quenched by aqueous saturated NH_4Cl solution (50 mL). The resulting solution was extracted with ethyl acetate (3 × 20 mL). The combined organic extract was washed with brine (20 mL), dried over anhydrous Na_2SO_4, filtered, and concentrated. The residue was purified by flash chromatography (25% ethyl acetate in petroleum ether as the eluent) to give the title compound as a white solid (330 mg, 25% yield). LCMS (ESI): mass calcd for $C_{23}H_{33}NO_6S$, 451.2; m/z found, 452.2 $[M + H]^+$; ^{1}H NMR (300 MHz, DMSO-d_6): δ 8.00 (s, 1H), 7.95 (d, J = 8.7 Hz, 2H), 7.88 (d, J = 8.7 Hz, 2H), 5.11 (s, 1H), 4.61 (s, 1H), 4.38 (t, J = 6.3 Hz, 2H), 4.12 (s, 2H), 3.25 (s, 3H), 1.71−1.81 (m, 2H), 1.54 (s, 6H), 1.41−1.54 (m, 2H), 1.17 (s, 6H), 0.97 (t, J = 7.5 Hz, 3H) ppm.

Preparation of Ethyl 2-((2-Butoxy-6-(2-hydroxy-2-methylpropoxy)-5-(4-(methylsulfonyl)phenyl)pyridin-3-yl)methoxy)-acetate (42). To a solution of 1-[[6-butoxy-5-(hydroxymethyl)-3-(4-methanesulfonylphenyl)pyridin-2-yl]oxy]-2-methylpropan-2-ol (**11**, 1.1 g, 2.60 mmol) in anhydrous THF (22 mL) at 0 °C was added NaH (60%, 417 mg, 10.4 mmol) in several batches. The mixture was stirred at 0 °C for 1 h, and then ethyl 2-bromoacetate (1.18 g, 7.06 mmol) was added dropwise. The reaction mixture was stirred at room temperature overnight. The mixture was quenched with acetic acid (10 mL) and water (50 mL). The mixture was extracted with ethyl acetate (3 × 30 mL). The organic layers were combined, dried over anhydrous Na_2SO_4, and concentrated to give the title compound as a colorless oil (910 mg, 69% yield). LCMS (ESI): mass calcd for $C_{25}H_{35}NO_8S$, 509.2; m/z found, 510.3 $[M - H]^+$.

Preparation of 1-((6-Butoxy-5-((2-hydroxyethoxy)methyl)-3-(4-(methylsulfonyl)phenyl)pyridin-2-yl)oxy)-2-methylpropan-2-ol (15). To a solution of ethyl 2-((2-butoxy-6-(2-hydroxy-2-methylpropoxy)-5-(4-(methylsulfonyl)phenyl)pyridin-3-yl)methoxy)-acetate (**42**, 910 mg, 1.34 mmol) in anhydrous THF (20 mL) at 0 °C was added $LiAlH_4$ (102 mg, 2.7 mmol). The reaction mixture was stirred at 0 °C for 2 h. The mixture was quenched by Fieser workup (water, 0.1 mL, followed by 15% aqueous NaOH, 0.3 mL; and then stirred for 10 min). The mixture was filtered, and the filtrate was concentrated. The residue was purified by flash chromatography (33−50% ethyl acetate in petroleum ether as the eluent) to give the title compound as a white solid (441 mg, 53% yield). LCMS (ESI): mass calcd for $C_{23}H_{33}NO_7S$, 467.2; m/z found, 468.1 $[M + H]^+$; ^{1}H NMR (300 MHz, DMSO-d_6): δ 7.95 (d, J = 8.7 Hz, 2H), 7.89 (d, J = 8.7 Hz, 2H), 7.86 (s, 1H), 4.62 (s, 2H), 4.45 (s, 2H), 4.35 (d, J = 6.0 Hz, 2H), 4.14 (s, 2H), 3.49−3.54 (m, 4H), 3.25 (s, 3H), 1.70−1.79 (m, 2H), 1.39−1.52 (m, 2H), 1.17 (s, 6H), 0.93 (d, J = 7.5 Hz, 3H) ppm.

Preparation of 2-Butoxy-6-(4-fluorophenyl)nicotinic Acid (43). To a mixture of 2-butoxy-6-chloronicotinic acid (**36c**, 4 g, 17.1 mmol), K_2CO_3 (10.6 g, 76.9 mmol), and 4-fluorophenylboronic acid (3.6 g, 25.6 mmol) in 1,4-dioxane (80 mL) and water (16 mL) under nitrogen was added $Pd(Ph_3P)_4$ (2.0 g, 1.7 mmol). The reaction mixture was heated and stirred at 80 °C overnight. The mixture was cooled to room temperature and then quenched with water (200 mL). The mixture was acidified to "pH" 1 using aqueous HCl solution (1 M), and then extracted with ethyl acetate (3 × 50 mL). The organic layers were combined, dried over anhydrous Na_2SO_4, and concentrated. The residue was purified by flash chromatography (50−70% ethyl acetate in petroleum ether as the eluent) to give the title compound as a white solid (2.1 g, 40% yield). LCMS (ESI): mass calcd for $C_{16}H_{16}FNO_3$, 289.1; m/z found, 288.2 $[M - H]^+$.

Preparation of 5-Bromo-2-butoxy-6-(4-fluorophenyl)-nicotinic Acid (44). To a solution of 2-butoxy-6-(4-fluorophenyl)-nicotinic acid (2.1 g, 6.9 mmol) in acetonitrile (40 mL) and trifluoroacetic acid (40 mL) was added NBS (1.6 g, 9.0 mmol). The reaction mixture was stirred at room temperature overnight. Water (500 mL) was added. The precipitate was collected by filtration, washed with water (2 × 40 mL), and dried in vacuo to give the title compound as a white solid (1.5 g, 57% yield). LCMS (ESI): mass calcd for $C_{16}H_{15}BrFNO_3$, 367.0; m/z found, 368.2 $[M + H]^+$.

Preparation of 2-Butoxy-6-(4-fluorophenyl)-5-(4-(methylsulfonyl)phenyl)nicotinic Acid (45). To a mixture of 5-bromo-2-butoxy-6-(4-fluorophenyl)nicotinic acid (**44**, 1.1 g, 2.87 mmol), K_2CO_3 (1.8 g, 12.9 mmol), and 4-(methylsulfonyl)-phenylboronic acid (630 mg, 3.15 mmol) in 1,4-dioxane (20 mL) and water (4 mL) was added $Pd(Ph_3P)_4$ (331 mg, 0.29 mmol) under nitrogen. The reaction mixture was heated with stirring at 80 °C overnight. The mixture was cooled to room temperature and quenched with water (60 mL). The mixture was acidified to "pH" 1 using aqueous HCl solution (1 M) and then extracted with ethyl acetate (3 × 20 mL). The combined organic extract was washed with brine (30 mL), dried over anhydrous Na_2SO_4, and concentrated. The residue was purified by

https://doi.org/10.1021/acs.jmedchem.1c00890
J. Med. Chem. 2021, 64, 11570−11596

flash chromatography (70% ethyl acetate in petroleum ether as the eluent) to give the title compound as a white solid (810 mg, 56% yield). LCMS (ESI): mass calcd for $C_{23}H_{22}FNO_5S$, 443.1; m/z found, 444.2 $[M + H]^+$.

Preparation of (2-Butoxy-6-(4-fluorophenyl)-5-(4-(methylsulfonyl)phenyl)pyridin-3-yl)methanol (16). To a solution of 2-butoxy-6-(4-fluorophenyl)-5-(4-(methylsulfonyl)phenyl)-nicotinic acid (**45**, 810 mg, 1.6 mmol) in anhydrous THF (16 mL) at 0 °C was added a THF solution (1 M) of BH_3·THF (4.7 mL, 4.7 mmol). The reaction mixture was stirred at room temperature for 3 h. The mixture was quenched with MeOH (10 mL) and water (50 mL), and the organic layer was separated. The aqueous layer was extracted with ethyl acetate (3 × 20 mL). The combined organic extract was washed with saturated aqueous $NaHCO_3$ (20 mL), brine (20 mL), dried over anhydrous Na_2SO_4, filtered, and concentrated. The residue was purified by reverse-phase prep-HPLC [Column, XBridge Prep C18 OBD column 19 × 150 mm 5umC-0013; mobile phase, phase A: water (10 mmol NH_4HCO_3 solution; phase B: MeCN from 56 to 74% in 7 min; detector, 254 nm)] to give the title compound as a white solid (416 mg, 61% yield). LCMS (ESI): mass calcd for $C_{23}H_{24}FNO_4S$, 429.1; m/z found, 430.1 $[M + H]^+$; ^1H NMR (300 MHz, DMSO-d_6): δ 7.86 (d, J = 8.4 Hz, 2H), 7.75 (s, 1H), 7.42 (d, J = 8.4 Hz, 2H), 7.31−7.37 (m, 2H), 7.10−7.17 (m, 2H), 5.30 (t, J = 5.4 Hz, 1H), 4.56 (d, J = 5.4 Hz, 2H), 4.40 (t, J = 6.3 Hz, 2H), 3.23 (s, 3H), 1.70−1.79 (m, 2H), 1.42−1.49 (m, 2H), 0.95 (t, J = 7.2 Hz, 3H) ppm.

Preparation of 2-Butoxy-6-(oxetan-3-ylmethoxy)nicotinic Acid (47a). To a mixture of 2-butoxy-6-chloronicotinic acid (**36c**, 20 g, 85 mmol), Cs_2CO_3 (83.1 g, 255 mmol), and oxetan-3-ylmethanol (18.7 g, 212 mmol) in toluene (600 mL) under nitrogen was added XPhos Pd G3 (1.4 g, 1.65 mmol). The reaction mixture was heated and stirred at 90 °C for 3 h. The mixture was cooled to room temperature and then quenched with water. The organic layer was separated, and the "pH" of the aqueous layer was adjusted to 1 using aqueous HCl solution (1 M). The aqueous solution was extracted with ethyl acetate. The organic layers were combined, dried over anhydrous Na_2SO_4, and concentrated to give the title compound as a white solid (19 g, 80% yield). LCMS (ESI): mass calcd for $C_{14}H_{19}NO_5$, 281.1; m/z found, 282.1 $[M + H]^+$.

Preparation of 2-Butoxy-6-((3-hydroxyoxetan-3-yl)-methoxy)nicotinic Acid (47b). To a mixture of 2-butoxy-6-chloronicotinic acid (**36c**, 2 g, 8.7 mmol), Cs_2CO_3 (8.6 g, 26.4 mmol), and 3-(hydroxymethyl)oxetan-3-ol (1.4 g, 13.4 mmol) in toluene (60 mL) under nitrogen was added XPhos Pd G3 (148 mg, 0.175 mmol). The reaction mixture was heated and stirred at 90 °C for 3 h. The mixture was cooled to room temperature and then quenched with water. The organic layer was separated, and the "pH" of the aqueous layer was adjusted to 1 using aqueous HCl solution (1 M). The aqueous solution was extracted with ethyl acetate. The organic layers were combined, dried over anhydrous Na_2SO_4, and concentrated to give the title compound as a white solid (1.4 g, 54% yield). LCMS (ESI): mass calcd for $C_{14}H_{19}NO_6$, 297.1; m/z found, 298.2 $[M + H]^+$.

Preparation of 2-Butoxy-6-((3-methyloxetan-3-yl)methoxy)-nicotinic Acid (47c). To a mixture of 2-butoxy-6-chloronicotinic acid (**36c**, 4 g, 17.4 mmol), Cs_2CO_3 (17 g, 52.2 mmol), and (3-methyloxetan-3-yl) methanol (4.4 g, 43.1 mmol) in toluene (120 mL) under nitrogen was added XPhos Pd G3 (295 mg, 0.349 mmol). The reaction mixture was heated and stirred at 90 °C for 3 h. The mixture was cooled to room temperature and then quenched with water. The organic layer was separated, and the "pH" of the aqueous layer was adjusted to 1 using aqueous HCl solution (1 M). The aqueous solution was extracted with ethyl acetate. The organic layers were combined, washed with brine, dried over anhydrous Na_2SO_4, and concentrated to give the title compound as a white solid (4.1 g, 80% yield). LCMS (ESI): mass calcd for $C_{15}H_{21}NO_5$, 295.1; m/z found, 296.1 $[M + H]^+$.

Preparation of 2-Butoxy-6-((1-hydroxycyclobutyl)-methoxy)nicotinic Acid (47d). To a mixture of 2-butoxy-6-chloronicotinic acid (**36c**, 20 g, 87.0 mmol), Cs_2CO_3 (85.1 g, 261 mmol), and 1-(hydroxymethyl) cyclobutan-1-ol (17.8 g, 174 mmol) in toluene (600 mL) under nitrogen was added XPhos Pd G3 (1.47 g, 1.74 mmol). The reaction mixture was heated and stirred at 90 °C overnight. The mixture was cooled to room temperature and then quenched with water (3 L). The organic layer was separated, and the "pH" of the aqueous layer was adjusted to 1 using aqueous HCl solution (1 M). The aqueous solution was extracted with ethyl acetate. The organic layers were combined, dried over anhydrous Na_2SO_4, and concentrated to give the title compound as a brown oil (15 g, 45% yield). LCMS (ESI): mass calcd for $C_{15}H_{21}NO_5$, 295.1; m/z found, 296.0 $[M + H]^+$.

Preparation of 5-Bromo-2-butoxy-6-(oxetan-3-ylmethoxy)-nicotinic Acid (48a). To a solution of 2-butoxy-6-(oxetan-3-ylmethoxy)nicotinic acid (**47a**, 19 g, 60.8 mmol) and acetic acid (18.3 g, 305 mmol) in acetonitrile (400 mL) was added NBS (13 g, 73 mmol). The reaction mixture was stirred at room temperature for 3 h. The mixture was concentrated under reduced pressure. The residue was triturated in ethyl acetate to give the title compound as a white solid (19.5 g, 85% yield). LCMS (ESI): mass calcd for $C_{14}H_{18}BrNO_5$, 359.0; m/z found, 360.0 $[M + H]^+$.

Preparation of 5-Bromo-2-butoxy-6-((3-hydroxyoxetan-3-yl)methoxy)nicotinic Acid (48b). To a solution of 2-butoxy-6-((3-hydroxyoxetan-3-yl)methoxy) nicotinic acid (**47b**, 1.4 g, 4.7 mmol) in acetonitrile (25 mL) and acetic acid (1.4 g, 23 mmol) was added NBS (1 g, 5.6 mmol). The reaction mixture was stirred at room temperature for 2 h. The mixture was concentrated. The residue was purified by reversal-phase Combi-Flash [MeCN/water (0.05% NH_4HCO_3) from 10% to 60% in 45 min] to give the title compound as a white solid (1.3 g, 73% yield). LCMS (ESI): mass calcd for $C_{14}H_{18}BrNO_6$, 375.0; m/z found, 376.2 $[M + H]^+$.

Preparation of 5-Bromo-2-butoxy-6-((3-methyloxetan-3-yl)-methoxy)nicotinic Acid (48c). To a solution of 2-butoxy-6-((3-methyloxetan-3-yl)methoxy) nicotinic acid (**47c**, 4.1 g, 13.9 mmol) and acetic acid (4.2 g, 69.4 mmol) in acetonitrile (80 mL) was added NBS (3 g, 16.9 mmol). The reaction mixture was stirred at room temperature for 3 h. The mixture was concentrated under reduced pressure. The residue was triturated in ethyl acetate to give the title compound as a white solid (4.5 g, 87% yield). LCMS (ESI): mass calcd for $C_{15}H_{20}BrNO_5$, 373.0; m/z found, 374.2 $[M + H]^+$.

Preparation of 5-Bromo-2-butoxy-6-((1-hydroxycyclobutyl)-methoxy)nicotinic Acid (48d). To a solution of 2-butoxy-6-((1-hydroxycyclobutyl)methoxy)nicotinic acid (**47d**, 15 g, 39.1 mmol) in acetonitrile (375 mL) was added NBS (7.66 g, 43.0 mmol). The reaction mixture was stirred at room temperature for 3 h. The mixture was concentrated under reduced pressure. The residue was triturated in ethyl acetate to give the title compound as a white solid (8 g, 50% yield). LCMS (ESI): mass calcd for $C_{15}H_{20}BrNO_5$, 373.0; m/z found, 374.1 $[M + H]^+$.

Preparation of 2-Butoxy-5-(4-(methylsulfonyl)phenyl)-6-(oxetan-3-ylmethoxy)nicotinic Acid (49a). To a mixture of 5-bromo-2-butoxy-6-(oxetan-3-ylmethoxy)nicotinic acid (**48a**, 10 g, 27.8 mmol), 4-(methylsulfonyl)phenylboronic acid (6.1 g, 30.5 mmol), and K_2CO_3 (17.3 g, 125 mmol) in 1,4-dioxane (200 mL) and water (20 mL) was added $Pd(Ph_3P)_4$ (3.2 g, 2.76 mmol) under nitrogen. The reaction mixture was heated with stirring at 80 °C overnight. The mixture was cooled to room temperature and quenched with water. The mixture was filtered to remove the solids. The filtrate was acidified to "pH" 1 using aqueous HCl solution (1 M), and then extracted with ethyl acetate. The combined organic extract was washed with brine, dried over anhydrous Na_2SO_4, and concentrated. The residue was triturated in ethyl acetate to give the title compound as a white solid (8 g, 66% yield). LCMS (ESI): mass calcd for $C_{21}H_{25}NO_7S$, 435.1; m/z found, 436.4 $[M + H]^+$.

Preparation of 2-Butoxy-6-((3-hydroxyoxetan-3-yl)-methoxy)-5-(4-(methylsulfonyl)phenyl)nicotinic Acid (49b). To a mixture of 5-bromo-2-butoxy-6-((3-hydroxyoxetan-3-yl)-methoxy)nicotinic acid (**48b**, 1.3 g, 3.5 mmol), (4-(methylsulfonyl)-phenyl)boronic acid (760 mg, 3.80 mmol), and K_2CO_3 (2.15 g, 15.6 mmol) in 1,4-dioxane (30 mL) and water (3 mL) was added $Pd(Ph_3P)_4$ (400 mg, 0.346 mmol) under nitrogen. The reaction mixture was heated with stirring at 80 °C overnight. The mixture was cooled to room temperature and quenched with water. The mixture was filtered to remove the solids. The filtrate was acidified to "pH" 1 using aqueous HCl solution (1 M), and then extracted with ethyl acetate. The

https://doi.org/10.1021/acs.jmedchem.1c00890
J. Med. Chem. 2021, 64, 11570−11596

combined organic extract was washed with brine, dried over anhydrous Na_2SO_4, and concentrated. The residue was triturated in ethyl acetate to give the title compound as a white solid (660 mg, 42% yield). LCMS (ESI): mass calcd for $C_{21}H_{25}NO_8S$, 451.1; *m/z* found, 452.3 $[M + H]^+$.

Preparation of 2-Butoxy-6-((3-methyloxetan-3-yl)methoxy)-5-(4-(methylsulfonyl)phenyl)nicotinic Acid (49c). To a mixture of 5-bromo-2-butoxy-6-((3-methyloxetan-3-yl)methoxy)nicotinic acid (**48c**, 4.5 g, 12.0 mmol), 4-(methylsulfonyl)phenylboronic acid (2.6 g, 13.0 mmol), and K_2CO_3 (7.5 g, 54.3 mmol) in 1,4-dioxane (90 mL) and water (9 mL) was added $Pd(Ph_3P)_4$ (1.4 g, 1.21 mmol) under nitrogen. The reaction mixture was heated with stirring at 80 °C overnight. The mixture was cooled to room temperature and quenched with water. The mixture was filtered to remove the solids. The filtrate was acidified to "pH" 1 using aqueous HCl solution (1 M), and then extracted with ethyl acetate. The combined organic extract was washed with brine, dried over anhydrous Na_2SO_4, and concentrated. The residue was purified by reverse-phase Combi-Flash [MeCN/water (0.05% NH_4HCO_3) from 10% to 40% in 45 min] to give the title compound as a white solid (2.2 g, 41% yield). LCMS (ESI): mass calcd for $C_{22}H_{27}NO_7S$, 449.2; *m/z* found, 450.3 $[M + H]^+$.

Preparation of 2-Butoxy-6-((1-hydroxycyclobutyl)-methoxy)-5-(4-(methylsulfonyl)phenyl)nicotinic Acid (49d). To a mixture of 5-bromo-2-butoxy-6-((1-hydroxycyclobutyl)-methoxy)nicotinic acid (**48d**, 8 g, 19.5 mmol), 4-(methylsulfonyl)-phenylboronic acid (4.28 g, 21.4 mmol), and K_2CO_3 (12.1 g, 87.5 mmol) in 1,4-dioxane (160 mL) and water (16 mL) was added $Pd(Ph_3P)_4$ (2.25 g, 1.95 mmol) under nitrogen. The reaction mixture was heated with stirring at 80 °C overnight. The mixture was cooled to room temperature and quenched with water. The mixture was filtered to remove the solids. The filtrate was acidified to "pH" 1 using aqueous HCl solution (1 M), and then extracted with ethyl acetate. The combined organic extract was washed with brine, dried over anhydrous Na_2SO_4, and concentrated. The residue was purified by reverse-phase Combi-Flash [MeCN/water (0.05% NH_4HCO_3) from 10% to 40% in 45 min] to give the title compound as a white solid (4.1 g, 45% yield). LCMS (ESI): mass calcd for $C_{22}H_{27}NO_7S$, 449.2; *m/z* found, 450.2 $[M + H]^+$.

Preparation of (2-Butoxy-5-(4-(methylsulfonyl)phenyl)-6-(oxetan-3-ylmethoxy)pyridin-3-yl)methanol (17). To a solution of 2-butoxy-5-(4-(methylsulfonyl) phenyl)-6-(oxetan-3-ylmethoxy)-nicotinic acid (**49a**, 8 g, 18.4 mmol) and triethylamine (2.3 g, 22.7 mmol) in anhydrous THF (200 mL) at 0 °C was added isobutyl chloroformate (3 g, 22 mmol). The mixture was stirred at 0 °C for 0.5 h, and then an aqueous suspension (2 mL) of $NaBH_4$ (1.4 g, 37.0 mmol) was added. The reaction mixture was stirred at room temperature for 2 h. The mixture was concentrated. The residue was purified by reverse-phase prep-HPLC (column, C-18, mobile phase, water (a)/MeCN (b), b %: 30%–80%, 35 min; detector, UV 210 nm) to give the title compound as a white solid (3.41 g, 44% yield). LCMS (ESI): mass calcd for $C_{21}H_{27}NO_6S$, 421.2; *m/z* found, 422.2 $[M + H]^+$; ^1H NMR (300 MHz, DMSO-d_6): δ 7.94 (d, J = 8.4 Hz, 2H), 7.82 (s, 1H), 7.82 (d, J = 8.4 Hz, 2H), 5.08 (t, J = 5.6 Hz, 1H), 4.65–4.74 (m, 2H), 4.57 (d, J = 6.4 Hz, 2H), 4.41–4.50 (m, 4H), 4.37 (t, J = 6.4 Hz, 2H), 3.32–3.49 (m, 1H), 3.24 (s, 3H), 1.65–1.80 (m, 2H), 1.36–1.53 (m, 2H), 0.95 (t, J = 7.4 Hz, 3H) ppm.

Preparation of 3-(((6-Butoxy-5-(hydroxymethyl)-3-(4-(methylsulfonyl)phenyl)pyridin-2-yl)oxy)methyl)oxetan-3-ol (18). To a solution of 2-butoxy-6-((3-hydroxyoxetan-3-yl)methoxy)-5-(4-(methylsulfonyl)phenyl)nicotinic acid (**49b**, 660 mg, 1.46 mmol) and triethylamine (178 mg, 1.76 mmol) in anhydrous THF (18 mL) at 0 °C was added isobutyl chloroformate (240 mg, 1.76 mmol). The mixture was stirred at 0 °C for 0.5 h, and then an aqueous suspension (0.2 mL) of $NaBH_4$ (111 mg, 2.93 mmol) was added. The reaction mixture was stirred at room temperature for 2 h. The mixture was concentrated. The residue was purified by reverse-phase prep-HPLC (column, C-18, mobile phase, water (a)/MeCN (b), *b* %: 20–50%, 35 min; detector, UV 210 nm) to give the title compound as a white solid (350 mg, 54% yield). LCMS (ESI): mass calcd for $C_{21}H_{27}NO_7S$, 437.2; *m/z* found, 438.2 $[M + H]^+$; ^1H NMR (300 MHz, DMSO-d_6): δ 7.97–7.87 (m, 4H), 7.85 (s, 1H), 4.57–4.48 (m, 8H), 4.38 (t, J = 6.5 Hz, 2H), 3.46 (br s, 2H), 3.25 (s, 3H), 1.80–1.68 (m, 2H), 1.54–1.36 (m, 2H), 0.95 (t, J = 7.4 Hz, 3H) ppm.

Preparation of (2-Butoxy-6-((3-methyloxetan-3-yl)-methoxy)-5-(4-(methylsulfonyl)phenyl)pyridin-3-yl)methanol (19). To a solution of 2-butoxy-6-((3-methyloxetan-3-yl)methoxy)-5-(4-(methylsulfonyl)phenyl)nicotinic acid (**49c**, 2.2 g, 4.9 mmol) and triethylamine (594 mg, 5.87 mmol) in anhydrous THF (55 mL) at 0 °C was added isobutyl chloroformate (802 mg, 5.87 mmol). The mixture was stirred at 0 °C for 0.5 h, and then an aqueous suspension (0.6 mL) of $NaBH_4$ (370 mg, 9.78 mmol) was added. The reaction mixture was stirred at room temperature for 2 h. The mixture was concentrated. The residue was purified by reverse-phase prep-HPLC (column, C-18, mobile phase, water (a)/MeCN (b), *b* %: 30–60%, 35 min; detector, UV 210 nm) to give the title compound as a white solid (746 mg, 35% yield). LCMS (ESI): mass calcd for $C_{22}H_{29}NO_6S$, 435.2; *m/z* found, 436.2 $[M + H]^+$; ^1H NMR (300 MHz, DMSO-d_6): δ 7.95 (d, J = 8.7 Hz, 2H), 7.84 (s, 1 H), 7.82 (d, J = 8.7 Hz, 2H), 5.10 (t, J = 5.7 Hz, 1H), 4.50–4.48 (m, 6H), 4.46 (t, J = 6.5 Hz, 2H), 4.29 (d, J = 5.7 Hz, 2H), 3.25 (s, 3H), 1.80–1.65 (m, 2H), 1.51–1.39 (m, 2H), 1.29 (s, 3H), 0.95 (t, J = 7.4 Hz, 3H) ppm.

Preparation of 1-(((6-Butoxy-5-(hydroxymethyl)-3-(4-(methylsulfonyl)phenyl)pyridin-2-yl)oxy)methyl)cyclobutan-1-ol (20). To a solution of 2-butoxy-6-((1-hydroxycyclobutyl)-methoxy)-5-(4-(methylsulfonyl) phenyl) nicotinic acid (**49d**, 4.1 g, 8.8 mmol) in anhydrous THF (82 mL) at 0 °C was added a THF solution (1 M) of BH_3·THF (27 mL, 27 mmol). The reaction mixture was stirred at room temperature for 5 h. The mixture was slowly quenched with MeOH (5 mL) dropwise and concentrated. The residue was purified by reverse-phase Combi-Flash chromatography [MeCN/water (0.05% NH_4HCO_3) from 45 to 65% in 30 min] to give the crude product (3.2 g). Then, SiliaMrtS DMT (0.5 g) and MeCN (100 mL) were added to the crude product. The mixture was stirred at room temperature for 2 h, and then filtered. The filtrate was concentrated to give the title compound as a white solid (2.85 g, 74% yield). LCMS (ESI): mass calcd for $C_{22}H_{29}NO_6S$, 435.2; *m/z* found, 436.2 $[M + H]^+$; ^1H NMR (300 MHz, DMSO-d_6): δ 7.94–7.82 (m, 4H), 7.82 (s, 1H), 5.21 (s, 1H), 5.07 (t, J = 4.2 Hz, 1H), 4.45 (d, J = 4.2 Hz, 2H), 4.39–4.34 (m, 2H), 4.34 (s, 2H), 3.24 (s, 3H), 2.13–1.94 (m, 4H), 1.78–1.63 (m, 3H), 1.55–1.39 (m, 3H), 0.95 (t, J = 6.8 Hz, 3H) ppm; Anal. Calcd for $C_{22}H_{29}NO_6S$: C, 60.67; H, 6.71; N, 3.22. Found: C, 60.32; H, 7.04; N, 3.17; Pd level 4.8 ppm.

Preparation of 1-((3-Bromo-6-butoxy-5-(hydroxymethyl)-pyridin-2-yl)oxy)-2-methylpropan-2-ol (50). To a solution of 5-bromo-2-butoxy-6-(2-hydroxy-2-methylpropoxy)nicotinic acid (**38c**, 100 g, 255 mmol) in anhydrous THF (2 L) at 0 °C was added a THF solution (1 M) of BH_3·THF (575 mL, 575 mmol). The reaction mixture was stirred at room temperature for 5 h. The mixture was quenched with MeOH (300 mL) and water (2 L), and then extracted with ethyl acetate (3 × 600 mL). The combined organic extract was washed with saturated aqueous $NaHCO_3$ (600 mL) and brine (600 mL), dried over anhydrous Na_2SO_4, filtered, and concentrated to give the title compound as a white solid (82 g, 81% yield). LCMS (ESI): mass calcd for $C_{14}H_{22}BrNO_4$, 347.1; *m/z* found, 348.0 $[M + H]^+$.

Preparation of 1-((6-Butoxy-5-(hydroxymethyl)-3-(4,4,5,5-tetramethyl-1,3,2-dioxaborolan-2-yl)pyridin-2-yl)oxy)-2-methylpropan-2-ol (51). To a mixture of 1-((3-bromo-6-butoxy-5-(hydroxymethyl)pyridin-2-yl)oxy)-2-methylpropan-2-ol (**50**, 82 g, 208 mmol), bis(pinacolato)diboron (105.6 g, 416 mmol), and potassium acetate (40.8 g, 416 mmol) in anhydrous 1,4-dioxane (800 mL) was added $Pd(dppf)Cl_2$ (15.2 g, 20.8 mmol) under nitrogen. The reaction mixture was heated with stirring at 100 °C overnight. The mixture was cooled to room temperature and diluted with water (1 L), and then extracted with ethyl acetate (3 × 400 mL). The combined organic extract was washed with brine (400 mL), dried over anhydrous Na_2SO_4, and concentrated to give the title compound as a crude product: a black solid (90 g, 67% yield). LCMS (ESI): mass calcd for $C_{20}H_{34}BNO_6$, 395.2; *m/z* found, 396.2 $[M + H]^+$.

Preparation of 6′-Butoxy-2′-(2-hydroxy-2-methylpropoxy)-5′-(hydroxymethyl)-[2,3′-Bipyridine]-5-sulfonamide (23). To a mixture of 1-(6-butoxy-5-(hydroxymethyl)-3-(4,4,5,5-tetramethyl-1,3,2-dioxa-borolan-2-yl)pyridin-2-yloxy)-2-methylpropan-2-ol (**51**,

https://doi.org/10.1021/acs.jmedchem.1c00890
J. Med. Chem. 2021, 64, 11570–11596

70 g, 115 mmol), 6-chloropyridine-3-sulfonamide (26.5 g, 138 mmol), and Na_2CO_3 (24.3 g, 229.5 mmol) in 1,4-dioxane (700 mL) and water (70 mL) was added Pd(dppf)Cl_2 (8.4 g, 11.5 mmol) under nitrogen. The reaction mixture was heated with stirring at 65 °C overnight. The mixture was cooled to room temperature and concentrated. The residue was diluted with water (500 mL), and then extracted with ethyl acetate (3 × 200 mL). The combined organic extract was washed with brine (200 mL), dried over anhydrous Na_2SO_4, and concentrated. The residue was purified by flash chromatography (50−80% ethyl acetate in petroleum ether as the eluent) to give a crude product. The crude product was dissolved in THF (200 mL) and SiliaMrtS DMT (3 g) was added. The mixture was stirred at room temperature overnight. The mixture was filtered, and the filtrate was concentrated. The residue was purified by reverse-phase prep-HPLC [Column, C-18, mobile phase, water (a, 0.1%TFA)/MeCN (b), *b* %: 20−57%, 12 min; detector, UV 254 nm] followed by recrystallization in acetonitrile to give the title compound as a white solid (15 g, 30% yield). LCMS (ESI): mass calcd for $C_{19}H_{27}N_3O_6S$, 425.2; *m*/*z* found, 426.2 $[M + H]^+$; ^{1}HNMR (400 MHz, DMSO-d_6): δ 9.00 (d, J = 2.0 Hz, 1H), 8.46 (s, 1H), 8.34 (d, J = 8.4 Hz, 1H), 8.18 (dd, J = 2.4, 8.4 Hz, 1H), 7.58 (s, 2H), 5.17 (t, J = 6.0 Hz, 1H), 4.73 (s, 1H), 4.46 (d, J = 5.6 Hz, 2H), 4.38 (t, J = 6.4 Hz, 2H), 4.21 (s, 2H), 1.71−1.78 (m, 2H), 1.40−1.49 (m, 2H), 1.22 (s, 6H), 0.95 (t, J = 6.8 Hz, 3H) ppm; Anal. Calcd for $C_{19}H_{27}N_3O_6S$: C, 53.63; H, 6.40; N, 9.88. Found: C, 53.45; H, 6.41; N, 9.95; Pd level < 4.4 ppm.

Human COX-2/COX-1 Enzymatic Assays. COX-2 is a bifunctional enzyme that catalyzes two sequential reactions starting with a COX reaction that oxidizes arachidonic acid to PGG2 and followed by a peroxidase reaction that reduces PGG2 to PGH2. COX-2 activity was assessed in an in vitro assay through coupling of the peroxidase activity with oxidation of ADHP to form resurofin, which is highly fluorescent with an excitation wavelength between 530 and 540 nm and an emission wavelength between 585 and 595 nm. The final assay buffer consisted of 30 nM recombinant human COX-2 and 25 mM arachidonic acid in 100 mM Tris−HCl, pH 8, containing 2 mM heme, 20 μM ADHP, 10 nM catalase, 0.1 mg/mL BSA, and 0.002% Tween-20. The K_m value under these conditions was determined to be 13 ± 3 μM. Test compound concentrations ranged from 50 μM to 0.85 nM prepared using a 11-step serial dilution (1:3) in pure DMSO. The serially diluted test compounds were spotted per well of a black 384-Proxiplate (Perkin Elmer) with DMSO maintained at 1% of the total assay volume. The background signal was measured from control wells containing assay buffer without arachidonic acid, which functions as low control (LC). High control (HC) values were generated using the reaction with enzyme but no compound treatment. Compounds were preincubated with enzyme for 60 min at room temperature. The substrate was added to initiate the reaction and the reaction mixture was incubated for 20 s. The reaction was quenched by adding 10 mM ascorbic acid (diverting oxidation of ADHP to that of ascorbic acid). Fluorescence was then measured in PheraStar with excitation at 540 nm and emission at 590 nm.

The COX-1 enzyme assay was identical to the COX-2 enzyme assay as described above with the exception that the arachidonic acid concentration in the COX-1 enzyme assay was maintained at 10 μM rather than at 25 μM as in the COX-2 assay. The K_m value of COX-1 was determined to be 2.8 ± 0.4 μM under the assay conditions.

COX-2/COX-1 RapidFire High-Throughput Mass Spectrometry Cellular Assay. The COX-2/COX-1 RapidFire mass spectrometric cellular assay monitors the conversion of arachidonic acid to PGD2 by COX1 and COX2. Tetracycline-inducible HEK 293 T-Rex cells (Thermo) overexpressed COX-2 or COX-1 via overnight promotion. Cells were adjusted to a given concentration (COX-2, 80,000 cells/mL; Cox-1, 30,000 cells/mL) in cell media supplemented with 1 μg/mL tetracycline (Sigma, T7660) and dispensed into Poly-D lysine (PDL)-coated 384-well cell culture plates (Greiner #655940), 100 μL/well, using a ThermoFisher MultiDrop Combi liquid handler. The plates were incubated overnight at 37 °C, 5% CO_2, 95% RH to induce COX-2 or COX-1 protein. Compounds were diluted fresh in DMSO (Sigma, 276855) and plated in Greiner 384-well PP plates (Greiner#781280). Using a Janus MDT liquid handler, a 3-fold titration was conducted for each compound (11pt. + vehicle control). 200 μL of tetracycline-free media (Life-Technologies 10566016) was dispensed into a 384-well deep well microplate (Greiner#781270) using the Combi. The Janus liquid handler was used to transfer 1 μL of each well from the compound plate (100% DMSO) and transfer it to the 200 μL of media and mix, creating 0.5% DMSO final concentrations of compounds in cell media. Spent media were removed from the overnight-induced PDL plates via plate flicking, and 30 μL of compound titrations in cell media were added atop PDL-attached cells. The plates were covered with a lid, centrifuged briefly (250*g*, 1 min), and incubated for 1 h at 37 °C. A MultiDrop Combi was used to dispense 30 μL/well of deuterated substrate (40 μM arachidonic acid-D11, AA-D11, Cayman Chemicals #10006758), which was diluted in tetracycline-free media. AA-D11 was dispensed with a small tube cassette due to the smaller tubing diameter and thus more vigorous mixing upon addition. Assay plates were covered with a lid, centrifuged, and incubated for 1 h at 37 °C. The Janus liquid handler was used to gently mix the media atop the cells now containing deuterated product PGD2-D11 and transfer 10 μL into 90 μL of Agilent RapidFire effluent containing internal standard PGD2-D4 (Cayman Chemicals #312010) (0.01% Formic Acid, 0.1% Tween 20, 0.025 μg/mL PGD2-D4). The assay plates were analyzed using a RapidFire high-throughput solid-phase extraction system (Agilent) coupled to a triple quadrupole mass spectrometer (AB SCIEX) to measure relative peak areas of PGD2-D11 and PGD2-D4. Due to the variable sip volume of the RF-MS system, quantification of product (PGD2-D11) via a relative peak area was divided by the relative peak area of internal control (PGD2-D4), for internal assay normalization. Peaks were integrated using the RapidFire integrator software. RF-MS sample loading was done on a miniature C4 column, Agilent "Cartridge A" (Agilent #G9303A). The RF-MS was tuned to capture the PGD2-D11 product at XIC 362.2/282.2 and the PGD2-d4 spiked in product at XIC 354.9/275.2 on a Sciex Triple Quad 4000 QTRAP.

Human Whole Blood COX-2/COX-1 Assays. The whole blood assay and related analytical procedure were previously described.[59] Briefly, DMSO solutions of test compounds (50,000, 33,300, 10,000, 3,000, 900, 270, 81.4, 24.4, 7.34, 2.20, 0.662, 0.199, and 0.0597 μM) were prepared. The test compound (1.8 μL) for each concentration was added into a 96 deep-well plate. Each of 300 μL freshly heparinized blood was used for COX-2 and COX-1 assays. The final compound concentrations ranged from 600 to 0.4 μM. The plate was covered with foil, vortexed at 800 rpm for 1 min, and then incubated at 37 °C/5% CO_2 for 1 h.

For the COX-2 assay, 10 μL of 300 μg/mL LPS solution was added to COX-2 plate for a 10 μg/mL LPS final concentration. The plate was covered with foil, vortexed at 800 rpm for 1 min, and then incubated at 37 °C/5% CO_2 overnight. 100 μL ice-cold PBS buffer was added to the wells and mixed by using a pipet 10 times. The plates were centrifuged at 1400 rpm at 4 °C for 10 min. The supernatant aliquot (50 μL) was transferred into 150 μL ELISA buffer and vortexed. The samples were analyzed using PGE_2 ELISA kits from Cayman Chemical Inc.

For the COX-1 assay, 2 μL of 2.25 mM calcium ionophore solution was added to the COX-1 plate for a 15 μM calcium ionophore final concentration. The plate was covered with foil, vortexed at 800 rpm for 1 min, and then incubated at 37 °C/5% CO_2 for 1 h with continuous shaking at 175 rpm. 100 μL ice-cold PBS buffer was added to the wells and mixed by using a pipet 10 times. The plates were centrifuged at 1400 rpm at 4 °C for 10 min. The supernatant aliquot (20 μL) was transferred into 180 μL ELISA buffer and vortexed. The samples were analyzed using TXB_2 ELISA kits from Cayman Chemical Inc.

Mouse Cassette PK Studies Following IV or Oral Dosing. The selected compounds were formulated together for the cassette dosing. Three fasted male C57BL/6J mice were administered a single intravenous (IV) bolus injection of 2 mg/kg in a solution of PEG400/water (70:30) at a dose volume of 2 mL/kg. Blood samples were collected at 0.08, 0.25, 0.5, 1, 2, 4, 6, 8, and 24 h postdose via dorsal metatarsal vein. Six fasted male C57BL/6J mice were administered a single oral dose of 10 mg/kg in a solution of PEG400/water (70:30) at a dose volume of 10 mL/kg. Blood samples were collected at 0.25, 0.5, 1, 2, 3, and 4 h postdose. Colon tissue was collected at 2 and 4 h postdose. For both studies, blood samples were collected into tubes containing

https://doi.org/10.1021/acs.jmedchem.1c00890
J. Med. Chem. 2021, 64, 11570−11596

the K_2EDTA anticoagulant and placed on wet ice. The plasma fraction was separated by centrifugation and frozen at −20 °C or lower until analysis. Colon tissue was collected at 2 and 4 h postdose. For both studies, blood samples were collected into tubes containing K_2EDTA anticoagulant and placed on wet ice. The plasma fraction was separated by centrifugation and frozen at −20 °C or lower until analysis. Colon tissue was homogenized with PBS at a ratio of 1:5 [colon weight (g) to PBS volume (mL)]. Plasma and colon samples were processed for analysis by protein precipitation using acetonitrile. The final compound concentration in colon (ng/mL) was corrected by multiplying by 6. Concentrations of the compound in plasma and colon were determined using a liquid chromatographic triple-quadrupole mass spectrometric method (Shimadzu HPLC coupled to an AAB API 5500 instrument; Quantification: MRM, Positive ion).

Metabolite Identifications from Incubations of Compound 11 with Human and Mouse Hepatocytes. The cryopreserved hepatocytes were thawed on ice and vials were placed in a 37 °C water bath for approximately 90 s and then immediately added to a prewarmed hepatocyte-thawing media. The cells were resuspended with the media and then centrifuged at 700*g* for 7 min at room temperature. The supernatant was discarded, and the cells were resuspended in 2 mL of Krebs−Henseleit buffer (KHB) containing 12.5 mM HEPES pH 7.4. Cell viability and yield were determined by Trypan Blue exclusion. The hepatocytes were then diluted in KHB to a cell concentration of 2×10^6 cells/mL (500 μL/well in 10 mL glass tubes). The tubes were placed on a rotary shaker in a humidifier incubator supplied with 5% CO_2 and allowed for 15 min acclimation at 37 °C prior to use. Compound **11** or positive control, diclofenac (10 μM), in KHB was then added to the hepatocytes to achieve a final compound concentration of 10 μM and a cell concentration of 1×10^6 cells/mL (1000 μL final incubation volume). Cells were incubated for 0 and 2 h. At the end of the incubation, cells were quenched with 3 volumes of ice-cold acetonitrile containing 0.02% formic acid, vortexed, and sonicated (3 min). Precipitated proteins were pelleted by centrifugation (3000 rpm, 10 min, 4 °C) and the supernatants were evaporated to dryness under a gentle stream of nitrogen. The resulting residues were reconstituted in 250 μL of water: acetonitrile (9:1) containing 0.01% formic acid with sonication and vortexing to aid solubilization of drug-derived materials prior to filtration using 0.45 μm nylon filter at 10,000*g* at room temperature for 10 min. The filtrate was transferred to a 96-well plate for liquid chromatography/tandem mass spectrometric (LC−MS/MS) analysis.

LC−MS/MS analysis: Accela HPLC coupled to LTQ-Orbitrap XL and operated in a positive ESI mode. Column: Betasil PHENYL-HEXYL (100 × 2.0 mm ID, 3 μm). Mobile phase A: 0.1% formic acid; mobile phase B: acetonitrile containing 0.1% formic acid. A nonlinear gradient with a flow rate of 0.2 mL/min was used throughout the analysis. Compound **11** underwent extensive metabolism in both species. The turnover at a 10 μM substrate concentration was 79.6% and ∼100% in mouse and human hepatocytes, respectively. The percentages of compound **11** and its derived metabolites in the incubation extracts were obtained based on the peak areas in LC/UV chromatograms.

Uptake of [^{18}F]-FDG in Established Polyps/Adenomas Present in the GI-Tract of Aged Apc$^{min/+}$ Mice Using Ex Vivo PET Imaging. The uptake of [^{18}F]-FDG by tissues is a marker for the tissue uptake of glucose, which in turn is closely correlated with certain types of tissue metabolism. After [^{18}F]-FDG is injected into a patient (or animal), a PET scanner can form two-dimensional or three-dimensional images of the distribution of [^{18}F]-FDG within the body. The spontaneous GI-tract tumor Apc^{min} (C57BL/6J-Apc^{Min}/J) was used that was approximately 16+ weeks of age. All mice were individually housed in IVC cages with 2 oz glass food hoppers (with metal food follower and lids) containing standard diet 5008 (powdered/meal form) and ad libitum water 4−5 days prior to the start of experiment. Day 1 (start of experiment), diet was changed to chow containing testing compound for 14 days (changed/topped off a minimum of 1× weekly). Body weights and food intake were measured at a minimum once weekly (more often if possible). Day 13, mice were fasted overnight for 12+ hour (for [^{18}F]-FDG imaging). Day 14 (ex vivo imaging), for the [^{18}F]-FDG imaging, mice were euthanized with CO_2, death confirmed by no response of paw-pinch reflex. Cardiac puncture was carried out to draw blood, which was transferred into EDTA containing tubes that were placed onto a rocker for 10 min. Mice were opened up and GI-tract was removed and placed onto paper towel. Kidneys, liver, heart, and stomach (opened and pinned) were taken out and placed in formalin (10% neutral buffer saline; NBF) for histopathology. GI was sectioned in duodenum, jejunum, ileum, and colon and opened up longitudinally. One section at a time was washed with clean cold PBS (∼300 mL) in a glass beaker (a separated glass beaker for each mouse). The tissue was placed onto a black-coated cork board and flattened out (proximal at top, lumen surface facing upwards). Approximately 0.5−1.0 cm of the proximal portions of each tissue were cut and placed into separate reweighed Eppendorf tubes. The remainder was photographed. Fresh PBS was squirted over top of sections to keep them from drying out. These were imaged using a PET scanner—20 min static scan on an ice pack/cold cork board. During scan, instruments were cleaned with PBS and EtOH, wiped dry. Contents of the glass beakers were placed in large plastic containers, as all radioactive ([^{18}F]) was kept for 24 h until it had decayed (10× half-life). Beakers were washed briefly with water, wiped, rinsed again, and wiped dry. After scanning, sections on board were carefully blotted to remove PBS, and formalin was added onto the sections (15−20 mL 10% NBF). After 3 h, each GI tract portion was swiss-rolled, pinned, and placed into a large white cassette and into formalin. Analyses were performed in R, version 3.3.2. ANOVA, adjusted for multiple comparisons in a linear regression model.

In Vivo Polyp Growth/Formation Inhibition within the GI-Tract of 4−5 weeks of Age Apc$^{min/+}$ Mice in a Prophylactic Setting. Fifty 4- to 5-week-old female C57BL/6J-Apc^{Min}/J mice were sourced from JAX labs and acclimated for 5−7 days. Mice were group housed in IVC-cages under a 12 h light: dark cycle at a temperature of 19 to 22 °C. Mice were fed an autoclaved powdered diet laboratory chow (5008) and water ad libitum. Mice were ear-tagged and tailed tattooed, which will be placed 5−7 days prior to the start of the study to identify each animal. The spontaneous GI-tract tumor Apc^{min} (C57BL/6J-Apc^{Min}/J) was used that was approximately 5+ weeks of age. Day 1 (start of experiment), diet was changed to chow containing testing compound for 84 days (12 weeks, with hoppers changed/topped off a minimum of 1× weekly). Body weights and food intake were measured at a minimum once weekly. On day 83, mice were fasted overnight for 12+ hour (for [^{18}F]-FDG imaging). On day 84 (ex vivo imaging), for the [^{18}F]-FDG imaging, mice were euthanized with CO_2, with death confirmed by no response of paw-pinch reflex. Cardiac puncture was carried out to draw blood, which was transferred into EDTA-containing tubes that were placed onto a rocker for 10 min. Mice were opened up and GI-tract was removed and placed onto paper towel. Kidneys, liver, heart, and stomach (opened and pinned) were taken out and placed in formalin (10% neutral buffer saline; NBF) for histopathology. GI was sectioned in duodenum, jejunum, ileum and colon, and opened up longitudinally. One section at a time was washed in clean cold PBS (∼300 mL) in a glass beaker (separated glass beaker for each mouse). The tissue was placed onto a black-coated cork board and flattened out (proximal at the top, lumen surface facing upwards). Approximately 0.5−1.0 cm of the proximal portions of each tissue (duodenum, jejunum, ileum, and colon) were cut and placed into separate reweighed Eppendorf tubes. The remainder was photographed. Fresh PBS was squirted over top of sections to keep them from drying out. These were imaged using a PET scanner—20 min static scan on ice pack/cold cork board. During scan, instruments were cleaned with PBS and EtOH, and wiped dry. Contents of the glass beakers were placed in large plastic containers, as all radioactive ([^{18}F]) was kept for 24 h until it had decayed (10 × half-life). Beakers were briefly washed with water, wiped, rinsed again, and wiped dry. After scan, sections on board were carefully blotted to remove PBS, and formalin was added onto of sections (15−20 mL 10% NBF). After 3 h, each GI tract portion was swiss-rolled, pinned, and placed into a large white cassette and into formalin.

Weight and tumor assessment: body weights were measured on a balance a minimum of once weekly. Mice were monitored daily for clinical signs of toxicity for the duration of the treatment. A sustained

https://doi.org/10.1021/acs.jmedchem.1c00890
J. Med. Chem. 2021, 64, 11570−11596

body weight loss greater than 15% of the initial body weight was considered as clinical toxicity, with the animal being humanely sacrificed. Tumor growth inhibition (TGI) values were determined from total ileum polyp area (sum of all polyp areas with diameter > 1 mm) following a daily oral dosing of 300 mg/kg as a suspension for 10–12 weeks, % TGI = $1 - (T_t/C_t)$, T_t = median tumor volume of treated at time t, and C_t = median tumor volume of control at time t. Analyses were performed in One-way ANOVA with Dunnett's Multiple comparisons test; or Two-way ANOVA with the Dunnett's Multiple Comparisons test using GraphPad Prism 7.0..

■ ASSOCIATED CONTENT

Supporting Information

The Supporting Information is available free of charge at https://pubs.acs.org/doi/10.1021/acs.jmedchem.1c00890.

Molecular modeling; molecular formula strings (PDB)

(CSV)

Assays and protocols: chemistry; metabolite identifications; PK; UGT phenotyping; glucuronidation K_m determination; survival extension; plots for derived free unbound fraction (fu %) in vivo potency; and HPLC traces of compounds **10**, **11**, **20**, **21**, **22**, and **23** (PDF)

■ AUTHOR INFORMATION

Corresponding Authors

Zhuming Zhang − *Discovery Chemistry, Janssen Research and Development, Spring House, Pennsylvania 19477, United States;* Present Address: Deerfield Discovery & Development, New York, NY, USA; orcid.org/0000-0002-5638-5320; Email: zzzhang_3000@yahoo.com

David C. Evans − *Drug Metabolism and Pharmacokinetics, Janssen Research and Development, Spring House, Pennsylvania 19477, United States*; Email: DCEvans@its.jnj.com

Authors

Avijit Ghosh − *Drug Metabolism and Pharmacokinetics, Janssen Research and Development, Spring House, Pennsylvania 19477, United States;* Present Address: Amgen Corporation, South San Francisco, CA, USA.

Peter J. Connolly − *Discovery Chemistry, Janssen Research and Development, Spring House, Pennsylvania 19477, United States*

Peter King − *Drug Metabolism and Pharmacokinetics, Janssen Research and Development, Spring House, Pennsylvania 19477, United States;* Present Address: Immuneering Corporation, San Diego, CA, USA.

Thomas Wilde − *Drug Metabolism and Pharmacokinetics, Janssen Research and Development, Spring House, Pennsylvania 19477, United States*

Jianyao Wang − *Drug Metabolism and Pharmacokinetics, Janssen Research and Development, Spring House, Pennsylvania 19477, United States;* orcid.org/0000-0003-2559-8849

Yawei Dong − *Chemistry, Pharmaron Beijing, Co. Ltd., Beijing 100176, P. R. China*

Xueliang Li − *Chemistry, Pharmaron Beijing, Co. Ltd., Beijing 100176, P. R. China*

Daohong Liao − *Chemistry, Pharmaron Beijing, Co. Ltd., Beijing 100176, P. R. China*

Hao Chen − *Chemistry, Pharmaron Beijing, Co. Ltd., Beijing 100176, P. R. China*

Gaochao Tian − *Discovery Technology and Molecular Pharmacology, Janssen Research and Development, Spring House, Pennsylvania 19477, United States*

Javier Suarez − *Discovery Technology and Molecular Pharmacology, Janssen Research and Development, Spring House, Pennsylvania 19477, United States*

William G. Bonnette − *Discovery Technology and Molecular Pharmacology, Janssen Research and Development, Spring House, Pennsylvania 19477, United States*

Vineet Pande − *Discovery Chemistry, Janssen Research and Development, B-2340 Beerse, Belgium*

Karen A. Diloreto − *Drug Metabolism and Pharmacokinetics, Janssen Research and Development, Spring House, Pennsylvania 19477, United States*

Yifan Shi − *Drug Metabolism and Pharmacokinetics, Janssen Research and Development, Spring House, Pennsylvania 19477, United States*

Shefali Patel − *Drug Metabolism and Pharmacokinetics, Janssen Research and Development, Spring House, Pennsylvania 19477, United States*

Beth Pietrak − *Discovery Technology and Molecular Pharmacology, Janssen Research and Development, Spring House, Pennsylvania 19477, United States*

Lawrence Szewczuk − *Discovery Technology and Molecular Pharmacology, Janssen Research and Development, Spring House, Pennsylvania 19477, United States*

Carlo Sensenhauser − *Drug Metabolism and Pharmacokinetics, Janssen Research and Development, Spring House, Pennsylvania 19477, United States*

Shannon Dallas − *Drug Metabolism and Pharmacokinetics, Janssen Research and Development, Spring House, Pennsylvania 19477, United States*

James P. Edwards − *Discovery Chemistry, Janssen Research and Development, Spring House, Pennsylvania 19477, United States*

Kurtis E. Bachman − *Oncology Discovery, Janssen Research and Development, Spring House, Pennsylvania 19477, United States*

Complete contact information is available at: https://pubs.acs.org/10.1021/acs.jmedchem.1c00890

Author Contributions

This manuscript was written through contributions of all authors. Z.Z., A.G., and P.K. contributed to this work while employed at Janssen Research and Development.

Notes

The authors declare no competing financial interest.

■ ACKNOWLEDGMENTS

The authors would like to thank Christopher Teleha (Janssen Research and Development) for his valuable insights into chemistry, and Karine Smans (Janssen Research and Development), Heather Murrey (Janssen Research and Development), and Kay Ahn (Janssen Research and Development) for their valuable insights into biology. We are also grateful to Wenqiong Wu (Pharmaron, Beijing, China) for her contributions to the synthesis of compounds described herein.

■ ABBREVIATIONS

COX, cyclooxygenase; NSAID, nonsteroidal anti-inflammatory drug; CRC, colorectal cancer; FDG, fluorodeoxyglucose; PET, positron emission tomography; PD, pharmacodynamics; APC,

adenomatous polyposis coli; MIN, multiple intestinal neoplasia; IVIVC, in vitro−in vivo correlation; FAP, familial adenomatous polyposis; PG, prostaglandin; PGE_2, prostaglandin E_2; RR, relative risk; CV, cardiovascular; PGI_2, prostacyclin; PDB, Protein Data Bank; ER, endoplasmic reticulum; HEK, human embryonic kidney; GSH, glutathione; NADPH, nicotinamide adenine dinucleotide phosphate hydrogen; PK, pharmacokinetics; SAR, structure−activity relationship; TGI, tumor growth inhibition; SGF, simulated gastric fluid; FaSSIF, fasted simulated intestinal fluid; ADME, absorption, distribution, metabolism, and excretion; HLM, human liver microsomes; MLM, mouse liver microsomes; MDCK-MDR1, Madin Darby canine kidney (MDCK) cells with the MDR1 gene (ABCB1); ADHP, 10-acetyl-3,7-dihydroxyphenoxazine; UGT, UDP-glucuronosyltransferases; PV, portal vein; HWB, human whole blood; PPB, plasma protein binding; LPS, lipopolysaccharide; DMSO, dimethyl sulfoxide; NBS, *N*-bromosuccinimide; ACN or MeCN, acetonitrile; AcOH, acetic acid; XPhos Pd G3, (2-dicyclohexylphosphino-2′,4′,6′-triisopropyl-1,1′-biphenyl)[2-(2′-amino-1,1′-biphenyl)]palladium(II) methanesulfonate; Cy_2NMe, *N*,*N*′-dicyclohexyl-carbodiimide; ESI, electrospray ionization; LiHMDS, lithium bis(trimethylsilyl)amide; EtOAc, ethyl acetate; DCM, dichloromethane; Red-Al, sodium bis(2-methoxyethoxy)aluminum hydride, boron trichloride; TFA, trifluoroacetic acid; THF, tetrahydrofuran; $CHCl_3$, chloroform; $Pd(dppf)Cl_2$, [1,1′-bis(diphenylphosphino)ferrocene]-dichloropalladium(II); MeOH, methanol; $Pd(Ph_3P)_4$, tetrakis-(triphenylphosphine)palladium(0)

REFERENCES

(1) Siegel, R. L.; Miller, K. D.; Fuchs, H. E.; Jemal, A. Cancer statistics, 2021. *Ca-Cancer J. Clin.* **2021**, *71*, 7−33.

(2) Fearon, E. R.; Vogelstein, B. A genetic model for colorectal tumorigenesis. *Cell* **1990**, *61*, 759−767.

(3) Radtke, F.; Clevers, H.; Riccio, O. From gut homeostasis to cancer. *Curr. Mol. Med.* **2006**, *6*, 275−289.

(4) Ranger, G. S. Current concepts in colorectal cancer prevention with cyclooxygenase inhibitors. *Anticancer Res.* **2014**, *34*, 6277−6282.

(5) Ricciardiello, L.; Ahnen, D. J.; Lynch, P. M. Chemoprevention of hereditary colon cancers: time for new strategies. *Nat. Rev. Gastroenterol. Hepatol.* **2016**, *13*, 352−361.

(6) Theisen, C. Chemoprevention: what's in a name? *J. Natl. Cancer Inst.* **2001**, *93*, 743.

(7) Burke, C. A.; Dekker, E.; Lynch, P.; Samadder, N. J.; Balaguer, F.; Hüneburg, R.; Burn, J.; Castells, A.; Gallinger, S.; Lim, R.; Stoffel, E. M.; Gupta, S.; Henderson, A.; Kallenberg, F. G.; Kanth, P.; Roos, V. H.; Ginsberg, G. G.; Sinicrope, F. A.; Strassburg, C. P.; van Cutsem, E.; Church, J.; Lalloo, F.; Willingham, F. F.; Wise, P. E.; Grady, W. M.; Ford, M.; Weiss, J. M.; Gryfe, R.; Rustgi, A. K.; Syngal, S.; Cohen, A. Eflornithine plus sulindac for prevention of progression in familial adenomatous polyposis. *N. Engl. J. Med.* **2020**, *383*, 1028−1039.

(8) Baron, J. A. Epidemiology of non-steroidal anti-inflammatory drugs and cancer. *Prog. Exp. Tumor Res.* **2003**, *37*, 1−24.

(9) Dubé, C.; Rostom, A.; Lewin, G.; Tsertsvadze, A.; Barrowman, N.; Code, C.; Sampson, M.; Moher, D.; U.S. Preventive Services Task Force. The use of aspirin for primary prevention of colorectal cancer: a systematic review prepared for the U.S. Preventive Services Task Force. *Ann. Intern. Med.* **2007**, *146*, 365−375.

(10) Rostom, A.; Dubé, C.; Lewin, G.; Tsertsvadze, A.; Barrowman, N.; Code, C.; Sampson, M.; Moher, D.; U.S. Preventive Services Task Force. Nonsteroidal anti-inflammatory drugs and cyclooxygenase-2 inhibitors for primary prevention of colorectal cancer: a systematic review prepared for the U.S. Preventive Services Task Force. *Ann. Intern. Med.* **2007**, *146*, 376−389.

(11) Burn, J.; Sheth, H.; Elliott, F.; Reed, L.; Macrae, F.; Mecklin, J.-P.; Möslein, G.; McRonald, F. E.; Bertario, L.; Evans, D. G.; Gerdes, A.-M.; Ho, J. W. C.; Lindblom, A.; Morrison, P. J.; Rashbass, J.; Ramesar, R.; Seppälä, T.; Thomas, H. J. W.; Pylvänäinen, K.; Borthwick, G. M.; Mathers, J. C.; Bishop, D. T.; Boussioutas, A.; Brewer, C.; Cook, J.; Eccles, D.; Ellis, A.; Hodgson, S. V.; Lubinski, J.; Maher, E. R.; Porteous, M. E.; Sampson, J.; Scott, R. J.; Side, L.; CAPP2 Investigators. Cancer prevention with aspirin in hereditary colorectal cancer (Lynch syndrome), 10-year follow-up and registry-based 20-year data in the CAPP2 study: a double-blind, randomised, placebo-controlled trial. *Lancet* **2020**, *395*, 1855−1863.

(12) Baron, J. A.; Sandler, R. S.; Bresalier, R. S.; Quan, H.; Riddell, R.; Lanas, A.; Bolognese, J. A.; Oxenius, B.; Horgan, K.; Loftus, S.; Morton, D. G.; APPROVe Trial Investigators. A randomized trial of rofecoxib for the chemoprevention of colorectal adenomas. *Gastroenterology* **2006**, *131*, 1674−1682.

(13) Higuchi, T.; Iwama, T.; Yoshinaga, K.; Toyooka, M.; Taketo, M. M.; Sugihara, K. A randomized, double-blind, placebo-controlled trial of the effects of rofecoxib, a selective cyclooxygenase-2 inhibitor, on rectal polyps in familial adenomatous polyposis patients. *Clin. Cancer Res.* **2003**, *9*, 4756−4760.

(14) Arber, N.; Eagle, C. J.; Spicak, J.; Rácz, I.; Dite, P.; Hajer, J.; Zavoral, M.; Lechuga, M. J.; Gerletti, P.; Tang, J.; Rosenstein, R. B.; Macdonald, K.; Bhadra, P.; Fowler, R.; Wittes, J.; Zauber, A. G.; Solomon, S. D.; Levin, B.; PreSAP Trial Investigators. Celecoxib for the prevention of colorectal adenomatous polyps. *N. Engl. J. Med.* **2006**, *355*, 885−895.

(15) Steinbach, G.; Lynch, P. M.; Phillips, R. K. S.; Wallace, M. H.; Hawk, E.; Gordon, G. B.; Wakabayashi, N.; Saunders, B.; Shen, Y.; Fujimura, T.; Su, L.-K.; Levin, B.; Godio, L.; Patterson, S.; Rodriguez-Bigas, M. A.; Jester, S. L.; King, K. L.; Schumacher, M.; Abbruzzese, J.; DuBois, R. N.; Hittelman, W. N.; Zimmerman, S.; Sherman, J. W.; Kelloff, G. The effect of celecoxib, a cyclooxygenase-2 inhibitor, in familial adenomatous polyposis. *N. Engl. J. Med.* **2000**, *342*, 1946−1952.

(16) Bertagnolli, M. M.; Eagle, C. J.; Zauber, A. G.; Redston, M.; Solomon, S. D.; Kim, K.; Tang, J.; Rosenstein, R. B.; Wittes, J.; Corle, D.; Hess, T. M.; Woloj, G. M.; Boisserie, F.; Anderson, W. F.; Viner, J. L.; Bagheri, D.; Burn, J.; Chung, D. C.; Dewar, T.; Foley, T. R.; Hoffman, N.; Macrae, F.; Pruitt, R. E.; Saltzman, J. R.; Salzberg, B.; Sylwestrowicz, T.; Gordon, G. B.; Hawk, E. T.; APC Study Investigators. Celecoxib for the prevention of sporadic colorectal adenomas. *N. Engl. J. Med.* **2006**, *355*, 873−884.

(17) FitzGerald, G. A.; Patrono, C. The coxibs, selective inhibitors of cyclooxygenase-2. *N. Engl. J. Med.* **2001**, *345*, 433−442.

(18) Simmons, D. L.; Botting, R. M.; Hla, T. Cyclooxygenase isozymes: the biology of prostaglandin synthesis and inhibition. *Pharmacol. Rev.* **2004**, *56*, 387−437.

(19) Gupta, R. A.; Dubois, R. N. Colorectal cancer prevention and treatment by inhibition of cyclooxygenase-2. *Nat. Rev. Cancer* **2001**, *1*, 11−21.

(20) Sankaranarayanan, R.; Kumar, D. R.; Altinoz, M. A.; Bhat, G. J. Mechanisms of colorectal cancer Prevention by aspirin-a literature review and perspective on the role of COX-dependent and -independent pathways. *Int. J. Mol. Sci.* **2020**, *21*, 9018.

(21) Benelli, R.; Venè, R.; Ferrari, N. Prostaglandin-endoperoxide synthase 2 (cyclooxygenase-2), a complex target for colorectal cancer prevention and therapy. *Transl. Res.* **2018**, *196*, 42−61.

(22) Sigthorsson, G.; Simpson, R. J.; Walley, M.; Anthony, A.; Foster, R.; Hotz-Behoftsitz, C.; Palizban, A.; Pombo, J.; Watts, J.; Morham, S. G.; Bjarnason, I. COX-1 and 2, intestinal integrity, and pathogenesis of nonsteroidal anti-inflammatory drug enteropathy in mice. *Gastroenterology* **2002**, *122*, 1913−1923.

(23) Bjarnason, I.; Scarpignato, C.; Holmgren, E.; Olszewski, M.; Rainsford, K. D.; Lanas, A. Mechanisms of damage to the gastrointestinal tract from nonsteroidal anti-Inflammatory drugs. *Gastroenterology* **2018**, *154*, 500−514.

(24) Fornai, M.; Antonioli, L.; Colucci, R.; Pellegrini, C.; Giustarini, G.; Testai, L.; Martelli, A.; Matarangasi, A.; Natale, G.; Calderone, V.; Tuccori, M.; Scarpignato, C.; Blandizzi, C. NSAID-induced enteropathy: are the currently available selective COX-2 inhibitors all the same? *J. Pharmacol. Exp. Ther.* **2014**, *348*, 86−95.

https://doi.org/10.1021/acs.jmedchem.1c00890
J. Med. Chem. 2021, 64, 11570−11596

(25) Seibert, K.; Zhang, Y.; Leahy, K.; Hauser, S.; Masferrer, J.; Perkins, W.; Lee, L.; Isakson, P. Pharmacological and biochemical demonstration of the role of cyclooxygenase 2 in inflammation and pain. *Proc. Natl. Acad. Sci. U.S.A.* **1994**, *91*, 12013−12017.
(26) Wang, D.; DuBois, R. N. Role of prostanoids in gastrointestinal cancer. *J. Clin. Invest.* **2018**, *128*, 2732−2742.
(27) Wang, D.; Dubois, R. N. The role of COX-2 in intestinal inflammation and colorectal cancer. *Oncogene* **2010**, *29*, 781−788.
(28) Kömhoff, M.; Guan, Y.; Shappell, H. W.; Davis, L.; Jack, G.; Shyr, Y.; Koch, M. O.; Shappell, S. B.; Breyer, M. D. Enhanced expression of cyclooxygenase-2 in high grade human transitional cell bladder carcinomas. *Am. J. Pathol.* **2000**, *157*, 29−35.
(29) Poon, R.; Smits, R.; Li, C.; Jagmohan-Changur, S.; Kong, M.; Cheon, S.; Yu, C.; Fodde, R.; Alman, B. A. Cyclooxygenase-two (COX-2) modulates proliferation in aggressive fibromatosis (desmoid tumor). *Oncogene* **2001**, *20*, 451−460.
(30) Benamouzig, R.; Uzzan, B.; Martin, A.; Deyra, J.; Little, J.; Girard, B.; Chaussade, S.; APACC Study Group. Cyclooxygenase-2 expression and recurrence of colorectal adenomas: effect of aspirin chemoprevention. *Gut* **2010**, *59*, 622−629.
(31) Tomozawa, S.; Tsuno, N. H.; Sunami, E.; Hatano, K.; Kitayama, J.; Osada, T.; Saito, S.; Tsuruo, T.; Shibata, Y.; Nagawa, H. Cyclooxygenase-2 overexpression correlates with tumour recurrence, especially haematogenous metastasis, of colorectal cancer. *Br. J. Cancer* **2000**, *83*, 324−328.
(32) Cha, Y. I.; DuBois, R. N. NSAIDs and cancer prevention: targets downstream of COX-2. *Annu. Rev. Med.* **2007**, *58*, 239−252.
(33) Wang, D.; DuBois, R. N. Eicosanoids and cancer. *Nat. Rev. Cancer* **2010**, *10*, 181−193.
(34) Wang, D.; Dubois, R. N. Prostaglandins and cancer. *Gut* **2006**, *55*, 115−122.
(35) Xia, D.; Wang, D.; Kim, S.-H.; Katoh, H.; DuBois, R. N. Prostaglandin E2 promotes intestinal tumor growth via DNA methylation. *Nat. Med.* **2012**, *18*, 224−226.
(36) Tanabe, T.; Tohnai, N. Cyclooxygenase isozymes and their gene structures and expression. *Prostaglandins Other Lipid Mediators* **2002**, *68*−*69*, 95−114.
(37) Oshima, M.; Dinchuk, J. E.; Kargman, S. L.; Oshima, H.; Hancock, B.; Kwong, E.; Trzaskos, J. M.; Evans, J. F.; Taketo, M. M. Suppression of intestinal polyposis in Apc delta716 knockout mice by inhibition of cyclooxygenase 2 (COX-2). *Cell* **1996**, *87*, 803−809.
(38) Fukutake, M.; Nakatsugi, S.; Isoi, T.; Takahashi, M.; Ohta, T.; Mamiya, S.; Taniguchi, Y.; Sato, H.; Fukuda, K.; Sugimura, T.; Wakabayashi, K. Suppressive effects of nimesulide, a selective inhibitor of cyclooxygenase-2, on azoxymethane-induced colon carcinogenesis in mice. *Carcinogenesis* **1998**, *19*, 1939−1942.
(39) Oshima, M.; Murai, N.; Kargman, S.; Arguello, M.; Luk, P.; Kwong, E.; Taketo, M. M.; Evans, J. F. Chemoprevention of intestinal polyposis in the Apcdelta716 mouse by rofecoxib, a specific cyclooxygenase-2 inhibitor. *Cancer Res.* **2001**, *61*, 1733−1740.
(40) Kohno, H.; Suzuki, R.; Sugie, S.; Tanaka, T. Suppression of colitis-related mouse colon carcinogenesis by a COX-2 inhibitor and PPAR ligands. *BMC Cancer* **2005**, *5*, 46.
(41) Arber, N.; Spicak, J.; Rácz, I.; Zavoral, M.; Breazna, A.; Gerletti, P.; Lechuga, M. J.; Collins, N.; Rosenstein, R. B.; Eagle, C. J.; Levin, B. Five-year analysis of the prevention of colorectal sporadic adenomatous polyps trial. *Am. J. Gastroenterol.* **2011**, *106*, 1135−1146.
(42) Solomon, S. D.; McMurray, J. J. V.; Pfeffer, M. A.; Wittes, J.; Fowler, R.; Finn, P.; Anderson, W. F.; Zauber, A.; Hawk, E.; Bertagnolli, M. Adenoma prevention with celecoxib (APC) study investigators. Cardiovascular risk associated with celecoxib in a clinical trial for colorectal adenoma prevention. *N. Engl. J. Med.* **2005**, *352*, 1071−1080.
(43) Lee, Y.; Kim, J.; Kim, H.; Kang, S.; Yoon, J.-H.; Kim, D.-D.; Kim, Y. M.; Jung, Y. N-succinylaspart-1-yl celecoxib is a potential colon-specific prodrug of celecoxib with improved therapeutic properties. *J. Pharm. Sci.* **2012**, *101*, 1831−1842.
(44) Lee, Y.; Kim, H.; Kim, W.; Yoon, J.-H.; Jeong, S. H.; Jung, Y. Colon-specific delivery of celecoxib is a potential strategy to improve toxicological and pharmacological properties of the selective Cox-2 inhibitor: implication in treatment of familiar adenomatous polyposis. *J. Drug Targeting* **2012**, *20*, 524−534.
(45) Filipski, K. J.; Varma, M. V.; El-Kattan, A. F.; Ambler, C. M.; Ruggeri, R. B.; Goosen, T. C.; Cameron, K. O. Intestinal targeting of drugs: rational design approaches and challenges. *Curr. Top. Med. Chem.* **2013**, *13*, 776−802.
(46) Hua, S. Advances in oral drug delivery for regional targeting in the gastrointestinal tract - influence of physiological, pathophysiological and pharmaceutical factors. *Front. Pharmacol.* **2020**, *11*, 524.
(47) Leonard, K. A.; Madge, L. A.; Krawczuk, P. J.; Wang, A.; Kreutter, K. D.; Bacani, G. M.; Chai, W.; Smith, R. C.; Tichenor, M. S.; Harris, M. C.; Malaviya, R.; Seierstad, M.; Johnson, M. E.; Venable, J. D.; Kim, S.; Hirst, G. C.; Mathur, A. S.; Rao, T. S.; Edwards, J. P.; Rizzolio, M. C.; Koudriakova, T. Discovery of a gut-restricted JAK inhibitor for the treatment of inflammatory bowel disease. *J. Med. Chem.* **2020**, *63*, 2915−2929.
(48) Tanwar, L.; Piplani, H.; Sanyal, S. Anti-proliferative and apoptotic effects of etoricoxib, a selective COX-2 inhibitor, on 1,2-dimethylhydrazine dihydrochloride-induced colon carcinogenesis. *Asian Pac. J. Cancer Prev.* **2010**, *11*, 1329−1333.
(49) El Miedany, Y.; Youssef, S.; Ahmed, I.; El Gaafary, M. The gastrointestinal safety and effect on disease activity of etoricoxib, a selective cox-2 inhibitor in inflammatory bowel diseases. *Am. J. Gastroenterol.* **2006**, *101*, 311−317.
(50) Tian, G.; Suarez, J.; Zhang, Z.; Connolly, P.; Ahn, K. Potent phenylpyridine and oxodihydrofuran inhibitors of cyclooxygenase-2: optimization towards long residence time with balanced internal energetics. *Biochemistry* **2021**, in press.
(51) Vauquelin, G.; Charlton, S. J. Long-lasting target binding and rebinding as mechanisms to prolong in vivo drug action. *Br. J. Pharmacol.* **2010**, *161*, 488−508.
(52) Sandborn, W. J.; Nguyen, D. D.; Beattie, D. T.; Brassil, P.; Krey, W.; Woo, J.; Situ, E.; Sana, R.; Sandvik, E.; Pulido-Rios, M. T.; Bhandari, R.; Leighton, J. A.; Ganeshappa, R.; Boyle, D. L.; Abhyankar, B.; Kleinschek, M. A.; Graham, R. A.; Panes, J. Development of gut-selective pan-Janus kinase inhibitor TD-1473 for ulcerative colitis: a translational medicine programme. *J. Crohns Colitis.* **2020**, *14*, 1202−1213.
(53) Plount Price, M. L.; Jorgensen, W. L. Analysis of binding affinities for celecoxib analogues with COX-1 and COX-2 from combined docking and monte carlo simulations and insight into the COX-2/COX-1 Selectivity. *J. Am. Chem. Soc.* **2000**, *122*, 9455−9466.
(54) Wang, J. L.; Limburg, D.; Graneto, M. J.; Springer, J.; Hamper, J. R. B.; Liao, S.; Pawlitz, J. L.; Kurumbail, R. G.; Maziasz, T.; Talley, J. J.; Kiefer, J. R.; Carter, J. The novel benzopyran class of selective cyclooxygenase-2 inhibitors. Part 2: the second clinical candidate having a shorter and favorable human half-life. *Bioorg. Med. Chem. Lett.* **2010**, *20*, 7159−7163.
(55) Orlando, B. J.; Malkowski, M. G. Crystal structure of rofecoxib bound to human cyclooxygenase-2. *Acta Crystallogr., Sect. F: Struct. Biol. Commun.* **2016**, *72*, 772−776.
(56) Yuan, C.; Smith, W. L. A cyclooxygenase-2-dependent prostaglandin E2 biosynthetic system in the Golgi apparatus. *J. Biol. Chem.* **2015**, *290*, 5606−5620.
(57) Troberg, J.; Järvinen, E.; Muniz, M.; Sneitz, N.; Mosorin, J.; Hagström, M.; Finel, M. Dog UDP-glucuronosyltransferase enzymes of subfamily 1A: cloning, expression, and activity. *Drug Metab. Dispos.* **2015**, *43*, 107−118.
(58) Esser, R.; Berry, C.; Du, Z.; Dawson, J.; Fox, A.; Fujimoto, R. A.; Haston, W.; Kimble, E. F.; Koehler, J.; Peppard, J.; Quadros, E.; Quintavalla, J.; Toscano, K.; Urban, L.; van Duzer, J.; Zhang, X.; Zhou, S.; Marshall, P. J. Preclinical pharmacology of lumiracoxib: a novel selective inhibitor of cyclooxygenase-2. *Br. J. Pharmacol.* **2005**, *144*, 538−550.
(59) Shi, Y.; Murrey, H. E.; Ahn, K.; Weng, N.; Patel, S. LC-MS/MS assay for the simultaneous quantitation of thromboxane B2 and prostaglandin E2 to evaluate cyclooxygenase inhibition in human whole blood. *J. Appl. Bioanal.* **2020**, *6*, 131−144.

https://doi.org/10.1021/acs.jmedchem.1c00890
J. Med. Chem. 2021, 64, 11570−11596

(60) Heijink, D. M.; Kleibeuker, J. H.; Nagengast, W. B.; Oosterhuis, D.; Brouwers, A. H.; Koornstra, J. J.; de Jong, S.; de Vries, E. G. E. Total abdominal 18F-FDG uptake reflects intestinal adenoma burden in Apc mutant mice. *J. Nucl. Med.* **2011**, *52*, 431−436.
(61) Senda, T.; Iizuka-Kogo, A.; Onouchi, T.; Shimomura, A. Adenomatous polyposis coli (APC) plays multiple roles in the intestinal and colorectal epithelia. *Med. Mol. Morphol.* **2007**, *40*, 68−81.
(62) McCart, A. E.; Vickaryous, N. K.; Silver, A. Apc mice: models, modifiers and mutants. *Pathol., Res. Pract.* **2008**, *204*, 479−490.
(63) Corpet, D. E.; Pierre, F. How good are rodent models of carcinogenesis in predicting efficacy in humans? A systematic review and meta-analysis of colon chemoprevention in rats, mice and men. *Eur. J. Cancer* **2005**, *41*, 1911−1922.
(64) Jacoby, R. F.; Seibert, K.; Cole, C. E.; Kelloff, G.; Lubet, R. A. The cyclooxygenase-2 inhibitor celecoxib is a potent preventive and therapeutic agent in the min mouse model of adenomatous polyposis. *Cancer Res.* **2000**, *60*, 5040−5044.
(65) Wieder, H. A.; Beer, A. J.; Lordick, F.; Ott, K.; Fischer, M.; Rummeny, E. J.; Ziegler, S.; Siewer, J. R.; Schwaiger, M.; Weber, W. A. Comparison of changes in tumor metabolic activity and tumor size during chemotherapy of adenocarcinomas of the esophagogastric junction. *J. Nucl. Med.* **2005**, *46*, 2029−2034.
(66) Egashira, I.; Takahashi-Yanaga, F.; Nishida, R.; Arioka, M.; Igawa, K.; Tomooka, K.; Nakatsu, Y.; Tsuzuki, T.; Nakabeppu, Y.; Kitazono, T.; Sasaguri, T. Celecoxib and 2,5-dimethylcelecoxib inhibit intestinal cancer growth by suppressing the Wnt/β-catenin signaling pathway. *Cancer Sci.* **2017**, *108*, 108−115.
(67) Montrose, D. C.; Zhou, X. K.; McNally, E. M.; Sue, E.; Yantiss, R. K.; Gross, S. S.; Leve, N. D.; Karoly, E. D.; Suen, C. S.; Ling, L.; Benezra, R.; Pamer, E. G.; Dannenberg, A. J. Celecoxib alters the intestinal microbiota and metabolome in association with reducing polyp burden. *Cancer Prev. Res.* **2016**, *9*, 721−731.
(68) Dubé, D.; Brideau, C.; Deschênes, D.; Fortin, R.; Friesen, R. W.; Gordon, R.; Girard, Y.; Riendeau, D.; Savoie, C.; Chan, C.-C. 2-Heterosubstituted-3-(4-methylsulfonyl)phenyl-5-trifluoromethyl pyridines as selective and orally active cyclooxygenase-2 inhibitors. *Bioorg. Med. Chem. Lett.* **1999**, *9*, 1715−1720.
(69) Drennen, B.; Scheenstra, J. A.; Yap, J. L.; Chen, L.; Lanning, M. E.; Roth, B. M.; Wilder, P. T.; Fletcher, S. Structural re-engineering of the α-helix mimetic JY-1-106 into small molecules: disruption of the Mcl-1-Bak-BH3 protein-protein interaction with 2,6-di-substituted nicotinates. *ChemMedChem* **2016**, *11*, 827−833.

https://doi.org/10.1021/acs.jmedchem.1c00890
J. Med. Chem. 2021, 64, 11570−11596